

MUSCULOSKELETAL MODELS IN HIGHLY DYNAMIC
MOTION: EFFECTS OF MODEL PARAMETERS AND
MENTAL STRESS



Dissertation
to obtain the doctoral degree
of Human Sciences
(Dr. sc. hum.)

of the
Faculty of Medicine
of the University of Regensburg

submitted by
Simon Auer

2023

Dean: Prof. Dr. med. Dirk Hellwig

Mentors: Prof. Dr. med. Markus Weber
Prof. Dr. med. Werner Krutsch

Supervisor: Prof. Dr.-Ing. Sebastian Dendorfer

Day of defense: 15.11.2023

Table of contents

List of Figures	3
List of Tables	4
Abstract	6
Zusammenfassung	7
1 Introduction	8
1.1 Mental stress	9
1.2 Muscle physiology	10
1.3 Relationship of mental stress and musculoskeletal loading	12
1.4 Musculoskeletal modeling	14
1.5 Research questions	19
2 Mental stress study	20
2.1 Introduction	20
2.2 Materials and Methods	22
2.3 Results	25
2.4 Discussion	28
2.5 Conclusion	31
3 Muscle model and recruitment study	32
3.1 Introduction	32
3.2 Materials and Methods	34
3.2.1 Experimental setup	34
3.2.2 Musculoskeletal modeling	35
3.2.3 Data processing	37
3.3 Results	38
3.3.1 Flexion and extension tasks	38
3.3.2 Sprinting tasks	38
3.4 Discussion	40
3.5 Conclusion	44
4 Addressing Human-Ground-Residuals	45
4.1 Introduction	45
4.2 Materials and Methods	46
4.2.1 Data acquisition	46
4.2.2 Musculoskeletal modeling	46

4.2.3	HGR reduction	47
4.2.4	Data processing	48
4.3	Results	49
4.4	Discussion	50
4.5	Conclusion	53
5	Discussion and Conclusion	54
5.1	Discussion	54
5.2	Conclusion	57
	Acknowledgments	67
	Declaration of authorship	68
	Appendix A: Supplementary material to chapter 3	69
	Appendix B: Supplementary material to chapter 4	79

List of Figures

1.1	Hebbian version of the Yerkes-Dodson law	9
1.2	Structural anatomy of a skeletal muscle	10
1.3	Functional structure of a sarcomere	11
1.4	Relationship between active and passive muscle force	12
1.5	Cascade of the biomechanical and mental load	13
1.6	Full body model of the AMMR.	14
1.7	Forward and inverse dynamics principle	15
1.8	Schematic view of the mechanical properties of the three-element Hill-type muscle model	18
2.1	Schematic view of the SpeedCourt	23
2.2	Front and back view of the employed musculoskeletal full body model from the AMMR	24
2.3	Results of the self-evaluation forms	26
3.1	Flexion and extension setup	35
3.2	Results of the Pearson correlation analysis for flexion/extension	39
3.3	Results of the Pearson correlation analysis for sprinting	40
3.4	Results of the SPM	41
4.1	Results of the HGR minimization for the OM models.	49
4.2	Results of the HGR minimization for the OP models.	50
4.3	Results of the HGR minimization for the IP models.	51
A.1	Muscle activity in EMG and AMS for sprinting.	78

List of Tables

2.1	Results of the musculoskeletal simulation for the participants (SpeedCourt)	27
2.2	Mean peak knee loadings and standard deviations.	28
3.1	Overview of the different muscle model and recruitment configurations . . .	37
3.2	Mean ρ , standard deviation and the 95% CI for flexion/extension	38
3.3	Mean ρ and the 95% CI for the different muscle models and recruitments of the sprints	38
3.4	Median DTWD and the 95% CI for the different muscle models and re- cruitments for the sprinting tasks	39
4.1	Overview of the HGR minimization approaches	47
4.2	Default and optimized segment mass distribution of the AMS.	50

Abbreviations

AMMR AnyBody Managed Model Repository
AMS AnyBody Modeling System
BF Biceps Femoris
CI confidence interval
CMA calculated muscle activity
COD change-of-direction
COM center of mass
DOF degrees of freedom
DTWD dynamic time warping distance
EMD electromechanical delay
EMG electromyography
GRF ground reaction forces
GRFP ground reaction force prediction
HGR human-ground-residuals
IMC inertial motion capture
IMU inertial measurement unit
JRF joint reaction forces
MMA measured muscle activity
OMC optical motion capture
PCSA physiological cross-sectional area
RF Rectus Femoris
RMSE root mean square error
RRA residual reduction algorithm
SPM statistical parametric mapping
ST Semitendinosus
VL Vastus Lateralis
VM Vastus Medialis
VMC video motion capture

Abstract

The analysis and understanding of highly dynamic movements is a fundamental part of biomechanics. Since sports injuries often involve the lower extremities and muscles, musculoskeletal models can help to prevent them. These models allow the calculation of ground and joint reaction forces as well as muscle forces and activities for individual muscle strands. One goal of this work is to use musculoskeletal models to investigate the influence of mental stress on lower extremity loading. Moreover, the models themselves are evaluated for highly dynamic movements and practical recommendations for action will be derived.

For this purpose, fast movements of youth competitive and amateur athletes will be recorded using different measurement systems. Subsequently, the models calculate the target parameters using inverse dynamics. Furthermore, measured and calculated muscle activities of the lower extremities are compared and artificial balancing forces (residuals) in the models are analyzed and minimization approaches are presented.

The investigation of muscle and joint loading under mental stress has shown that the response to mental stress is highly individual. Athletes may experience a significant increase in muscle and knee forces with a simultaneous decrease in performance. The comparison of measured and calculated muscle activity proved the reliability of the models also for highly dynamic movements. With the frequently used default settings in the model and optical and inertial motion capture, the muscle activities in the model could be calculated reliably. The residual forces were highest, when the model transitioned from foot-ground contact to no contact and vice versa. By adjusting the settings of the kinematic filter and the ground reaction force prediction, the residuals were reduced by up to 54%.

The analysis of musculoskeletal loading under mental stress has shown that the models can make a valuable contribution to the biomechanical analysis of highly dynamic movements. Subsequently, the models have also proven to be a reliable tool for the analysis of highly dynamic movements when the calculated parameters as well as the model-specific optimization options are reviewed. With this in mind, these models can contribute to further understand highly dynamic movements and prevent muscle injuries in athletes.

Zusammenfassung

Die Analyse und das Verständnis hochdynamischer Bewegungen ist ein fundamentaler Bestandteil der Biomechanik. Da Sportverletzungen häufig die unteren Extremitäten und Muskeln betreffen, können muskuloskelettale Modelle dazu beitragen, sie zu vermeiden. Diese Modelle ermöglichen die Berechnung von Boden- und Gelenkreaktionskräften sowie von Muskelkräften und -aktivitäten für einzelne Muskelstränge. Ein Ziel dieser Arbeit ist es, mit Hilfe von muskuloskelettalen Modellen den Einfluss von mentalen Belastungen auf die Belastung der unteren Extremitäten zu untersuchen. Darüber hinaus werden die Modelle selbst für hochdynamische Bewegungen evaluiert und praktische Handlungsempfehlungen abgeleitet.

Zu diesem Zweck werden schnelle Bewegungen von jugendlichen Leistungs- und Freizeitsportlern mit verschiedenen Messsystemen aufgezeichnet. Anschließend berechnen die Modelle mittels inverser Dynamik die Zielparameter. Weiterhin werden gemessene und berechnete Muskelaktivitäten der unteren Extremitäten verglichen sowie künstliche Ausgleichskräfte (Residuen) in den Modellen analysiert und Minimierungsansätze vorgestellt.

Die Untersuchung der Muskel- und Gelenkbelastung unter mentalem Stress hat gezeigt, dass die Reaktion auf mentalen Stress sehr individuell ist. Bei einzelnen Personen kann es zu einem deutlichen Anstieg der Muskel- und Kniegelenkreaktionskräfte bei gleichzeitiger Leistungsminderung kommen. Der Vergleich von gemessener und berechneter Muskelaktivität beweist die Zuverlässigkeit der Modelle auch bei hochdynamischen Bewegungen. Mit den häufig verwendeten Standardeinstellungen im Modell und der vielseitigen Bewegungserfassung konnten die Muskelaktivitäten im Modell zuverlässig berechnet werden. Die Residualkräfte waren am höchsten, wenn das Modell von Fuß-Boden-Kontakt zu keinem Kontakt und umgekehrt übergang. Durch Anpassung der Einstellungen des kinematischen Filters und der Berechnung der Bodenreaktionskraft konnten die Residualkräfte um bis zu 54% reduziert werden.

Die Analyse der muskuloskelettalen Belastung unter psychischer Beanspruchung hat gezeigt, dass die Modelle einen wertvollen Beitrag zur biomechanischen Analyse von hochdynamischen Bewegungen leisten können. In der Folge haben sich die Modelle auch bei der Überprüfung der berechneten Parameter sowie der modellspezifischen Optimierungsmöglichkeiten als zuverlässiges Werkzeug für die Analyse hochdynamischer Bewegungen erwiesen. Daher können die Modelle dazu beitragen, hochdynamische Bewegungen besser zu verstehen und Muskelverletzungen bei Sportlern vorzubeugen.

Chapter 1

Introduction

Understanding fast movements in sports or in everyday life is an essential part of biomechanics. The main goals of sports biomechanics studies are the improvement of performance and the prevention of injuries (Bussey 2002). While performance analysis usually has its focus on kinematic and kinetic outputs such as running times, exerted force or repetitions, injury prevention often concentrates on intrinsic parameters like joint reaction forces (JRF) and moments or muscle activity and muscle forces.

In amateur and professional sports muscle injuries of the players are a major problem. However, the injury mechanisms and types differ from the usual occupational diseases and, since professional athletes often are highly paid, the costs for their outages are high. In addition, there are the individual health consequences of the injuries for the athletes themselves. Consequently, it is beneficial for the teams, the society and the players to prevent injuries of athletes. A large proportion of sports injuries are caused by muscular problems as they make almost a third of all injuries (Ekstrand et al. 2011a). In addition, many injuries are potentially caused or facilitated by mental stress (Jansen et al. 2019). Therefore, it is of enormous importance to be able to grasp and analyze these connections. By understanding the complex and intricate processes involved in dynamic motions, it is possible to optimize movements in sports or prevent injuries in general.

For these reasons, the use of musculoskeletal models to analyze fast, highly dynamic movements has increased noticeably in recent years. Musculoskeletal models that allow deep insight into athletes and the forces acting internally can help to better understand injury mechanisms and causes, and consequently prevent damage. While conventional investigations are often limited to one or two time slots due to fixed force plates, models allow for more extensive research because they provide more complete data. Since these models were initially developed for slower movements or orthopedic research, they have been tested and validated thoroughly for these kinds of applications (Rasmussen et al. 2001; Wu et al. 2009; Andersen et al. 2010; Fluit et al. 2014). Nevertheless, a comprehensive assessment of these models in highly dynamic movements has yet to be made.

1.1 Mental stress

Although it is commonly described as emotional pain, the definition of mental stress is ambiguous. There are many different manifestations of mental stress, as it can occur in the form of major events (crises), daily hassles, or environmental situations (Jones 2001). Regardless of its form, mental stress is considered a major public health issue with significant social and economic consequences. This is because mental stress can lead to a variety of physical and psychological health problems, such as anxiety, depression, sleep disturbances, cardiovascular diseases, and impaired cognitive function (Pastorino and Doyle-Portillo 2019). Selye (1976) defined stress as a nonspecific response of the body to any demand placed on it and divided it into eustress and distress. Eustress refers to the positive form of stress that can be motivating and lead to personal growth, while distress refers to the negative form of stress that can be harmful and cause anxiety, depression, or other mental health problems. This reaction to stress is described by the Hebbian version of the Yerkes–Dodson law (Figure 1.1).

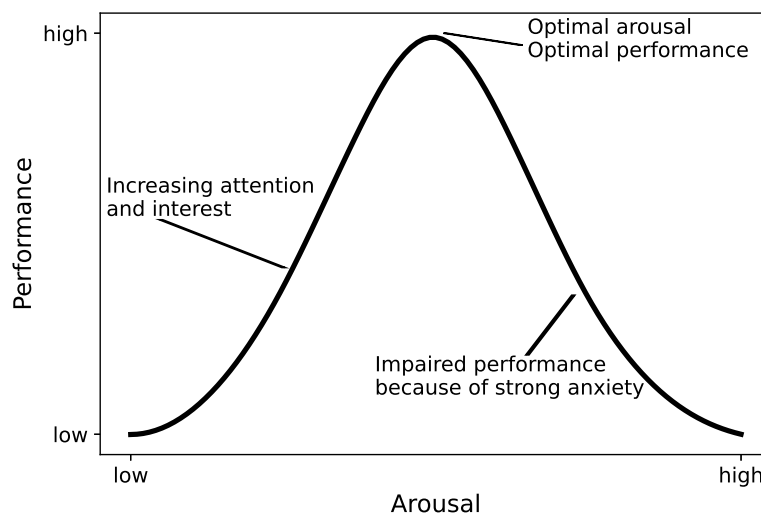


Figure 1.1: Hebbian version of the Yerkes-Dodson law. The law describes the human reaction to different levels of stress. The Hebbian version leaves out that hyperarousal does not adversely impact simple tasks. Figure adapted from Diamond et al. (2007).

In addition, Lazarus and Folkman’s transactional model of stress (Lazarus and Folkman 1984) describes how individuals evaluate the demands of a situation and their ability to cope with those demands, which in turn affects their level of stress.

Overall, there are many theoretical frameworks that attempt to explain the causes and consequences of mental stress. However, it is widely recognized that mental stress is a complex phenomenon influenced by various biological, psychological and social factors. Therefore, a multidisciplinary approach is needed to fully understand and effectively address mental stress in individuals and populations and research its cause.

There are many causes of mental stress. Some common causes of mental stress include interpersonal conflict, financial difficulties, work-related stressors, major life events (such as divorce, job loss, or the death of a loved one), and chronic health problems. Environmental factors such as noise, air pollution, and overcrowding can also contribute to mental stress. Moreover, individual factors such as personality traits, coping mechanisms and resilience can play an important role in the development and management of mental stress (Selye 1976; Cooper 1986). For athletes in particular, the pressure to perform at a high level and to meet the expectations of coaches, teammates, and fans can contribute to psychological stress. Especially in sports, eustress can also be experienced when an athlete is motivated and energized by the challenge of competition, leading to improved performance. However, when stress becomes chronic and overwhelming, it can lead to negative outcomes such as burnout, injury, and mental health disorders such as anxiety and depression. For athletes in particular, a healthy mix of eu- and distress, as shown in Figure 1.1, can be important in order to be able to perform accordingly.

However, the principle of increasing performance with rising stress levels is not undisputed. In recent literature, for example, there is growing doubt about the empirical basis for this theory (Corbett 2015). Consequently, there is still room for the investigation of mental stress and its actual effects on sports.

1.2 Muscle physiology

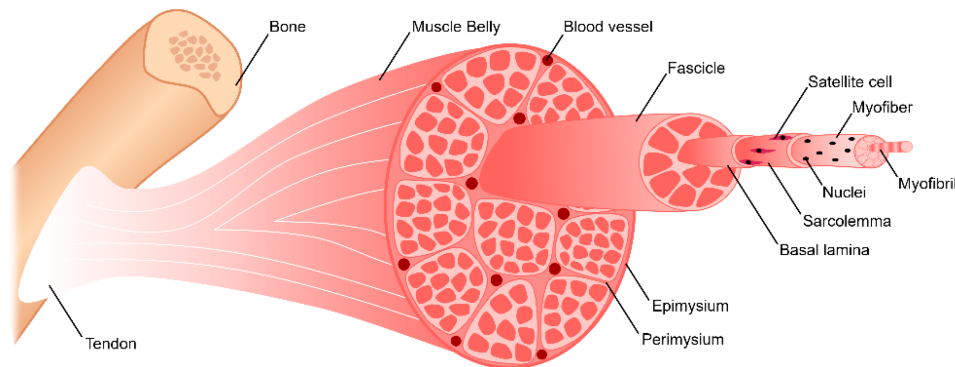


Figure 1.2: Structural anatomy of a skeletal muscle. Adapted from Carnes and Pins (2020).

Humans have several types of muscles. Skeletal, smooth, and cardiac muscles are the three main types of muscles in the human body. However, since this thesis is mainly about skeletal muscles, the other types will not be discussed in this text. Skeletal muscles are attached to the bones and allow the skeleton to move. These muscles are responsible for voluntary movements, such as walking and talking, and account for about 40% of total human weight. Skeletal muscles are called striated muscles because of the striated pattern

formed by the arrangement of actin and myosin filaments. A single muscle consists of several muscle bundles, each of which is composed of individual muscle fibers. Figure 1.2 describes the structural anatomy of a skeletal muscle.

The muscle fibers are multinucleated, meaning they contain multiple nuclei, which are essential for protein synthesis and maintaining cellular metabolism. Muscle fibers are also composed of multiple myofibrils made up of sarcomeres, the basic functional unit of muscle contraction. Sarcomeres contain two types of protein filaments, actin and myosin. The sliding of these two filaments past each other is responsible for muscle contraction, which is triggered by the release of acetylcholine, a neurotransmitter that binds to receptors on the muscle fibers. The functional structure of a sarcomere is described in Figure 1.3.

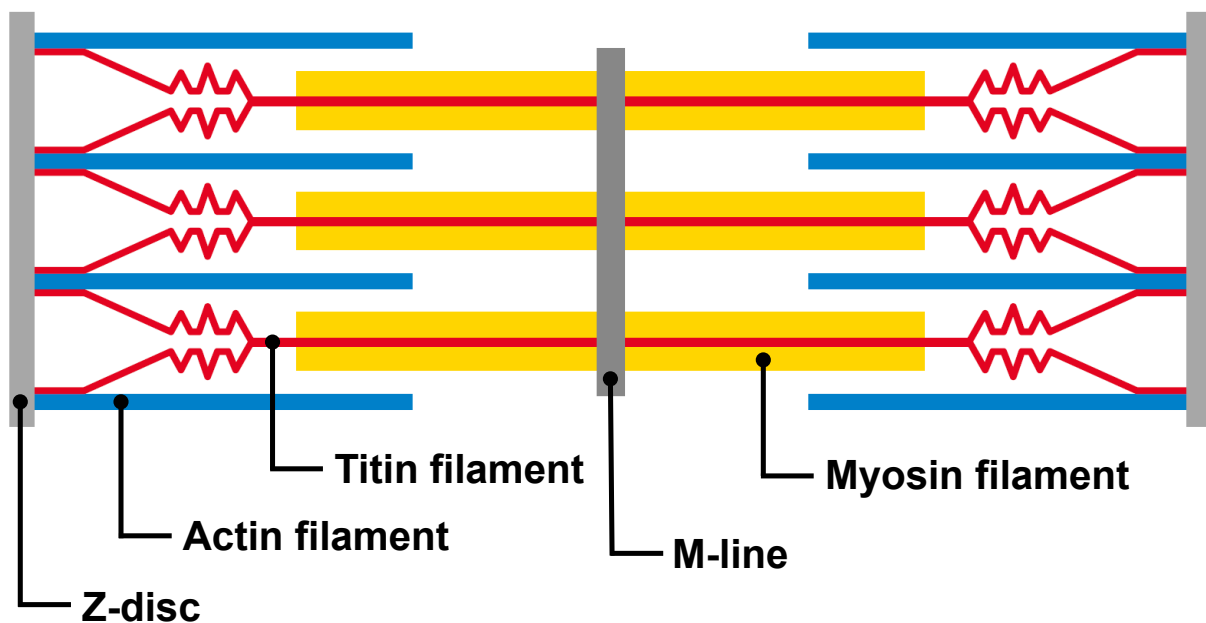


Figure 1.3: Functional structure of a relaxed sarcomere. The myosin filaments in the middle of the sarcomere and actin filaments interlock with each other. The titin filaments bind the actin filaments to the Z-discs and serve as elastic feathers during contraction. The M-line in the middle connects the Myosin filaments. Adapted from Brandes et al. (2019, p. 131).

To control skeletal muscle strength, muscle fibers are grouped into motor units. They describe a set of muscle fibers that are activated by a motoneuron. Consequently, to generate more muscle force, more motor units are activated and vice versa. In addition to the number of activated motor units, muscle force is also regulated by the variation in action potential frequency. By increasing the frequency, a superposition of individual muscle activations is achieved, resulting in higher muscle force. There are large motor units with predominantly slow twitch fibers (Type I) and small motor units with mainly fast twitch fibers (Type II). While the small motor units are typically responsible for precise movements, the large motor units are usually involved in rough or holding movements.

Muscles can produce passive forces in addition to active ones. Unstimulated, resting muscles exert a passive force when stretched beyond their resting length. The passive force exerted increases in a non-linear relationship with increasing stretch, implying an increasing Young's modulus as a function of muscle stretch. The slope varies for different skeletal muscles and depends on the different titin isoforms and the content and cross-linking of the collagen fibers. Passive muscle force is also added to the muscle force when active force is applied. Thus, muscle stretch affects both active and passive muscle force. The relationship between active and passive muscle force is described in Figure 1.4.

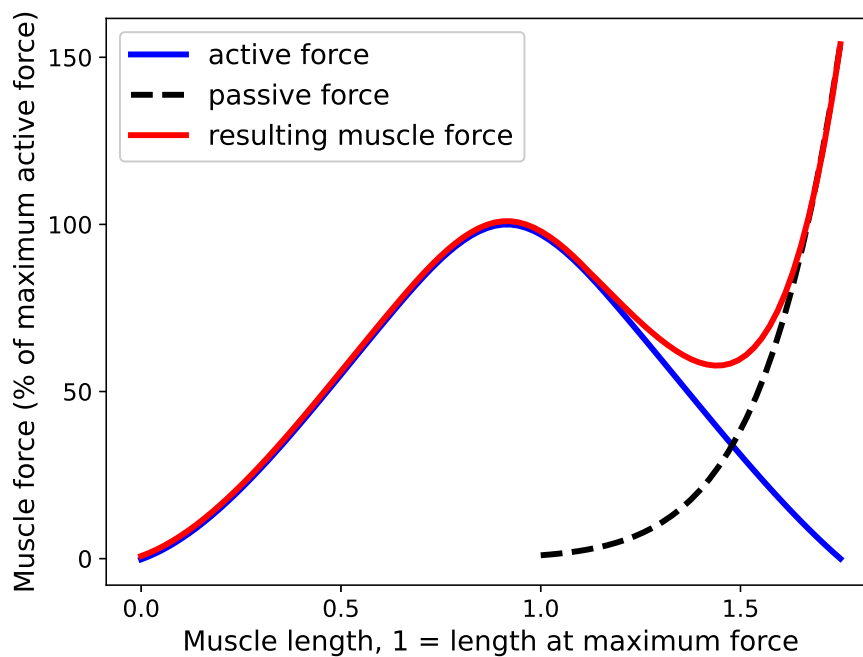


Figure 1.4: Relationship between active and passive muscle force

1.3 Relationship of mental stress and musculoskeletal loading

This section is also part of a contribution published in "*Die Orthopädie*" under the title "Kombinierter Einfluss von psychologischen und biomechanischen Faktoren auf die muskulären Belastungen beim Fußballspielen. Ein neuer Ansatz zur Prävention von Muskelverletzungen?" (Auer et al. 2023).

Study results indicate that psychological factors are also associated with the risk of sports injuries. Personality traits such as anxiety and an associated reduced ability to cope with stressful situations in the form of negative life events or everyday stress have been identified as indicators. This has been demonstrated in cross-sectional and prospective studies (Alahmad et al. 2020; Ivarsson et al. 2013). In addition to this individual level, risk factors can additionally be identified in the interpersonal domain. This can be seen,

for example, in correlations between the coach-athlete relationship and an increased risk of injury (Pensgaard et al. 2018). Previous injuries also represent a stress factor that can lead to increased anxiety and thus to a vicious circle (Jansen et al. 2019). The risk of injury also increases additionally with the duration of the stress. For example, increased stress over three to four weeks leads to a significantly increased risk of injury (McCall et al. 2018). In order to assess the risk of injury, multiple factors must therefore be taken into account, which act directly or indirectly on the musculature.

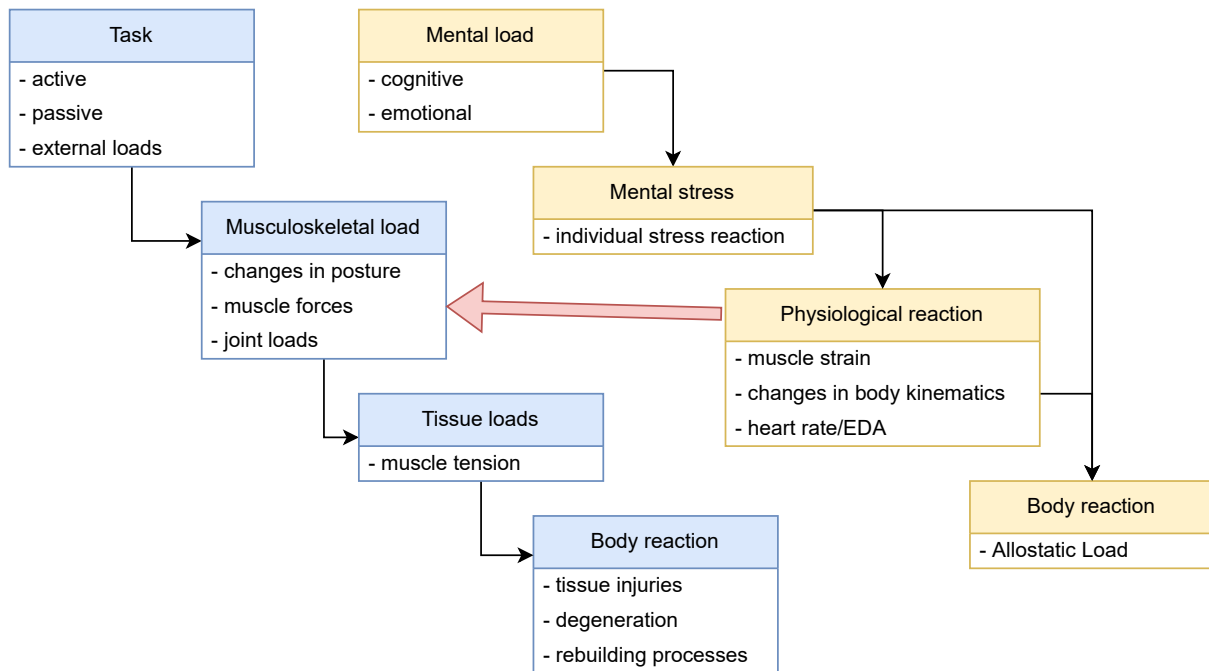


Figure 1.5: Cascade of the biomechanical and mental load. Adapted from Auer et al. (2023).

The effects of biomechanical and mental loads can be summarized in a cascade structure (Figure 1.5). In the case of biomechanical loads, activities such as sprints lead in the first stage to musculoskeletal loads in the form of, for example, muscle and joint forces or ligament strains. The integral loads on structures can also be represented at a further level of discretization as tissue loads such as muscle tension or joint compression. From the point of view of structural mechanics, this level is usually used to further describe changes in tissue structure such as the development of injuries, or the initiation of remodeling processes or degeneration. Analogously, in a first stage, the influence of mental loads, for example of a cognitive or emotional nature, can lead to mental stress depending on moderating factors such as individual evaluation processes, from which a psychical reaction can result. Typical measurable physical reactions to a higher mental stress are an altered heart rate and skin conductance, an increase in muscle tone and altered body kinematics (Selye 1976; Lundberg et al. 2002). Here is an obvious cross-connection between mental and biomechanical loads. The physiological responses to the mental loads

directly influence the biomechanical loads at the muscular level, through an increase in preload and conditioned by the altered body kinematics. Nevertheless, there is little to no literature investigating the effects of mental stress on individual muscles.

1.4 Musculoskeletal modeling

This section is based on the information available in the *AnyBody Tutorials* (AnyBody Technology 2023). Other references are given, if applicable.

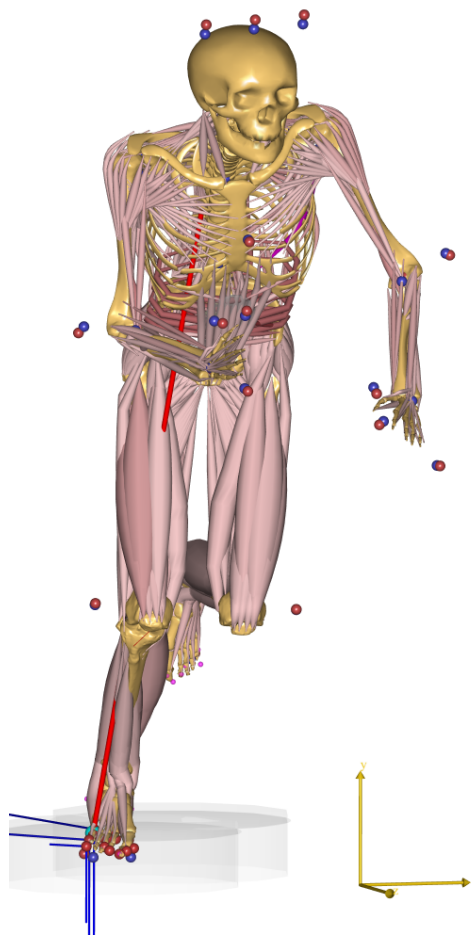


Figure 1.6: Full body model of the AnyBody Managed Model Repository (AMMR). The bones are depicted in beige, muscles in salmon. The blue and red lines at the bottom represent the ground reaction forces (GRF).

Musculoskeletal models are a special field of multi-body dynamics. A popular application for musculoskeletal models is the AnyBody Modeling System (AMS) (AnyBody Technology A/S, Aalborg, Denmark) with its open-code model library, the AnyBody Managed Model Repository (AMMR). The models consist of rigid bodies, representing human bones, actuators acting as muscles and other important support-components such

as tendons and ligaments (Figure 1.6). The joints defining the connection between the modeled bones imitate the functionality of the anatomical human joints. The musculoskeletal models in the AMS are based on an inverse dynamics approach. While other musculoskeletal models are based on forward dynamics and calculate the motion on the given forces, inverse dynamics models calculate forces and moments based on a given motion and defined inertial properties.

Forward dynamics:

$$F \longrightarrow \frac{F = m a}{F = m \ddot{x}} \longrightarrow \int \int \longrightarrow x$$

Inverse dynamics:

$$x \longrightarrow \frac{d^2}{dt^2} \longrightarrow \frac{F = m a}{F = m \ddot{x}} \longrightarrow F$$

Figure 1.7: Simplified principles of the forward and inverse dynamics approaches. F represents the occurring forces, m the objects mass, a and \ddot{x} the acceleration, x the motion and t the time.

Muscle recruitment

Since the models are based on an inverse dynamics approach, they can calculate internal and external parameters through differentiation of a given motion (Figure 1.7). However, the human body consists of hundreds of muscles and bones interacting in many complex configurations. Additionally, since there are many more muscles involved in the movement than there would be necessary to balance the body's degrees of freedom (DOF), the human body is a kinetically overdetermined system. This problem is solved mathematically by formulating the boundary conditions, internal and external forces, and movements as an optimization problem. It minimizes internal forces in respect of given motion and if applicable external forces. With this approach, the kinetics of individual body parts can be calculated (Damsgaard et al. 2006).

Since rigid body systems need actuators that exert forces on the system, a major part of inverse dynamics is muscle recruitment. In humans as well as in musculoskeletal models, this part is taken by muscles attached to the bones. In humans this involves the detachment of cross bridges and the re-uptake of calcium as two energy-consuming processes (Praagman et al. 2003; Praagman et al. 2006) and the human body strives to

minimize energy consumption. In terms of inverse dynamics, the process of balancing a given external load through muscle activation is called muscle recruitment and is described as an optimization problem. The equilibrium equations can be organized like

$$C * f = r \quad (1.1)$$

with f as a vector of muscle and joint forces, r as a vector of external and inertia forces and C as the matrix of equation coefficients. f is restricted to positive numbers, since muscles can only exert forces in one direction. Furthermore, the human musculoskeletal system is highly complex and redundant since there is more than one muscle to perform a certain movement. Mathematically, this results in more unknowns in the equilibrium equation than it has equations and consequently infinitely many solutions. The optimization problem for the muscle recruitment can be described as follows:

$$\begin{aligned} & \text{minimize} && G(f^{(M)}) \\ & \text{subject to} && C * f = r \\ & && f_i^{(M)} \geq 0, i = 1 \dots n^{(M)} \end{aligned} \quad (1.2)$$

$G(f^{(M)})$ is the target function of the optimization problem, that can have different forms in the AMS. Ideally, the target function should represent the physiological muscle activation exactly but since this isn't possible, there are different approximations taking the numerical peculiarities of the AMS into account. The simplest approximation of physiological muscle recruitment is a linear combination of muscles where the target function looks like this:

$$G = \sum_i \frac{f_i}{N_i} \quad (1.3)$$

N_i represent the normalization factors, which usually is the individual muscle strength and causes strong muscles to work more than weak muscles. Practically, this means that the AMS only recruits the minimum number of muscles necessary to balance the system, although this is non-physiological. In order to improve the physiological behavior of the musculoskeletal model, one can introduce a polynomial to the target function

$$G = \sum_i \left(\frac{f_i}{N_i} \right)^p \quad (1.4)$$

where the power p increases the synergy between muscles. The higher p gets, the higher the synergy is and an infinite p would mean maximum synergy. Nevertheless, increasing the power of the polynomial decreases numerical stability of the model and therefore, the default value is $p = 2$ for motion capture models with ground reaction force

prediction (GRFP) and $p = 3$ for all other models. However, there's also the possibility to use a recruitment algorithm that allows for minimum fatigue by minimizing the maximum relative load in the muscles. This can mathematically be described by setting $p = \infty$. Since an infinite p would lead to hard, non-physiological on- and offsets of muscle activity, it can be combined with a quadratic term:

$$\begin{aligned}
 & \text{minimize} && G = \beta + \epsilon * \sum_i \left(\frac{f_i}{N_i} \right)^2 \\
 & \text{subject to} && \frac{f_i^{(M)}}{N_i} \leq \beta, \text{ for } i = 1 \dots n^{(M)} \\
 & && C * f = r \\
 & && f_i^{(M)} \geq 0, \text{ for } i = 1 \dots n^{(M)}
 \end{aligned} \tag{1.5}$$

Here β describes the numerical representation of an infinite p in Equation 1.4 in the AMS and ϵ is a factor to weigh the additional quadratic term. In practice, this formulation of the muscle recruitment optimization algorithm leads to a simultaneous reduction of all muscle activities with soft on- and offset for the individual activities. Nevertheless, when independent model parts are used in the same application, this recruitment algorithm leads to unreasonable results and therefore should be handled with care.

Muscle modeling

Besides muscle recruitment, there are also different ways of modeling muscles in musculoskeletal models and since the muscle force is dependent on the used muscle model, muscle modeling consequently influences the muscle recruitment. For modeling, one has to distinguish between the kinematic implementation of the muscle, which determines the muscle's path from origin to insertion and the kinetic representation which defines the muscle's strength and other properties depending on the muscle's kinematics.

One way to define the muscle paths is by giving specific points (nodes) in the musculoskeletal model to which the muscle is attached and follows a straight line between two points. The first and last point transfer the muscle force in the muscle's longitudinal direction while the via points only transfer forces along the line that bisects the angle formed by the muscle on the two sides of one via point. Although this makes muscle pathing quite simple and kinematically robust, this approach is limited in creating complex geometrical muscle pathings that change with different joint angles. Therefore, one can additionally use geometrical shapes as wrapping surfaces for the muscles. By, for example, combining cylindrical surfaces with via points one can create complex and physiological muscle pathings.

The muscle properties can be defined in multiple ways in the AMS. The most often used properties are the *simple muscle model* and the *Hill-type muscle model*. The simple muscle model calculates the muscle's strength depending on its physiological cross-sectional area (PCSA) and a strength index (SI) acting as a scaling factor. Consequently, the muscle force (F_M) is calculated as follows:

$$F_M = SI * PCSA \quad (1.6)$$

The three-element Hill-type muscle model calculates the muscle force depending on the active properties of the muscle fibers (F_{CE}), the elasticity of the tendon (F_T) and also the passive stiffness of the muscle fibres (F_{PE}):

$$F_M = F_{CE} + F_{PE} + F_T \quad (1.7)$$

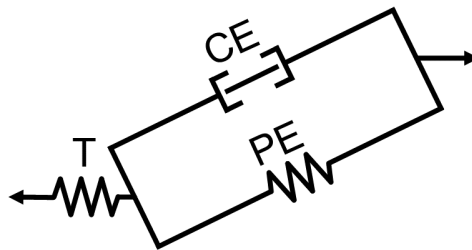


Figure 1.8: Schematic view of the mechanical properties of the three-element Hill-type muscle model. It consists of a contractile element (CE), a passive element (PE), and an elastic element (T).

A schematic view of the mechanical properties is shown in Figure 1.8 and the concepts for this model in the AMS are adopted from Zajac (1989). Although the described properties are not the only ones in the model, they are often used in different combinations and there is little literature on the practical implications in highly dynamic movements.

1.5 Research questions

It is well known that mental stress promotes muscular injuries in competitive sports (Ivarsson and Johnson 2010; Ivarsson et al. 2013; Jansen et al. 2019), but the exact mechanisms are unknown. There are suggestions that psychological stress can lead to force peaks in the (leg) muscles, but detailed studies are lacking. Musculoskeletal models are ideally suited for these research questions, as they allow analysis of muscle forces at the level of individual muscle strands. This problem is addressed in chapter 2 and refers to research question 1.

Further on, the musculoskeletal models used in these studies are tested and validated for normal and slow movements only. Investigations regarding muscle modeling, muscle recruitment and activation in musculoskeletal models in highly dynamic movements like sprinting are rare. Consequently, these models need to be evaluated for such applications, which leads to research question 2 and is treated in chapter 3.

As preliminary investigations have shown, musculoskeletal models driven by motion capture inherit artificial balancing forces (human-ground-residuals (HGR)), influencing the calculated results. In order to investigate the height and effects of the HGR on musculoskeletal models and approaches to minimize them, research question 3 is addressed in chapter 4.

The research questions are formulated as follows:

1. How does the muscle and joint reaction force behave under the influence of mental stress in elite junior football players for highly dynamic, sports related motions?
2. Does the musculoskeletal model's muscle activity in the lower extremities match the physiological muscle activation in highly dynamic motion, and what's the influence of different muscle modeling options?
3. When and to what extent do HGR occur in simulations of highly dynamic motions and how can their occurrence be influenced?

Each of the following chapters deals with a separate research question.

Chapter 2

Musculoskeletal loading under mental stress in football-related movements

This chapter addresses research question 1: "how do the muscle and joint reaction forces behave under the influence of mental stress in elite junior football players for highly dynamic, sports related motions?" The text and figures are mostly based on the papers "Mental stress reduces performance and changes musculoskeletal loading in football-related movements" published in *Science and Medicine in Football* by Auer et al. (2021) and "Effect of mental demand on knee forces in professional youth soccer players" published in the *ISBS Proceedings Archive: Vol. 38* by Auer et al. (2020).

2.1 Introduction

Despite its popularity, football bears a considerable injury risk. Injuries to the thigh muscles are common in amateur and professional football, representing almost a third of all injuries (Ekstrand et al. 2011b). These can lead to a range of costs, including financial costs associated with treatment and those associated with long-term recovery and absence from training or competition. Further, there is a high risk of injury recurrence and subsequent injury (Ekstrand et al. 2011b). These injuries usually occur in non-contact or overuse situations (Loose et al. 2019; McCall et al. 2018). Half of the injuries occur during matches (Junge et al. 2002), and these matches involve a high physical workload combined with psychological aspects. Psychological aspects have previously been identified as potential risk factors for injury (Ivarsson and Johnson 2010; Ivarsson et al. 2013; Jansen et al. 2019; Junge et al. 2002). These psychological reactions occurred in the form of cognitive anxiety and changed mood states, which led to increased cortisol and testosterone levels (Slimani et al. 2017). Besides professional players, players in semi-professional and

elite junior football have a comparably high risk of injury, especially on the musculature (Loose et al. 2019). These competition levels are characterized by the same high ambitions and physical demands of the players as in professional football. Mendez-Villanueva et al. (2013) reported an average running distance of 8450 m for U17 players, while it was 8810 m for adults (Rebello et al. 2014). Rebello et al. (2014) additionally reported an average heart rate of 85% of the maximum heart rate of the U17 stating similar physical effort for youth and adult players.

Since it is a considerable risk for injury (Arnason et al. 2004), this work aims to examine the effects of mental stress in the form of additional attention-grabbing tasks in highly dynamic motion. The effects of this kind of mental stress on the body have been studied before, with arithmetic tasks used as a form of mental stress (Lundberg et al. 2002; Nimbarte et al. 2012; Wijsman et al. 2013). Others used short-term memory tests (Bloemsaat et al. 2005; Wijsman et al. 2013), negative/unsupportive language (Marras et al. 2000) or additional cognitive tasks (Srinivasan et al. 2016). There, muscle activity in the upper extremities and back was increased significantly under stress. Also, muscles were active even though there was no physical necessity for this. In addition to higher muscle tone, compression and shear forces in the spine increased (Marras et al. 2000).

While these studies (Bloemsaat et al. 2005; Lundberg et al. 2002; Marras et al. 2000; Wijsman et al. 2013) consistently detected higher biomechanical loading under mental stress, some information is still missing. The motion is mostly quasi-static or low dynamic since they arise from workplace ergonomics. Moreover, most studies focus on muscle activities, lacking kinetic information of internal parameters like muscle or joint reaction forces, since collecting such information is quite difficult.

For this purpose, musculoskeletal simulation is a valuable tool. Such software has been used in different sports-related fields to analyze internal biomechanical parameters. Ali et al. (2014) investigated non-contact ACL injury rates in single-leg landings using individualized 3D musculoskeletal models of the human body. Although they could only indirectly validate the internal forces, this was the first study to report joint reaction and muscle forces during single-leg landings. Skals et al. (2017) gave another example of analyzing highly dynamic motion. They examined predicted ground reaction forces and moments for running, side-cutting and vertical jumping with human body models. They found that the estimates are comparable to measured ground reaction forces (median Pearson's correlation coefficient, $r = 0.99$) and moments as well as joint flexion moments (median $r = 0.93$) and resultant joint reaction forces (median $r = 0.97$). Hence, musculoskeletal simulation opens the possibility of adequately mapping highly dynamic movements using motion capture and musculoskeletal modeling.

Although current studies (Ivarsson and Johnson 2010; Ivarsson et al. 2013; Jansen et al. 2019; Junge et al. 2002) show that mental stress increases the injury risk for competitive footballers, there is a lack of research into the exact injury mechanisms. Most studies refer to longer-term exposure to stress. To the best of the authors' knowledge, there are no studies investigating the acute occurrence of mental stress in the form of an additional attention-grabbing, mental task and its effects on the peak muscle force of competitive footballers. Hence, the purpose of this study was to examine the musculoskeletal reaction of elite junior football players exposed to mental stress in highly dynamic motion. In particular, we want to analyze the players' performance in terms of running speed and the changes in exerted muscle force in the lower extremities with and without an additional mental stressor.

2.2 Materials and Methods

For this study, professional youth football players were subjected to mental stress while performing standardized, sports-specific movements. The kinetics of these movements are computed with inverse dynamics software. Ethical approval was obtained in advance by the University of Regensburg (Number: 15-101-0137).

Participants

Twelve football players from a German U17 elite junior football team of a 2nd Bundesliga club were tested. The mean age was 15.9 ± 0.3 years. The average weight was 72.5 ± 5.3 kg and the mean height was 1.80 ± 0.06 m. The players' mean training time per week was 7.5 ± 0.5 h. All players granted their informed consent. Players with a muscle injury within six weeks before the testing were excluded from the study.

Study Design and Protocol

This study was performed in a SpeedCourt (Globalspeed GmbH, Hemsbach, Germany), where the test subjects completed two runs. The SpeedCourt System is a 4×4 m field with twelve integrated pressure plates and a screen in front of it (Figure 2.1). The pressure plates are connected to a computer, which detects foot contacts and highlights the target field on the screen. This system has already been used to recreate standardized, sports-related change-of-direction (COD) maneuvers (Achenbach et al. 2019; Düking et al. 2016). The running route was designed as a so-called star run (Achenbach et al. 2019). The players started in the center field, touched a randomly highlighted outer field, and returned to the center. Each outer field had to be touched two times to get evenly distributed motion patterns for each participant in one run. The screen in front only highlights the

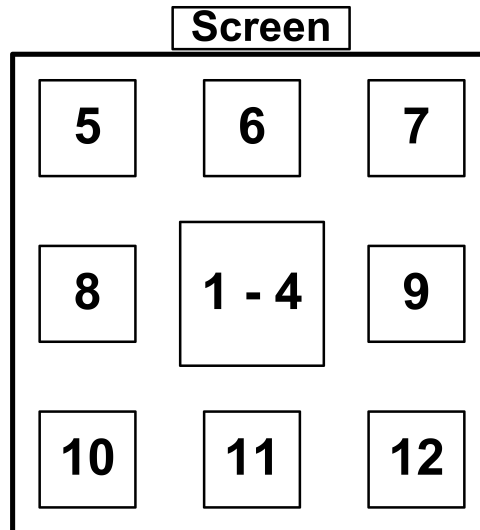


Figure 2.1: Schematic view of the SpeedCourt system. The fields 1-4 in the middle are treated as one field in this study.

current target field. Running times were measured through the system, starting with the first and ending with the last foot contact on the center field. Before the test, the players were introduced to the SpeedCourt system and the stressor.

The first run (baseline) was performed without any external stressor, with the instruction to run as fast as possible. After a five-minute break for rest, the players ran again. The runs were limited to two runs to avoid a learning effect and fatigue. During the second run, the test subjects had to perform a modified version of the d2 attention test (Brickenkamp et al. 2016) as a mental stressor. For this purpose, a second screen in front of the court displayed the letters d and p with one to four dashes. The players had to affirm every d with exactly two dashes and negate every other case. This test was selected to recreate a football-related stress situation of a physically demanding challenge combined with an attention-grabbing task. The answers to the displayed test were not assessed. After each run, the players had to fulfil the NASA-TLX workload scale to evaluate the runs: physical demand ("How much physical activity was required?"), mental demand ("How much mental and perceptual activity was required?"), performance ("How successful were you in performing the task?"), exertion ("How hard did you have to work (mentally and physically) to accomplish your level of performance?"), and frustration ("How irritated, stressed, and annoyed versus content, relaxed, and complacent did you feel during the task?") (Hart and Staveland 1988). The ratings ranged from zero (low) to ten (high). The NASA-TLX ensured the validity of the stressor compared to the baseline.

Data Processing and Musculoskeletal Simulation

Twelve motion capture infrared cameras (Vicon Motion Systems, Oxford, UK) captured the runs with a sampling rate of 120 Hz. Afterwards, the data was filtered using a second-order Butterworth filter with an 8 Hz cut-off frequency and used as input for the AnyBody Modeling System (AMS) (v. 7.2), a musculoskeletal simulation software (AnyBody Technologies, Aalborg, Denmark). Figure 2.2 shows the model used in this study. The software uses an inverse dynamics approach to calculate internal (joint reaction forces (JRF), muscle forces, muscle activities) and external kinetics (ground reaction forces (GRF)). In our study, we modified a full-body model from the AnyBody Managed

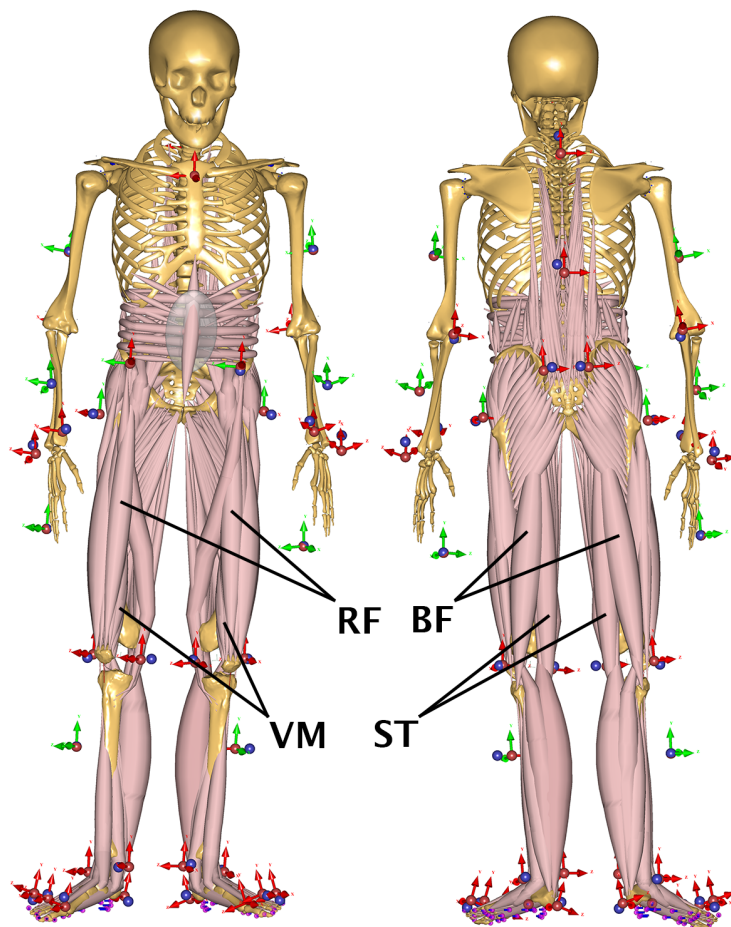


Figure 2.2: Front and back view of the employed musculoskeletal full body model from the AnyBody Managed Model Repository (AMMR). The investigated muscles are highlighted. The blue and red dots represent the motion capture marker set, which is transferred from the recording software to the AMS.

Model Repository (AMMR)(v. 2.2.0). The model from the AMMR has already been validated previously (Skals et al. 2017). In this study, the muscle forces of the M. Rectus Femoris (RF), M. Semitendinosus (ST), M. Biceps Femoris (BF) and M. Vastus Medialis (VM) as injury-prone muscles in adults as well as in elite youth players (Ekstrand et al. 2011b; Nilsson et al. 2016) were investigated along with knee JRF. Ekstrand et al. (2011b)

reported 3.1 injuries per 1000 match hours for the hamstring muscles and 1.3 injuries/1000 match hours for the quadriceps muscles for an age group of 16-21 y. These are the highest and third-highest incidences of muscle injuries in this age group. Antero-posterior (AP), medio-lateral (ML) and proximo-distal (PD) forces of both knees were determined and normalized to the participants' body weight.

For the analysis, only the contact phases of the outer fields (5-12) were regarded to compare similar motion patterns. The contact phase was defined as the period from 0.6 s before to 0.6 s after the foot's ground contact within the target field. From the contact phase, the peak forces of the parameters mentioned above were analyzed. Furthermore, contact phases were compared for matching field numbers with/without mental stress. Differences in mean peak muscle force and percentage change were calculated between baseline and stress conditions. The peak force of each parameter was determined by averaging the peaks of the particular contact phases. Therefore, within-subject variability is reduced and the effect of possible outliers in one field is minimized.

Statistical Analysis

All statistical tests were performed using the SciPy package (v. 1.2.1) in Python (v. 3.7.6). The results of the running times were tested with a t-test for two related samples, and the effect size was determined with Cohen's d . NASA-TLX results were compared using a two-sided Wilcoxon signed-rank test. The effect size was obtained using Spearman's rank correlation coefficient (r_s). The confidence interval (CI) was calculated for the NASA-TLX parameters, the running time, and the mean difference of the particular muscle forces. The level of significance for all tests was 0.95.

2.3 Results

Stressor evaluation and kinematics

The NASA-TLX identified an effect of the mental stressor. The results specific to the mental demand components of the NASA-TLX supported an association with the condition where players were under mental stress. Specifically, the runs carried out without mental stress (5.8 ± 2.5) were rated less mentally demanding than with stressor (8.5 ± 1.7); $p = 0.006$, $r_s = 0.37$. The mental demand was rated 2.25 points (CI: [1.09, 3.41]) higher on average under mental stress. Physical demand under stress was averagely rated 6.7 ± 2.1 , while the baseline had a mean rating of 6.5 ± 1.7 , showing no significant difference between ratings for physical demand ($p = 0.777$, $r_s = 0.45$). The mean increase in the stress condition was 0.17 (CI: [-0.86, 1.20]). The parameters performance ($p = 0.191$, $r_s = 0.50$), effort ($p = 0.526$, $r_s = 0.56$) and frustration ($p = 0.359$, $r_s = 0.12$) were not rated significantly

different either. The time demand was rated significantly different ($p = 0.039, r_s = 0.77$). Figure 2.3 shows the results from the self-evaluation. Regarding the kinematics, the velocity in runs under mental stress was significantly lower than in the baseline runs ($p < 0.001, d = -1.62$). In terms of time, the players ran on average 35.7 ± 1.8 s in the control condition but 39.9 ± 3.3 s under mental stress. The average running-time increase under mental stress was 4.25 s (CI: [2.94, 5.56]).

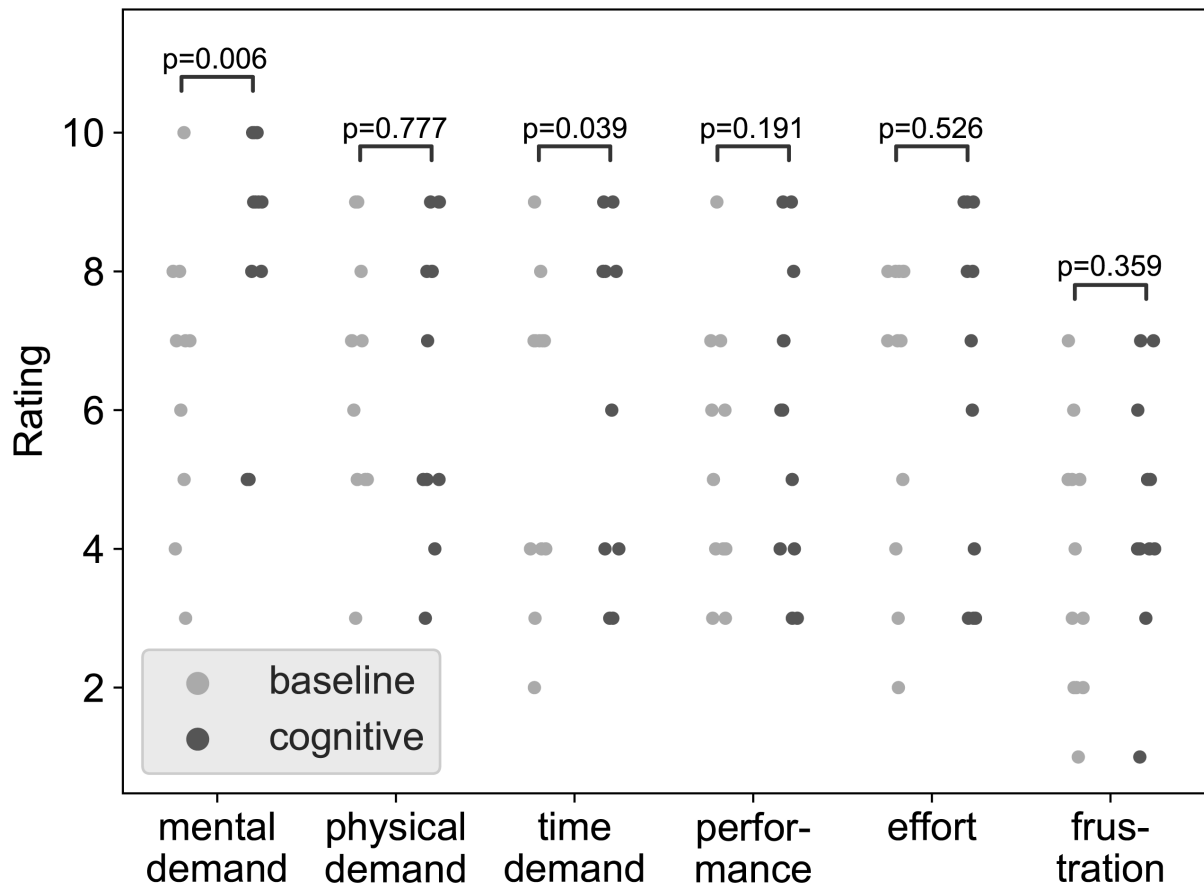


Figure 2.3: Results of the self-evaluation forms. The light grey points represent the feedback after the baseline runs, while the black points are from the stressor runs. The mental demand was rated significantly higher under cognitive stress ($p = 0.006, r_s = 0.37$) with equally rated physical demand ($p = 0.777, r_s = 0.45$).

Musculoskeletal simulation

For the baseline and the mental stressor, 204 simulations were executed, resulting in 408 datasets. Table 2.1 shows the results of the musculoskeletal simulation. If the muscles are viewed separately, a very heterogeneous picture emerges. On the one hand, there are partial differences in the stress reaction between left and right, and on the other hand, there are differences between the individual muscles themselves. The ST on the right side consistently shows reduced muscle force under stress, while it also indicates

Table 2.1: Results of the musculoskeletal simulation for the participants. The investigated muscles were m. RF, m. VM, m. BF and m. ST. The table presents the mean difference between stressor muscle force and baseline and the mean peak loading in the baseline runs in %BW and the relative change. Mean values and CI are reported for the different parameters.

Parameter/Player	1	2	3	4	5	6	7	8	9	10	11	12	\bar{x}, CI		
RF	right	Delta (%BW)	-35	16	23	-12	-36	-32	-20	-13	-48	14	9	-21	-13, [-26, 0]
		Mean (%BW)	171	172	126	204	175	166	280	163	177	153	169	209	180 [160,201]
		rel. change	-20%	9%	18%	-6%	-21%	-19%	-7%	-8%	-27%	9%	5%	-10%	-4% [-12, 4]
	left	Delta (%BW)	-8	71	5	-3	-146	8	-11	-18	65	27	-14	-9	-3 [-32, 27]
		Mean (%BW)	117	140	185	182	290	168	239	200	178	153	221	148	185 [159, 211]
		rel. change	-7%	51%	3%	-2%	-50%	5%	-5%	-9%	37%	18%	-6%	-6%	2 [-11, 16]
VM	right	Delta (%BW)	-24	24	-2	-14	-28	-31	-11	-5	-17	-53	-12	2	-14 [-25, -4]
		Mean (%BW)	148	162	141	135	134	129	166	131	143	199	179	156	152 [143, 162]
		rel. change	-16%	15%	-1%	-10%	-21%	-24%	-7%	-4%	-12%	-27%	-7%	1%	-12% [-17, -7]
	left	Delta (%BW)	-29	87	-7	-10	-40	23	25	-11	64	-6	44	-24	10 [-12, 31]
		Mean (%BW)	160	138	160	137	173	119	142	156	140	176	176	150	152 [143, 162]
		rel. change	-18%	63%	-4%	-7%	-23%	19%	18%	-7%	46%	-3%	25%	-16%	8% [-7, 22]
BF	right	Delta (%BW)	4	-11	-13	-9	-60	-10	-19	-8	-27	4	-55	-17	-18 [-29, -7]
		Mean (%BW)	73	76	89	118	165	107	107	127	183	82	119	71	110 [90,129]
		rel. change	5%	-14%	-15%	-8%	-36%	-9%	-18%	-6%	-15%	5%	-46%	-24%	-15% [-23, -7]
	left	Delta (%BW)	-13	-14	20	33	-19	-11	43	10	-52	-11	-18	-2	-3 [-17, 11]
		Mean (%BW)	109	89	55	93	115	99	122	92	119	93	88	98	98 [88, 107]
		rel. change	-12%	-16%	36%	35%	-17%	-11%	35%	11%	-44%	-12%	-20%	-2%	-1% [-15, 22]
ST	right	Delta (%BW)	-4	-5	-5	-4	-38	-12	-12	-7	-14	-6	-30	-11	-12 [-18, -6]
		Mean (%BW)	46	48	58	62	100	66	54	79	85	51	69	47	64 [55, 73]
		rel. change	-9%	-10%	-9%	-6%	-38%	-18%	-22%	-9%	-16%	-12%	-43%	-23%	-16% [-24, -9]
	left	Delta (%BW)	-4	-7	9	3	-16	-19	3	-2	-19	-17	-7	3	-6 [-11, -1]
		Mean (%BW)	63	48	37	58	69	69	75	61	61	63	49	55	59 [53, 65]
		rel. change	-6%	-15%	24%	5%	-23%	-28%	4%	-3%	-31%	-27%	-14%	5%	-9% [-18, 0]

increased values on the left side. The situation is similar for the ST, which has only a few increased muscle forces on the right side but more on the left. The VM responds similarly. Conversely, this means a more frequent increase in muscle force under stress on the left side. In the RF, the left and right changes are more or less the same, with force increases being higher on the left. The players also show different reactions to mental stressors. For some, this has little or no effect on peak muscle force (04/08). For these players, the percentage changes under stress are relatively small. Meanwhile, other players (05/09) show comparatively frequent high changes in force under mental stress. It can also be seen that the direction of change differs from subject to subject. While for VM, ST and BF muscle forces are almost exclusively reduced under stress, there are increases and decreases to the same extent in the RF.

Table 2.2 shows the mean peak loadings of the parameters for baseline and attention task during the runs. No significant difference is found between the mean baseline and

Table 2.2: Mean peak loadings (%BW) and standard deviations of the investigated knee forces for the two run types.

	Left AP	Left ML	Left PD	Right AP	Right ML	Right PD
Baseline	693±247	109±61	511±195	659±388	101±48	489±284
Stressor	697±286	106±63	472±155	610±209	94±41	457±141

stressor runs ($p < 0.05$). The mental demand lead to equally high knee loadings, with no divergent effect for any parameter. While the knee joint reaction forces appear to be slightly higher on the left side, this effect accounts for both the baseline and the stressor.

2.4 Discussion

Muscle forces in the lower extremities, knee forces and performance under stress were analysed in highly dynamic motion. The collected data shows that running velocity was decreased in football players when subjected to an additional mental stressor. The potential implications of the results may be a reduced performance. Furthermore, this stressor led to a change in muscle force in the lower extremities for almost half of the inspected muscle parameters. Nonetheless, knee forces were not affected and there were some differences in how this impacted specific muscles across individuals.

The athletes' reduced performance can be seen best in a significantly increased running and reaction time, which raises from averagely 35.7 s to 39.9 s (+4.2 s $\hat{=}$ +12%) under mental stress. Only two players were equally fast in both runs. Nevertheless, their rating of mental demand in the NASA-TLX was comparable to the others. This could imply a greater tolerance to stress for some players, although the perception is the same. All other athletes needed longer for the stressor runs. However, this performance drop under stress cannot be seen clearly in the athletes' musculoskeletal loading. Although the low number of players does not allow a common statement, some athletes may be more affected in the extensor muscles RF and VM, and others in the flexor muscles BF and ST. Additionally, one must acknowledge that an individual interpretation of muscle forces can be subject to errors since within-subject-variability influences these results (Atkinson and Batterham 2015). Nevertheless, this is counteracted by averaging the muscle forces over all fields for the individual players. For more sophisticated individual interpretation, adjustments to the study protocol are necessary.

An interesting aspect of the results is that the knee and muscle forces are not lower in general under mental stress, although longer reaction and running times indicate lower velocities. Previous studies stated that the muscle and ground reaction forces are higher

with increasing walking or running speeds (Dorn et al. 2012; Fukuchi et al. 2019; Weinhandl et al. 2017). Conversely, this should mean that the knee, muscle and ground reaction forces are lower under mental stress due to lower running speed. However, the force level under stress is the same as without. A further examination of the center of mass (COM) shows that the velocity in the contact phase is not reduced in general. Thus, lower running speed only occurs between the contact phases and can only explain some of the lower peaks under stress, whereas the majority presumably has different causes. Previous studies on mental stress have shown that changes in kinematics (e.g., longer reaction time or altered movements) can occur under its effects (Higuchi et al. 2002). Marras et al. (2000) and Lundberg et al. (2002) found increased muscle activity under mental stress and even active muscles without physical demand. Higuchi et al. (2002) stated changed movement strategies under stress. Lohse and Sherwood (2012) suggested that an internal focus of attention disrupts efficient motor control. In light of that, the up- and downward fluctuations of the peak muscle force can be induced by a different movement behavior and non-physiological muscle activation in the form of disrupted efficient motor control under mental stress (Swanik et al. 2007). Nevertheless, the players' psychological personality profiles, e.g., introversion/extroversion, thinking/feeling, were not considered in this study. Marras et al. (2000) and Nimbarte et al. (2012) indicate that they influence the players' stress response. Therefore, the players react individually to stress. The muscle force changes, which are listed herein, come exclusively from a change in kinematics since the AMS calculates the forces solely through the kinematic input and cannot create a stress-induced increase of the muscle tone. Previous studies have shown that under stress, there is an increase in muscle tone up to activity without physical necessity (Bloemsaat et al. 2005; Lundberg et al. 2002; Marras et al. 2000; Nimbarte et al. 2012; Srinivasan et al. 2016; Wijsman et al. 2013). Nonetheless, it is challenging to generate an artifact-free electromyography (EMG) signal during such complex and highly dynamic movements. These aspects should be considered in future studies. Furthermore, this study only addresses the contact phases, which excludes information about the rest of the run. However, this is necessary to be able to compare the different contact points.

Since the experimental condition in this study is relatively new, the protocol is subjected to some limitations. Although generally established methods were used, they had to be adjusted to the particular environment. One central point is the complexity of the movements. The randomization of the route in the SpeedCourt has a considerable effect of unequal movement sequences. Thus, every time a field is approached, the direction and speed are slightly different from the second attempt. This makes a simple comparison of the stressor and baseline runs difficult. Nevertheless, each attempt's start and endpoint are the same (middle-outer field), minimizing deviations. By considering the contact phases of ± 0.6 s to the turning point, this deviation is minimized additionally,

and a learning effect for the players is avoided. Besides that, the SpeedCourt system has already been utilized in sports-related studies in the recent past (Achenbach et al. 2019; Bartels et al. 2016; Born et al. 2016; Düking et al. 2016; Zinner et al. 2017). Its application ranges from focusing on using the SpeedCourt system to help identify factors for improving performance and preventing and rehabilitating from injury. Another aspect of limitation is the muscle recruitment algorithm of the AMS. For this study, a quadratic target function for the optimization problem was used for numeric stability, as suggested by other studies (Skals et al. 2017). This algorithm is responsible for the numerical activation of the muscles and, consequently, their exerted force. However, it can only work with the kinematic input from the motion capture and lacks information on real muscle activation since the numerical muscle activation is based on an optimization algorithm. Besides that, it is commonly used for faster movements (David et al. 2017; Sakai et al. 2018), and its validity for these applications has already been investigated (Skals et al. 2017).

To the best of our knowledge, this is the first study that has researched into highly dynamic movements and mental stress using musculoskeletal simulation. On the one hand, the SpeedCourt system has already been used to create game-situation-like motion sequences (Achenbach et al. 2019; Düking et al. 2016). On the other hand, the established musculoskeletal software allows the examination of muscle forces in such movements without the complex equipment of EMG (Damsgaard et al. 2006; Skals et al. 2017). Also, the modified d2 attention test may be a suitable method of inducing mental stress to the test persons. The mental and time demands were rated significantly higher under the influence of the d2 test, while there was no significant difference in physical demand. The other parameters were rated equally as well. Thus, the test only affects mental stress and does not affect perceived physical stress or performance. This study combines established methods to expose players to a mental task while performing highly dynamic movements. However, the combination of these is novel and needs further validation to yield a proper representation of in-game situations in football. In addition to that, the questionnaires have proven to be a practical way of assessing stress. While physiological parameters such as electrodermal activity or heart rate variability are more precise than questionnaires, they lose their validity in physically demanding activities. The inevitable sweating of the test subjects and the varying exposure makes the results of the measurements uninterpretable. Hence, the questionnaire remains a reliable alternative to these tests. Although questionnaires are always answered subjectively, especially in the investigated age group, the self-evaluation forms in combination with the increased running times support the reliability. The details on the NASA-TLX are found in the literature (Hart and Staveland 1988).

Properly managing stress may be an underrepresented aspect for injury prevention in football players so far. Hence, future studies could research into this association and evaluate programs to direct these stressors to avoid motion patterns prone to injury during football activity. For the practical routine in elite junior football, this study shows that a mental stress-inducing task is associated with decreased performance and can change musculoskeletal loading patterns. Additionally, it might imply that mental preparedness for stress situations in players represents a vital role in successful football play and may be considered in training planning for the season.

2.5 Conclusion

This study aimed to analyze the effect of stress on the velocity and muscle forces of athletes. To this end, twelve young competitive athletes were exposed to mental stress during highly dynamic movements. The mental stress task was found to be associated with a lower velocity in a controlled lab environment. Additionally, changes in peak muscle forces were observed. For the first time in football medicine, this data quantifies an association between mental stress with reduced football players' performance and changes in muscle force.

Chapter 3

Implications of different muscle models and recruitment configurations in musculoskeletal models of sprinting movements

Although musculoskeletal models are well tested for a number of applications, there is little information on how they behave in highly dynamic situations. Especially data concerning muscle modeling, muscle recruitment and muscle activation is rare. Consequently, this chapter addresses research question 2: "Does the musculoskeletal model's muscle activity in the lower extremities match the physiological muscle activation in highly dynamic motion, and what's the influence of different muscle modeling options?".

3.1 Introduction

Musculoskeletal simulations have played a vital role in biomechanics research for quite some time. They are used in the field of orthopedics (Benditz et al. 2018; Putzer et al. 2016; Weber et al. 2016), ergonomics (Larsen et al. 2020; Reilly and Kontson 2020) and the recent years, more and more in sports biomechanics (Auer et al. 2021; Dupré et al. 2019; Sakai et al. 2018). Since musculoskeletal models allow a deep insight into the human body, they are valuable tools for detailed research without complex and invasive measurement methods. Nevertheless, model validity is inevitable if parameters such as ground reaction forces, joint reaction forces or muscle activities are researched without additional measurement equipment like force plates or implanted load cells. Hence, musculoskeletal models were a matter of research themselves to prove the reliability of their outputs (Dupré et al. 2019; Karatsidis et al. 2019; Wibawa et al. 2016).

Various parameters influence the models' outputs. First of all, the kinematic is a crucial factor. If the given kinematic model input has insufficient quality the model results are deficient. Optical motion capture (OMC) is often used as kinematic input for these calculations due to its accuracy (Aurang et al. 2017). However, the growing applications of musculoskeletal models in sports biomechanics increased the urge to perform measurements in the field. Hence, inertial motion capture (IMC), has gained importance in recent years because it does not require cameras and can therefore be used nearly anywhere (Karatsidis et al. 2019).

Secondly, kinematic input can be excellent, but the results remain unusable if the musculoskeletal model is misdesigned in terms of boundary conditions. Especially, when ground reaction forces (GRF) and moments are predicted through the model without measuring them with force plates, the boundary conditions need to be set correctly. Karatsidis et al. (2019) evaluated model-predicted GRF and joint angles during gait recorded with OMC and IMC. They had test subjects walk slowly, normal and fast and investigated the correlation of the predicted and measured GRF and the correlation of sagittal plane joint angles of ankle, knee and hip of IMC- and OMC-driven models. They determined a Pearson correlation of $0.80 \leq \rho \leq 0.97$ for the predicted GRF and $0.95 \leq \rho \leq 0.99$ for the ankle, knee and hip joint angles with an IMC-driven musculoskeletal model.

Additionally, the model's accuracy depends on its anatomy. The calculated parameters strongly rely on the implemented model geometry e.g. in terms of muscle wrapping. Wibawa et al. (2016) compared measured muscle activity (MMA) from the leg to calculated muscle activity (CMA) for walking, forward hopping and side jumping. They used an optical motion capture system, including force plates, to produce kinematic and kinetic input for the musculoskeletal model. They found visually comparable activity patterns. However, their Pearson correlation coefficients ranged from -0.25 to 0.82 over all movements. Another study on CMA and MMA in the thigh has found a higher correlation. Dupré et al. (2019) found a strong correlation between CMA and MMA for sprinting and running, while the correlation decreased for side-cutting manoeuvres. Their mean ρ ranged from 0.57 for cutting manoeuvres to 0.81 for walking. They determined $-0.42 \leq \rho \leq 0.96$ for the investigated thigh and shank muscles for sprinting.

In addition to the type of kinematic input and model geometry, CMA is dependent on the model configuration. The most common configuration for the motion capture models of the AnyBody Modeling System (AMS) is a simple muscle model, where the muscle activity is dependent solely on the physiological cross-sectional area (PCSA) and a scaling factor. For the muscle recruitment optimization problem, a target function with a quadratic exponent is the preset choice. However, the AMS also features three-element Hill-type muscle models, where passive properties of the muscles are taken into account. Furthermore, the optimization problem has different target functions, though their effect in complex movements is poorly investigated.

IMC-driven musculoskeletal models have been investigated in the past and reproduce valid results regarding predicted GRF and joint kinematics. Furthermore, these models show a good agreement of MMA and CMA with OMC-input. However, to the authors' best knowledge, there are no investigations on the agreement of MMA and CMA when IMC is used as kinematic input, especially in dynamic movements like sprinting. Hence, IMC is a valid kinematic input for many model aspects but needs further investigation. Furthermore, although the anatomy does not change in highly dynamic situations, the physiological muscle recruitment differs (Higashihara et al. 2010). Additionally, the influence of different muscle recruitment criteria on muscle activity in dynamic musculoskeletal simulations is currently unknown. Thus, this study aimed to analyze the agreement of numerical and measured muscle activity in dynamic movements using GRF prediction and IMC as well as the effect of different muscle recruitment criteria and muscle models on the numerical muscle activity.

3.2 Materials and Methods

For this study, 20 test subjects (all male) with a mean age of 26.0 ± 3.7 y were recruited and granted informed consent. The average height was 1.82 ± 0.06 m, and the mean weight was 80.6 ± 8.2 kg. Exclusion criteria were chronic musculoskeletal diseases or acute injuries to the lower limbs in the last three months before the study. However, data from all participants could be included in the evaluation. The procedures performed in this study were in accordance with the 1964 Helsinki Declaration and its later amendments or comparable ethical standards.

3.2.1 Experimental setup

After an individual warm-up, the subjects conducted three different tasks. Firstly, they executed five knee flexion (prone, 0° - 90°) and extension (sitting, 90° - 0°) movements for the left and right leg at an audio signal as fast as possible (Figure 3.1). Afterwards, they performed five sprints of 10 m on artificial turf resulting in a total running distance of 50 m. The turning points were marked as solid lines on the ground, which had to be crossed before turning by 180° . Motion was captured at 240 Hz using 17 IMC sensors (MVN Link, Xsens Technologies B.V., NL) for a full-body setup. Simultaneously, ten surface-electromyography (EMG) sensors (Trigno IM, Delsys Inc., USA) measured muscle activity of five thigh muscles on each thigh at 1111 Hz. These muscles were Rectus Femoris (RF), Vastus Medialis (VM), Vastus Lateralis (VL), Biceps Femoris (BF) and Semitendinosus (ST).



Figure 3.1: Experimental setup for flexion (top) and extension movements. Left side describes the initial and right side the maximum position.

3.2.2 Musculoskeletal modeling

The motion capture data served as input for the simulation of the flexion/extension movements and the sprints with musculoskeletal modelling software (AMS v. 7.3.3, AnyBody Technology, DK). For this study, the pre-configured model from the AnyBody Managed Model Repository (AMMR) (v.2.3.4, Lund et al. (2021)) with IMC-input was chosen since this is the most commonly used configuration for this kind of musculoskeletal analysis. The inverse dynamics software uses an algorithm to calculate internal and external forces, including muscle activities. Details on the AMS muscle recruitment can be found in section 1.4.

For this study, two different approaches for the formulation of the optimization problem's target function are selected. On the one hand a quadratic polynomial target function (Equation 1.4) was chosen, since it is the pre-defined configuration for IMC-driven musculoskeletal models in the AMS. Another pre-defined configuration for muscle recruitment in the AMS is the increase of power in the target function. In order to improve the synergy between muscles, the power of the term can be increased, and an infinite exponent reaches maximum synergy. However, numerically this would lead to very hard on- and offsets of muscle activity, which is not physiological, since human muscles cannot apply forces immediately. Therefore, a quadratic term as in Equation 1.4 is added to the infinite-power. Now, the target function represents the two energy-consuming processes of muscle contraction and creates softer on- and offsets of muscle activities (Praagman et al. 2003; Praagman et al. 2006). The optimization problem is now formulated as in Equation 1.5 and serves as second option for the muscle recruitment's target function. Due to the combination of a term with an infinite power polynomial and a quadratic term in the target function, this muscle recruitment criterion is also called "composite muscle recruitment".

Further on, two different muscle models were used in the musculoskeletal models. The simple muscle model calculates the muscle force only through a scaling factor (SI) and the PCSA:

$$F_M = SI * PCSA \quad (3.1)$$

Furthermore, a three-element Hill-type muscle model was used for the simulations, where the muscle force depends on the active properties of the muscle fibres (F_{CE}), the elasticity of the tendon (F_T) and also the passive stiffness of the muscle fibres (F_{PE}):

$$F_M = F_{CE} + F_{PE} + F_T \quad (3.2)$$

A schematic view of the mechanical properties is shown in Figure 1.8. The passive properties of the Hill-type muscle model are determined in a calibration sequence before the actual inverse dynamics calculation. For this study, the pre-defined calibration sequence of the AMS was used since this is the most common workflow (Lund et al. 2021). It uses pre-defined joint angles of each joint and calculates the passive fiber length of each muscle of the respective joints.

With the two different muscle models and the two different target functions for the muscle recruitment, there are four possible configurations for the calculations of CMA: a simple muscle model with a quadratic target function for the muscle recruitment (S2), a simple muscle model with composite target function (SC), a Hill-type muscle model with quadratic muscle target function (H2) and a Hill-type muscle model with composite target function (HC). An overview of the four different configurations is shown in Table 3.1.

Table 3.1: Overview of the different configurations regarding the calculation of muscle forces (muscle model) and the target function of the muscle recruitment minimization problem.

	S2	SC	H2	HC
Muscle model:	$F_M = SI * PCSA$	$F_M = SI * PCSA$	$F_M = F_{CE} + F_{PE} + F_T$	$F_M = F_{CE} + F_{PE} + F_T$
Muscle recruitment:	$G = \sum_i \left(\frac{f_i}{N_i}\right)^2$	$G = \beta + \epsilon * \sum_i \left(\frac{f_i}{N_i}\right)^2$	$G = \sum_i \left(\frac{f_i}{N_i}\right)^2$	$G = \beta + \epsilon * \sum_i \left(\frac{f_i}{N_i}\right)^2$

3.2.3 Data processing

Raw EMG data was filtered with a second-order bandpass Butterworth filter with 10 Hz and 500 Hz cut-off frequencies. Additionally, the linear envelope of the EMG data was formed with a fourth-order low-pass Butterworth filter with a cut-off frequency of 6 Hz. Finally, to account for the electromechanical delay (EMD) between the onset of muscle activation and the onset of muscle force, the linear envelope of the EMG data was right-shifted by 40 ms (Zhou et al. 1995).

Motion Capture data was filtered with a 12.5 Hz cut-off frequency second-order low-pass Butterworth filter before being loaded into the musculoskeletal model. For the sprint analysis, the second sprint-cycle of each of the 10 m runs was taken from right heel strike to right heel strike to minimize effects of the turning points and analyze the movement at its highest velocity. Additionally, time steps where none of the feet had ground contact in the musculoskeletal model were removed to avoid an influence of human-ground-residuals (HGR) on the muscle activity. These five trials per subject were normalized to the maximum activity in the measured and calculated data, respectively. Afterwards, the mean curve from the five trials was created for MMA as well as CMA.

In order to compare MMA and CMA, the Pearson correlation coefficient ρ and the root mean square error (RMSE) of the mean curves was determined. The Pearson correlation coefficient was interpreted according to Cohen (1988), where $\rho \leq 0.29$ should be considered as low correlation, $0.30 \leq \rho \leq 0.49$ as moderate correlation $0.50 \leq \rho$ as strong correlation. In addition to determining the Pearson correlation coefficient, MMA and CMA of sprinting was analyzed using statistical parametric mapping (SPM) (Pataky 2012), where the recorded curves were tested for statistically significant differences over their course using random field theory (Friston 2006). Furthermore, the sprint curves were compared using dynamic time warping distance (DTWD) (Keogh and Ratanamahatana 2005). The analyses were performed using Python (v. 3.7.6) with the scipy (v. 1.7.2), spm1d (v. 0.4.0) and dtadistance (v. 2.3.2) packages. The level of confidence for all statistical tests was 0.95.

3.3 Results

With five periods for each kinematic setting, 20 test subjects and four different muscle recruitment/configuration scenarios, 400 musculoskeletal simulations have been run for every kinematic setting. All three kinematic settings thus include 800 datasets for each muscle and, since the left and right leg muscle activity is investigated.

3.3.1 Flexion and extension tasks

Table 3.2 shows the overall flexion/extension results of the Pearson correlation analysis of the different muscle configurations summarized for all muscles. All muscle configurations and recruitment types bear a strong mean correlation with Hill-type muscles performing slightly better than simple muscles.

Table 3.2: Mean ρ , standard deviation and the 95% confidence interval (CI) for the different flexion and extension scenarios. BF and ST were analyzed for flexion and RF, VM and VL for extension.

	S2	SC	H2	HC
Mean $\rho \pm \text{STD}$	0.57 \pm 0.16	0.57 \pm 0.16	0.61 \pm 0.16	0.61 \pm 0.16
[CI]	[0.54, 0.59]	[0.54, 0.59]	[0.59, 0.64]	[0.59, 0.64]

When the muscles are considered individually, there is no noticeable difference between them. Not even between flexion and extension muscles. Although the correlation is slightly higher overall for the VM and VL flexors, the differences are within the range of the standard deviation.

3.3.2 Sprinting tasks

The overall results of the Pearson correlation for all scenarios are depicted in Table 3.3. The overall results show a strong correlation for the S2 and SC scenarios and a moderate one for the H2 and HC scenarios. Additionally, the different muscle recruitment types do not yield remarkable differences in median ρ or the confidence interval (CI).

Table 3.3: Median ρ and the 95% CI for the different scenarios of sprinting. Median values were taken due to the non-normal distribution of ρ -values.

	S2	SC	H2	HC
Median ρ	0.57	0.57	0.45	0.45
[CI]	[0.52, 0.61]	[0.52, 0.61]	[0.40, 0.49]	[0.40, 0.49]

However, the particular correlations are different for the investigated muscles (Figure 3.3). For example, the highest correlation of median [CI] $\rho = 0.68$ [0.58, 0.79] can be

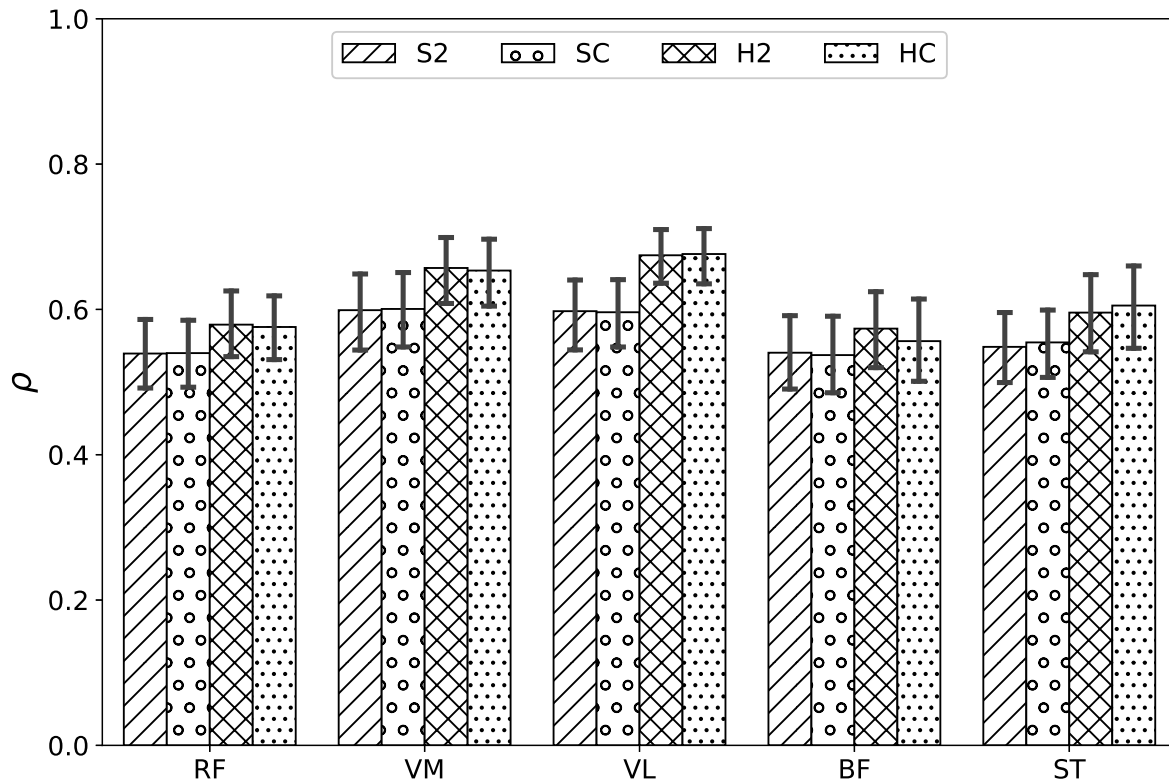


Figure 3.2: Results of the Pearson correlation analysis for the flexion/extension tasks. The chart is grouped by muscle, and the different bars represent the median ρ and the confidence interval (CI) of the muscle for the four configurations S2, SC, H2 and HC.

found in the ST muscles for both S2 and SC. On the other hand, the lowest correlation is found in the RF muscles for the S2 and SC scenarios with a median [CI] ρ of 0.27 [0.19, 0.35], meaning a low correlation of MMA and CMA.

The DTWD analysis in Table 3.4 shows that the distance between MMA and CMA is bigger for the H2 and HC scenario. At the same time, there is only a small difference between the two different muscle recruitment criteria.

Table 3.4: Median DTWD and the 95% CI for the different scenarios of the sprinting tasks. Median values were taken due to the non-normal distribution of DTWD-values.

	S2	SC	H2	HC
Median DTWD	1.18	1.19	1.38	1.38
[CI]	[1.09, 1.28]	[1.10, 1.29]	[1.27, 1.49]	[1.27, 1.49]

An exemplary result of the SPM analysis is shown in Figure 3.4. The SPM revealed that CMA and CMA are not significantly different over most of the course. Lower correlation coefficients show more different ranges than high ones. However, in all data sets, the areas of difference are limited to rather small sections, so that no statistically significant difference can be established for a predominant part of the muscle activity.

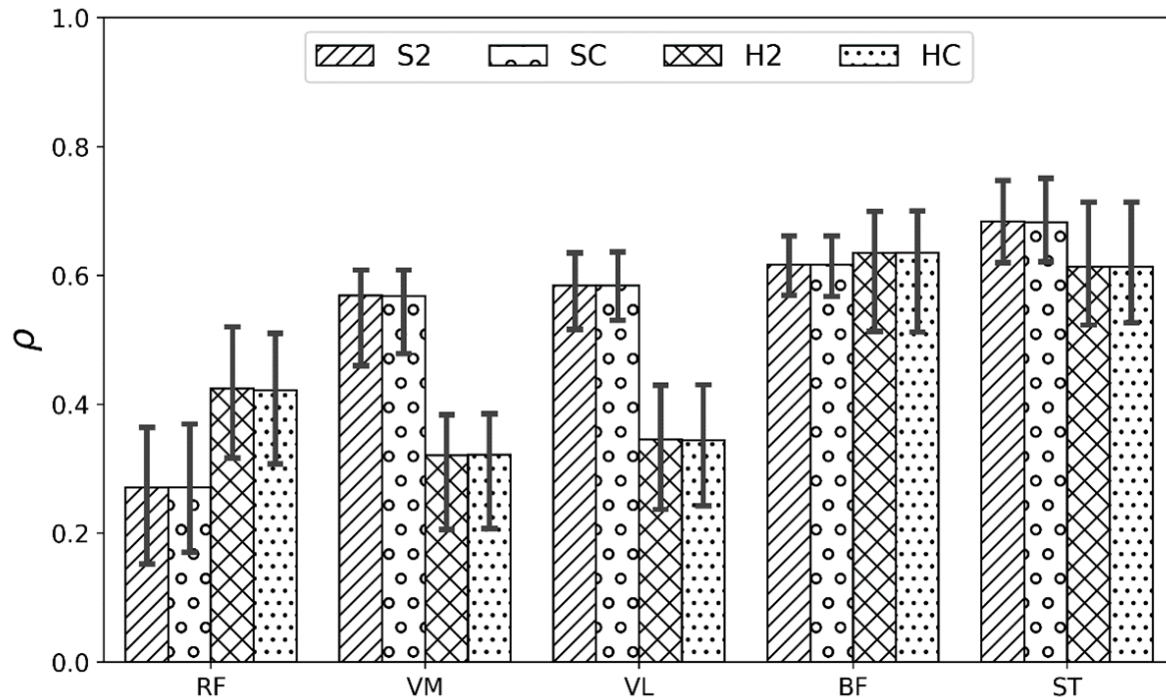


Figure 3.3: Results of the Pearson correlation analysis for sprinting. The chart is grouped by muscle, and the different bars represent the median ρ and the CI of the muscle for the four configurations S2, SC, H2 and HC.

Since the S2 scenario is the default configuration and often used, the MMA and CMA graphs of all subjects for the S2 sprinting scenarios can be found in Appendix A.

3.4 Discussion

The study aimed to analyze the effect of different muscle recruitment criteria and muscle models on the correlation of numerical and measured muscle activity in dynamic movements using GRF prediction and IMC. The Pearson correlation reveals a strong correlation for flexion/extension tasks and an overall moderate to strong correlation of MMA and CMA for sprinting tasks. However, in sprinting tasks, except for RF and BF, the simple muscle model produces a higher correlation of MMA and CMA. In the flexion/extension tasks, the Hill-type muscle model's correlation is slightly higher than the simple muscles' correlation. No noticeable difference was found between the different muscle recruitment criteria.

MMA and CMA agree the most in extension for VL when a Hill-type muscle model is used with $\rho = 0.68 \pm 0.12$. Although the overall level of agreement is higher for Hill-type muscles, the differences between the muscles models is within the standard deviation. The correlation of the individual muscles ranges from $\rho = 0.54$ to $\rho = 0.68$ over all muscle types and recruitment criteria, hence the individual muscles are on a comparable level regardless of the model configuration.

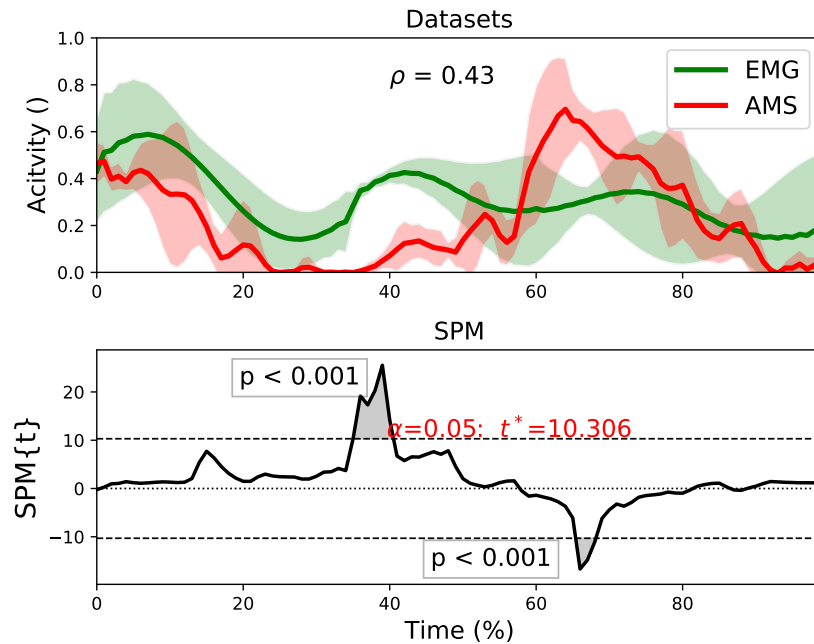


Figure 3.4: Exemplary result of a univariate SPM analysis for one muscle-dataset of one subject with $\rho=0.43$. The upper part describes the MMA in green and the CMA in red as mean curve with standard deviation for the five recordings for each muscle. The bottom part represents the corresponding SPM results. Sections, where statistically significant differences between MMA and CMA were detected, are marked gray with corresponding p-values.

In sprinting, ST bears the best correlation of MMA and CMA with $\rho = 0.68$ [0.58, 0.79] for S2 and SC. The second best-correlating muscle is the BF with $\rho = 0.64$ [0.53, 0.74] for the HC scenario. Overall, the flexor muscles have a higher correlation than the extensor muscles regardless of muscle or recruitment type, which is stronger when the Hill-type muscle model is used. This leads to the conclusion, that the muscle wrapping in the AMS is represented better for knee flexor muscles and therefore leading to higher correlations. Since the Hill-type muscle model requires a calibration sequence to determine the passive properties of the muscle, this calibration sequence influences the CMA.

It is noticeable that the correlation for the Hill-type muscle model for extension only is at a similar level to the correlation for simple muscles, whereas for extensions in sprints the Hill-type correlation is much lower. In flexion, whether sprinting or isolated, the difference is not as pronounced. This may be due to the fact that the pure flexion/extension movements are much more controlled and isolated with regard to the application of force by the muscles. As a result, physiological parameters of the Hill-model that are inadequately estimated by the model may not have such a strong effect on the CMA. In particular, inaccurate parameters can lead to deviations in the anterior thigh muscles, which are not pure flexors but are also responsible to a certain extent for internal/external rotation and knee stabilization.

The different muscle recruitment criteria of the AMS have little to no influence on the CMA. Regardless of muscle model or location, the difference in correlation is minimal because the flexor and extensor muscles are not fully loaded during sprinting or flexion/extension. Hence, there is no need for further synergy, which the composite muscle recruitment criterion would provide. Furthermore, the results from the DTWD analysis are consistent with the Pearson correlation. The DTWD in the simple muscle model scenarios is considerably lower than in the Hill-type muscle model scenarios.

Although only a few other studies are investigating MMA and CMA in dynamic movements, the results of this study's correlation analysis are comparable to the results from the literature. Dupré et al. (2019) investigated the agreement of MMA and CMA for running as well. They found a strong correlation for VM ($\rho = 0.93$), VL ($\rho = 0.92$), and negative correlation of BF ($\rho = -0.59$). However, they used a different model of the AMMR with a knee that has more degrees of freedom (DOF). This might explain the higher Pearson correlation.

Another study performed by Wibawa et al. (2016), also using optical motion capture and measured GRF, investigated muscle activity of EMG and musculoskeletal models in one-legged forward hopping and side jumping. They also found a moderate to strong correlation between MMA and CMA for the thigh muscles. They calculated the Pearson correlation of $\rho = 0.25$ for the RF, 0.68 (VM), 0.69 (VL), 0.51 (BF) and $\rho = 0.41$ (ST) for forward hopping. For side jumping they calculated $\rho = 0.41$ (RF), $\rho = 0.81$ (VM), $\rho = 0.82$ (VL), $\rho = 0.31$ (BF) and $\rho = 0.31$ (ST). The different movements might explain the higher correlation in VM and VL combined with a lower correlation in BF and ST.

However, some limitations have to be taken into consideration. First of all, the knee joint in the standard model of the AMMR is modeled as a hinge joint, allowing only flexion/extension movements and neglecting rotation and abduction/adduction. This simplification might lead to a change in numerical muscle activation since only flexion/extension movements are possible, and the activity of muscles that participate in rotation or abduction/adduction may be underrepresented. Although the effect of missing degrees of freedom cannot be avoided totally, the chosen muscles are mainly responsible for flexion/extension movements, which minimizes this effect.

The usage of a general EMD also bears some limitations. CMA and MMA's optical investigation often shows similar characteristics of peaks and valleys, but they seem to be shifted on the x-axis. For many individual curves, the x-shift is mainly eliminated by considering the EMD. Although some x-shifts remain when using a constant EMD for all muscles and subjects, most of the curves fit well. The determination of individual EMD would only provide minor improvements. However, neither Pearson correlation analysis nor SPM take into account time shifts between curves. Anyway, the DTWD analysis confirms the results of the Pearson correlation with a smaller DTWD for scenarios with a higher ρ .

Nevertheless, the results only allow conclusions about the curves' shape due to the normalization of signals to the maximum value. Hence, when analysing CMA's absolute height, e.g. maximum voluntary contraction (Konrad 2005), tests or other methods to quantify muscle activity have to be performed.

The results imply that inertial motion capture as kinematic input for musculoskeletal models is suited for calculating thigh muscle activities in sprinting movements. The moderate to strong correlation between the thigh muscles' MMA and CMA lead to this conclusion. In addition, the SPM showed that even at low to moderate correlations, there were no statistically significant differences for the predominant range of MMA and CMA. Thus, when the results of the SPM are considered in addition to the correlation, we find a high level of agreement between MMA and CMA. However, not all muscles perform equally. For example, in this study, BF and ST had the highest ρ during sprinting, while VM and VL had the highest ρ in the study of Wibawa et al. (2016) during side and forward jumping. This circumstance suggests that the correlation of the individual muscles' MMA and CMA depends on the movement itself. This is supported by the fact that muscle wrapping plays a crucial role in numerical muscle activation (Vondrák et al. 2006). The muscle wrapping is dependent on the chosen musculoskeletal model. The Twente Lower Extremity Model (Pieri et al. 2018), the default model configuration for the lower extremities of the AMS, was used, while other studies used lower extremity models with, e.g. more degrees of freedom to the knee (Dupré et al. 2019). However, this study aimed to investigate the most common configuration to draw conclusions for the general application of the model.

Additionally, this study showed that one could use GRF prediction for highly dynamic movements to calculate reliable muscle activities. Although the GRF prediction itself has already been proven to be valid, even for highly dynamic situations (Skals et al. 2017), the influence on CMA when using this method had been investigated. Although the peak correlation between CMA and MMA is not as high as in musculoskeletal simulations using measured GRF, the overall ρ is in the same range (Dupré et al. 2019; Wibawa et al. 2016).

With the increasing use of GRF prediction and the rise in studies of highly dynamic motions, many simulations were using quadratic muscle recruitment (Dupré et al. 2019; Skals et al. 2017). Although only flexion/extension tasks and sprinting movements have been investigated in this study, other studies have shown the validity of quadratic muscle recruitment for various activities (Andersen 2018). Moreover, this study showed that this recruitment type is suitable for fast movements and has no drawback compared to supposedly more dedicated composite muscle recruitment types.

3.5 Conclusion

The study aimed to analyze the effect of different muscle recruitment criteria and muscle models on the correlation of numerical and measured muscle activity in dynamic movements using GRF prediction and IMC. The Pearson correlation reveals an overall moderate to strong correlation of MMA and CMA. Except for RF and BF, the simple muscle model produces a higher correlation of MMA and CMA. Additionally, the simple muscle model proved to be a reliable muscle model for sprinting simulations. Furthermore, the quadratic muscle recruitment did not show any disadvantages in the correlation between MMA and CMA. Altogether, the study shows that IMC as kinematic input and the usage of GRF prediction is suitable for calculating thigh muscle activities in sprinting movements. Moreover, the most common configuration of the AMS models produces reliable results of CMA.

Chapter 4

Addressing Human-Ground-Residuals in dynamic musculoskeletal simulation

Preliminary tests have shown that residual forces can occur to a considerable degree in highly dynamic motions. Therefore, further investigation into the characteristics of residual forces in highly dynamic motions is warranted. Hence, this chapter deals with research question 3: "When and to what extent do HGR occur in simulations of highly dynamic motions and how can their occurrence be influenced?"

4.1 Introduction

The fields of application for musculoskeletal models has widened in the last years. After initially (and still) being used in orthopaedics and ergonomics (Benditz et al. 2018; Larsen et al. 2020), these models have gradually found broader use. Nowadays, it is common to utilize musculoskeletal software, such as the AnyBody Modeling System (AMS), also in sports biomechanics (David et al. 2017; Dupré et al. 2019). However, musculoskeletal models are sensitive to the given kinematics and the modeled boundary conditions. Since none of the models is a perfect representation of the real person and motion capture also involves some inaccuracy, the models include forces acting on the hip to balance the deviations. These forces are often referred to as "human-ground-residuals (HGR)". Although artificial forces like the HGR are necessary for numerical stability, they effect the actual results of the musculoskeletal simulations and have to be monitored closely. If the HGR are too high, the computations become questionable as they can be considered as a reference value for the realistic representation of the actual movement and boundary conditions in the model. Usually, these forces are rather small and they should not exceed 5% of the "net external force" (Hicks et al. 2015).

Mayo and Ojeda (2020) investigated HGR in gait using calculated ground reaction forces (GRF). They used two different methods to perform the inverse dynamics calculations including estimated GRF, which were compared with measured ones. They found average HGR up to 69 %BW in vertical direction but also up to 64 %BW in the transversal plane. Pallarès-López et al. (2019) introduced a new residual reduction procedure and compared it to OpenSim’s existing residual reduction algorithm (RRA). For this purpose, they recorded kinematics of 6 subjects performing single leg triple hops and performed an inverse dynamics analysis. In order to minimize the HGR they implemented the recorded kinematics into an optimization algorithm with the HGR as constraints. Although they were able to reduce the HGR by over 98%, performing an optimization at each step of the inverse dynamics calculation is timely and computationally consuming, which limits its use. Faber et al. (2018) experienced vertical HGR of over 30 %BW for normal walking. They managed to completely eliminate the HGR without even considering them as balancing forces by optimizing marker and joint positions as well as the segments’ centers of mass. However, their approach is limited to the use of measured GRF and normal walking and also used a two-dimensional inverse dynamics model instead of a three-dimensional.

Obviously, the studies on HGR are rare, especially concerning the AMS. Hence, it is the aim of this study to approach HGR by investigating their occurrences in dynamic motion and find a way to minimize these artificial forces in the musculoskeletal models. In particular, dynamic motions, where the model temporarily has no ground contact are investigated. Furthermore, several HGR-optimization approaches are evaluated to determine the occurrence of these forces for different kinematic inputs.

4.2 Materials and Methods

4.2.1 Data acquisition

For this study, the kinematics of one test subject were recorded. The male subject (28 y, 1.86 m, 83.3 kg) performed a squat jump on two force plates (3D Force Plate 9260, Kistler Instrumente GmbH, Germany). Kinematics were recorded at 240 Hz using optical motion capture cameras (Vicon Vero v. 2.2, Vicon Motion Systems, UK) as well as inertial motion capture sensors (MVN Link, Xsens Technologies B.V., NL) in order to investigate the influences of the type of kinematic data collection. The force plates measured the GRF at 960 Hz. The kinetic and kinematic recordings were synchronized to match the timestamps.

4.2.2 Musculoskeletal modeling

Kinematic and kinetic data served as input for the AMS (v.7.3). Three different models were adapted from the AnyBody Managed Model Repository (AMMR):

- kinematic input from optical motion capture and kinetic data from the force plates (=OM),
- kinematic input from optical motion capture and ground reaction force prediction (GRFP) (=OP),
- kinematic input from inertial motion capture and GRFP (=IP).

Since the HGR were expected to be the highest, when there was no contact of the model's feet with the ground or right before losing/regaining contact, the jumps were analyzed from 1 s before to 1 s after the no-ground-contact period.

4.2.3 HGR reduction

Since the GRFP and the HGR are strongly related in the AMS and the segment mass distribution as well as the kinematics are known to influence the HGR (Ojeda et al. 2016), these model properties are assessed in the optimization process as well as the cut-off frequency of the kinematic filter.

The OP and IP models were optimized regarding the detection height and velocity of the GRFP and the segment mass distribution. Furthermore, the segment mass distribution of the IP model is optimized. Table 4.1 gives an overview of the pursued minimization approaches. Two different optimization methods are used for all approaches. In preliminary investigations, a gradient-based minimization algorithm with a sequential least squares programming solver is applied. Since this procedure did not produce a solution differing from the initial guess, a stochastic approach is introduced for this study. The "*differential evolution*" from Storn and Price (1997) is a heuristic method to minimize continuous functions. All optimization procedures were conducted using Python (v.3.7.6) with the *anypytools* package (v.1.6.0) and the *scipy* package (v.1.7.2). Exemplary Python code for the optimization procedures of segment masses and GRFP can be found in Appendix B.

Table 4.1: Overview of the HGR minimization approaches that have been applied to the different model configurations. Details on the exact application of the approaches are described in the following paragraphs.

Adjustments/model type	OM	OP	IP
filter cut-off frequency	7.5 Hz, 12.5 Hz	7.5 Hz, 12.5 Hz	5 Hz, 7.5 Hz, 12.5 Hz
GRFP parameters	no	detection height, max velocity	detection height, max velocity
segment mass distribution	no	no	thorax, lower body

Optimization of the GRFP parameters

The main parameters influencing the GRFP are the thresholds for the detection height and maximum velocity of the contact nodes. These limits define the range in which a potential ground contact is detected. Hence, these two parameters were modified to minimize the HGR. The bounds were set to height=0.005...0.3 m and velocity=0.1...15 $\frac{m}{s}$. The velocity's initial guess was set to the default value of the AMS (=0.8 $\frac{m}{s}$) while the height was chosen manually to create a reasonable on- and offset of the GRFP in accordance with the Xsens ground contact detection. Hence, the height limit was set to 0.35 m. In order to account for the actual ground contact determined by the force plates or the motion capture system, a weighted penalty term adding the absolute difference in contact time was included to the target function.

Optimization of the segment mass distribution

Since the mass distribution of the AMS is based on cadaver studies and the distribution is known to influence the HGR it was subject of another optimization approach. The individual segment masses of all model segments excluding the head and arms were optimized within boundaries of $\pm 25\%$ to their default configuration in the AMS which served as initial guess. The range and initial guess are shown in Table 4.2. Furthermore, the minimization problem was subjected to the constraint that the overall change of mass must be $< 5\%$.

Kinematic data filtering

The kinematic data is known to have great influence on the HGR (Hicks et al. 2015). While others propose optimizing the joint angles at every time step of the kinematic data, here a more general approach is presented by adjusting the cut-off frequency of the musculoskeletal model's kinematic filter. As 12.5 Hz were proposed by Winter (2009) for dynamic motions, 12.5 Hz, 7.5 Hz and 5 Hz were chosen as options for the cut-off frequency. This ensures the comparison of an established frequency as well as stronger kinematic smoothing with the lower ones.

4.2.4 Data processing

In order to compare the different optimization methods to the default model, the HGR and GRF were analyzed. Maximum occurring HGR value over the analyzed time slot was considered in its own as well as in relation to the maximum occurring GRF as *net external force*. All forces were normalized to the subject's body weight.

4.3 Results

In total 11 different model configurations were examined regarding their maximum GRF and their maximum HGR. The force plates measured maximum GRF of 238 %BW during the landing phase of the counter-movement jump. When the OM models (Figure 4.1) were run with a kinematic filter's cut-off frequency of 12.5 Hz, the maximum HGR are at 62 %BW. This results in a share of 26.1% of HGR of the GRF as net external force. When the filter's cut-off frequency is set to 7.5 Hz, the HGR are reduced to 45 %BW (18.9% net external force).

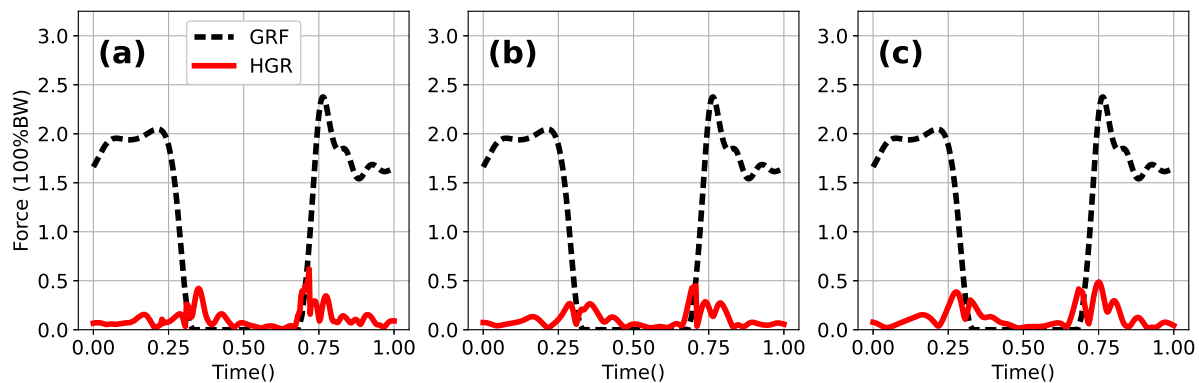


Figure 4.1: Results of the HGR minimization for the OM models. (a) 12.5 Hz cut-off frequency for the kinematic filter, (b) 7.5 Hz cut-off frequency for the kinematic filter, (c) 5 Hz cut-off frequency for the kinematic filter.

Figure 4.2 depicts the GRF and HGR results for the OP models. The baseline model with a kinematic filter cut-off frequency of 12.5 Hz calculates maximum GRF of 256 %BW and maximum HGR of 42 %BW, resulting in a HGR-share of 16.4%. Using a cut-off frequency of 7.5 Hz reduces the maximum GRF and HGR to 235 %BW and 29 %BW, respectively (12.3% net external force). When, in addition to a lower cut-off frequency, the GRFP detection height and velocity are optimized, the maximum HGR go down to 27 %BW (11.5% net external force).

For the IP models three different cut-off frequencies are compared (Figure 4.3 a-c) in addition to the optimization of segment mass distribution and GRFP settings (Figure 4.3 d-f). Initially, with a cut-off frequency of 12.5 Hz, the maximum GRF are 275 %BW with the HGR being 37 %BW (13.5% net external force). A cut-off frequency of the kinematic filter of 7.5 Hz sets the maximum GRF to 246 %BW and the HGR to 27 %BW (11.0% net external force). Lowering the cut-off frequency to 5 Hz reduces the maximum GRF to 225 %BW and raises the HGR to 39 %BW (17.3% net external force). When the segment mass distribution is optimized (Table 4.2), the HGR/GRF ratio goes down to 12.9%, however the maximum GRF and HGR rise to 319 %BW and 41 %BW respectively. The optimization of the GRFP alone does not yield any changes in maxi-

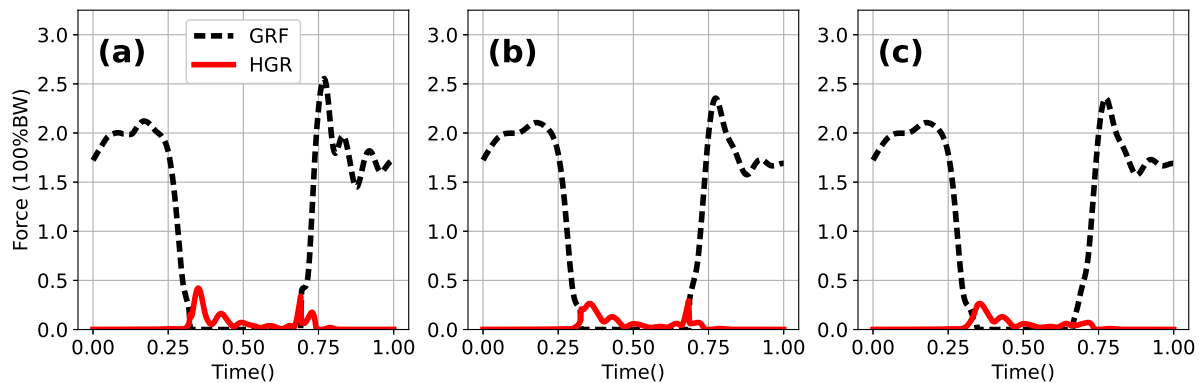


Figure 4.2: Results of the HGR minimization for the OP models. (a) 12.5 Hz cut-off frequency for the kinematic filter, (b) 7.5 Hz cut-off frequency for the kinematic filter, (c) 7.5 Hz cut-off frequency for the kinematic filter and optimized GRFP settings.

Table 4.2: Default and optimized relative segment mass distribution of the AMS.

segment masses	thorax	lumbar	pelvis	thigh	shank	foot
default	19%	14%	14%	10%	5%	2%
optimized	17%	23%	17%	12%	6%	2%

imum HGR or GRF compared to the original model. However, when the kinematic filter’s cut-off frequency is set to 5 Hz, the optimization of the GRFP brings the HGR down to 17 %BW, resulting in a share of 7.6% at 225 %BW maximum GRF.

4.4 Discussion

The aim of the study was to investigate and minimize the HGR musculoskeletal simulations of dynamic movements. Consequently, a counter-movement jump of one subject was simulated with the AMS for different model configurations. In general, the investigation has shown that in a jump simulation with measured GRF, HGR of up to 62 %BW can occur, which corresponds to a proportion of 26.1% of the net external force. When the GRF are calculated, 37 %BW HGR occur at the peak at 12.5 Hz cut-off frequency of the kinematic filter. Regardless of the kinematic input, a reduction of the cut-off frequency also leads to a decrease of the maximum HGR. Additionally, an optimization study for the GRFP settings can help to reduce the HGR even more.

The investigation found HGR that ranged from 37 %BW to 62 %BW without any optimization approaches. This is in accordance with literature data, that determined HGR of 30 %BW (Faber et al. 2018) and 69 %BW (Mayo and Ojeda 2020) for gait. The maximum reduction of HGR was achieved for the IP models, where HGR were reduced by 54% from 36 %BW to 17 %BW by decreasing the kinematic filter cut-off frequency in combination with an optimization of GRFP settings. However, Pallarès-López et al. (2019)

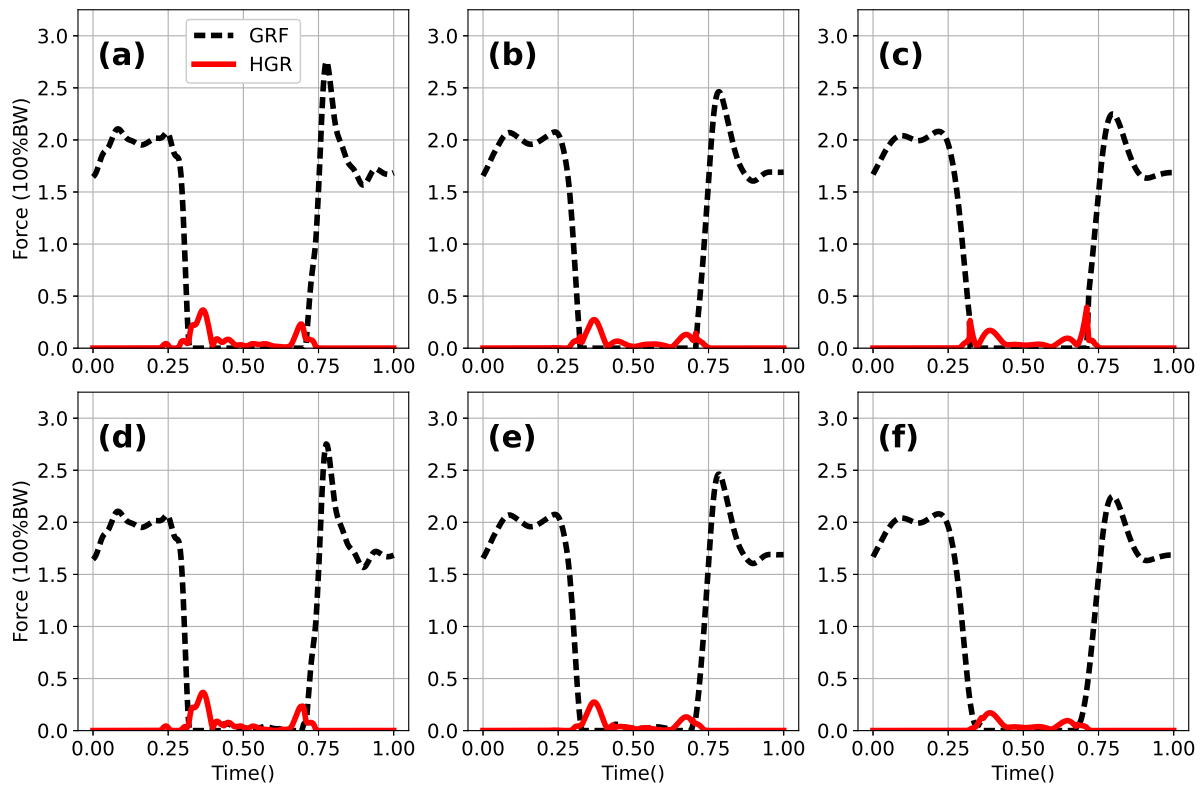


Figure 4.3: Results of the HGR minimization for the IP models. (a) 12.5 Hz cut-off frequency for the kinematic filter, (b) 7.5 Hz cut-off frequency, (c) 5 Hz cut-off frequency, (d) 12.5 Hz cut-off frequency and optimized segment mass distribution, (e) 12.5 Hz cut-off frequency and optimized GRFP settings, (f) 5 Hz cut-off frequency and optimized GRFP settings.

managed a reduction of over 98% by optimizing each time step of the inverse dynamics calculation. While this approach delivers an efficient minimization of HGR, it probably is computationally demanding, which limits its use. Thus, the proposed procedure allows a considerable reduction of HGR by 54% with a simple methodology. In order to minimize the HGR, the segment mass distribution was optimized, like Riemer and Hsiao-Wecksler (2009) and Fritz et al. (2019) proposed. Despite lowering the share of HGR, the total HGR even increased when the segment mass distribution was optimized. On the one hand, Riemer and Hsiao-Wecksler (2009) used a two-dimensional model and additionally optimized the joint angles. On the other hand, the used optimization algorithm allowed an increase of the total body mass by 5%, which led to overall higher forces in the model and consequently higher HGR.

Although the segment mass distribution optimization delivered a solution by minimizing the share of HGR, it did not perform as expected. The absolute body weight rose, revealing weaknesses in the framework conditions of the optimization algorithm. Most importantly, an increase of body weight share for the lumbar spine of 9% to 23% is remarkable. Although the standard data of the model are largely based on cadaver data

from older individuals, and younger people, such as the subject here, can be assumed to have a greater weighting of the lower body, the current subject was in no way extremely athletic, which would fit such a severe shift. Some optimization drawbacks could be improved by minor adjustments of the algorithm's settings, but it might be appropriate to re-evaluate the chosen optimization method for the segment mass distribution.

The high HGR of 62 %BW for the OM models show that HGR are a major issue in musculoskeletal simulations of dynamic movements. Although the kinetic boundary conditions are recorded with two force plates as gold standard, the HGR were the highest in these models. It can be concluded that musculoskeletal models with calculated GRF may be better suited to simulate dynamic motion. Not only are dynamic motions rarely limited to only two ground contacts, GRFP models can be fine-tuned in the calculation of GRF to mitigate HGR. However, the risk of "hiding" the HGR in the GRF should not be disregarded even if the results show that the calculated GRF are close to the measured ones after the optimization of the parameters.

Furthermore, it can be stated that the HGR are primarily dependent on the kinematics, since especially the adjustment of the kinematic filter led to a decrease of the HGR. Moreover, optimization of the segment mass distribution (Riemer and Hsiao-Wecksler 2009) as proposed in the literature, did not really produce any improvement. Consequently, depending on the absolute level of the HGR, it may be promising to optimize the kinematics. An adjustment of the cut-off frequency of the kinematic filter seems to be a feasible way due to the noticeable reduction of the HGR by 54%. Optimizing each time step (Pallarès-López et al. 2019) brings an even better reduction of the HGR, but is also more computationally intensive.

It is noticeable that the peaks of HGR are mostly in the transition phases from ground contact to no ground contact and vice versa. This can be observed more clearly in the models with GRFP than in the models with measured GRF, but the HGR are also highest in the transition phases. In the latter, the HGR are also significant in the ground contact phases, whereas in the GRFP models they are virtually non-existent in the contact phases. On the one hand, this is due to the fact that the GRFP models have the possibility to compensate for the HGR above them due to the nature of the GRFP. On the other hand, it is also important to consider which areas of the simulation are relevant to the problem at hand. Thus, if the transition phases from contact to no contact are not of interest, the influences of the HGR on the results are likely to be smaller.

It should be noted that this HGR minimization approach was only conducted for one subject and movement only. Especially the optimization of segment mass distribution is dependent on the subjects actual body composition. Thus, although in this case the optimization of mass distribution didn't bring any improvements to the HGR, this could bear enhancements for other subjects. Since the GRFP, just like the HGR is implemented in the AMS as artificial muscles, it is possible that the AMS simply transfers forces,

initially exerted by the HGR feature, to the GRF. In the process, the investigated HGR are reduced, although they are actually still exerted in the GRF. However, the GRFP is a reliable and valid feature of the AMS (Skals et al. 2017) and the predicted GRF in the OP and IP models only differ slightly from the measured GRF. Moreover, it must be mentioned that a reduction of the cut-off frequency also means a loss of kinematic information. Thus, corresponding adjustments must not be made across the board but must be applied with caution. As the HGR are to a certain degree also an indicator for the computational error in musculoskeletal models (Ojeda et al. 2016), in this specific case lowering the cut-off frequency also led to an error minimization.

4.5 Conclusion

This study aimed to investigate and minimize HGR for a counter-movement jump by adjusting kinematics and optimizing the GRFP settings and has shown that HGR can be considerably large in standard simulations and can affect the results. The region of interest plays an important role, since the ground contact phases are hardly influenced by HGR, whereas GRFP models show significantly lower HGR. In addition, there are application-dependent possibilities to reduce the HGR. A small improvement is achieved by optimizing the GRFP parameters and an adjustment of the cut-off frequency of the kinematic filter has a noticeable influence on the occurrence and the amount of HGR. However, in order to reduce the occurring HGR below limit values suggested by the literature or even completely eliminate them more elaborate methods are necessary. With the presented approach, however, it is possible to reduce the influence of HGR on the model output considerably by simple adjustments.

Chapter 5

Discussion and Conclusion

5.1 Discussion

The aim of this work was to investigate highly dynamic movements of competitive athletes, as well as to evaluate the behavior of musculoskeletal models during such motions. Specifically, the performance and musculoskeletal load of youth competitive football players under the influence of mental stress was investigated by providing players with additional cognitive tasks during change of direction maneuvers. Moreover, an evaluation of muscle activation in the musculoskeletal models was performed by comparing measured and calculated muscle activity during fast movements. In a further step, numerical inaccuracies of these models (HGR) during the calculation of highly dynamic movements were systematically investigated and optimization approaches were presented.

Investigating research question 1 "How does the muscle and joint reaction force behave under the influence of mental stress in elite junior football players for highly dynamic, sports related motions?" revealed an interesting behavior of muscle and joint reaction force under stress. The additional cognitive load for the elite junior football players led to individual physiological and biomechanical reactions of the athletes. While some showed considerate de- or increases in muscle and knee forces, others had comparable force levels regardless of external stress reception.

Research question 2 was "Does the musculoskeletal model's muscle activity in the lower extremities match the physiological muscle activation in highly dynamic motion, and what's the influence of different muscle modeling options?". The examinations of EMG and AMS muscle activities for different muscle recruitment and muscle modeling configurations showed, that EMG and AMS fit quite well. Since the different configurations didn't differ much, the AMS most common configuration with a simple muscle model and a quadratic target function for the muscle recruitment's optimization problem delivered reliable muscle activities for fast flexion and extension tasks as well as sprinting movements.

With research question 3 "When and to what extent do HGR occur in simulations of highly dynamic motions and how can their occurrence be influenced?" another model reliability aspect was addressed. It was shown that HGR occur in simulations of highly dynamic motion especially during changes of ground contact of the feet to no ground contact. With optimizations to the GRFP and adjustments to the kinematic filter's cut-off frequency, the HGR can be reduced, although not eliminated completely.

The particular investigations in this thesis have shown that musculoskeletal models can make a valuable contribution to research in the field of highly dynamic biomechanical issues. In the experimental series on musculoskeletal loading under mental stress, the athletes responded very differently to the stimuli. Most subjects experienced a reduction in performance and changes in muscle and knee loading. Some exhibited significant peaks in bracing during runs under stress.

Although the number of participants in the study reported here was too small to draw general conclusions, the findings suggest that athletes in states of mental stress, particularly with an additional attention-demanding task, may be at increased risk for injury due to the non-physiological change in loading in the musculoskeletal apparatus. Studies with a larger subject population may help in the future to identify athletes at high risk in general or vulnerable body areas in particular. This work has shown that a stressful scenario can be created with simple means and that musculoskeletal models in a highly dynamic setup are suitable to identify such stress induced changes.

Evaluation of measured and calculated muscle activity has further supported the reliability of musculoskeletal models in highly dynamic movements. In particular, for flexion/extension-only movements, the correlation was mostly strong. For sprint movements, the correlation of muscle activities was somewhat lower, overall in the moderate to strong range, however, they were also in the range of those found by the literature in similar studies (Wibawa et al. 2016). Although higher correlations were also calculated in other studies (Dupré et al. 2019), this was probably due to the much tighter boundary and environmental conditions for those studies. In this work, broader frameworks were set with, compared to marker-based motion capture as the gold standard, somewhat less accurate inertial motion capture (Blair et al. 2018) and calculated rather than measured ground reaction forces. Additionally, deliberate attention was paid to presets and standard models of the model library, which have wide application. However, the investigations proved that it is possible to calculate reliable muscle activities and consequently muscle forces even with these. Though, it is to be noted that only the thigh musculature was evaluated here.

In further work, other body regions such as the lower leg, thorax or upper extremities can be considered. Similar results can be expected due to the general numeric muscle recruitment algorithm. Furthermore, in highly dynamic movements, the thigh musculature is often the subject of investigation. Consequently, it can be concluded that musculoskele-

tal (standard) models fed with motion data from inertial or also video-based motion capture paired with calculated ground reaction forces can be used to analyze highly dynamic movements.

As a final step, the HGR minimization approaches can contribute to additional model validity. From the analysis, it appears that the kinematic input has a significant influence on the occurrence of artificial balancing forces in the musculoskeletal model. By reducing the cutoff frequency of the Butterworth low-pass filter in the model, the HGR can be significantly reduced. In addition, optimization of the GRFP settings brings further reduction. Thus, the interaction of kinematic fitting and GRFP optimization leads to a better computational result with less HGR. Nevertheless, it has not been possible to bring the relative contribution of HGR to the maximum occurring forces below 10%, which is considered a reference value for HGR in the literature (Hicks et al. 2015). These 10%, nonetheless, refer to normally fast motions. In the case of the examined highly dynamic movements, a higher HGR level is to be expected in principle due to the greater accelerations occurring.

However, the investigations into HGR minimization have also shown that the optimization approaches may well be subject to error. By optimizing the segment mass distribution to reduce HGR, a relative decrease in HGR has occurred, but a simultaneous increment in body mass combined with an increase in GRF and HGR has ultimately led to an absolute rise in HGR. Given that musculoskeletal models are often based on cadaver studies of older subjects, it is reasonable for the future to optimize the segment mass distribution to the specific subjects. Still, the framework of the optimization procedure needs to be narrowly defined after the literature has shown that this optimization can help (Fritz et al. 2019). In the end, there are already simple adjustments to minimize HGR by adapting the cutoff frequency and the GRFP settings, whereas depending on the problem, further, special minimization approaches have their justification.

In summary, musculoskeletal models are well suited to answer specific questions in highly dynamic movements. Although there is still some potential for enhancement, which needs further intensive research, the models produce reliable muscle activities on the one hand and on the other hand there are simple possibilities to reduce numerical inaccuracies caused by the input kinematics and thus to calculate the loads more stable and reliable.

5.2 Conclusion

For practical applications this means that we have models that we can safely use for research questions in sports or other dynamic settings. First of all, the study on the influence of stress on muscle loading has shown how such complex issues can be addressed in a close to real-world experimental setting. In particular, the further advancement of markerless motion capture technology will simplify such studies further. Due to the fact that with markerless motion capture the subjects have to be prepared with much less effort, considerably more subjects can be investigated, which is especially necessary when dealing with stress with often individual reactions in order to draw general conclusions from the examinations. The experimental setup presented in this work can easily be adapted to markerless motion capture and essential components for stress generation and evaluation as well as analysis can be adopted. This lays a foundation for further and in-depth investigations of the exact mechanisms inherent to the cascade of biomechanical and mental load (Figure 1.5). A better understanding of the precise relationships between injuries and mental stress will ultimately lead to improved preventive measures in amateur and professional sports.

With the evaluation of muscle recruitment and muscle modeling in musculoskeletal models, studies regarding skeletal muscle loading have a broader basis for assessing the results in terms of their accuracy and reliability. With the knowledge of the behavior of different muscle models and muscle recruitment criteria, the results of the studies on stress are also supported but not limited to them. Further studies investigating either the performance of individual muscles and muscle groups or muscle injuries independent of stress are also conceivable. With research into the exact injury development mechanisms, new prevention programs can be developed or existing ones can be further improved and the health of athletes can be promoted. Due to the possibility of application in more dynamic settings, use in post-injury care is also possible. In sports rehabilitation, for example, problems and progress in muscle development can be addressed.

Last but not least, the study of HGR has also shown that musculoskeletal models are suitable for studies in highly dynamic movements. Although HGR also occur to a greater extent there, they can be reduced and the time of occurrence also plays a role. For practice, this means that especially, but not exclusively, attention must be paid to HGR in simulations of highly dynamic motions, as they can have a significant influence on the results. However, with the approaches presented in this paper, it is possible to get a grip on the HGR and reduce their influence. In general, it is necessary to always check the results of the calculations and ensure the correct setting of the boundary conditions in the musculoskeletal model.

Bibliography

- Achenbach, L., W. Krutsch, M. Koch, F. Zeman, M. Nerlich, and P. Angele (2019). “Contact times of change-of-direction manoeuvres are influenced by age and the type of sports: a novel protocol using the SpeedCourt system”. In: *Knee Surgery, Sports Traumatology, Arthroscopy* 27.310, pp. 991–999. DOI: 10.1007/s00167-018-5192-z.
- Alahmad, T. A., P. Kearney, and R. Cahalan (2020). “Injury in elite women’s soccer: a systematic review”. In: *The Physician and sportsmedicine* 48.3, pp. 259–265. DOI: 10.1080/00913847.2020.1720548.
- Ali, N., M. S. Andersen, J. Rasmussen, D. G. E. Robertson, and G. Rouhi (2014). “The application of musculoskeletal modeling to investigate gender bias in non-contact ACL injury rate during single-leg landings”. In: *Computer Methods in Biomechanics and Biomedical Engineering* 17.14, pp. 1602–1616. DOI: 10.1080/10255842.2012.758718.
- Andersen, M. S., J. Rasmussen, D. K. Ramsey, and D. L. Benoit (2010). “Validation of Knee Joint Models – An In Vivo Study”. In: *6th World Congress of Biomechanics (WCB 2010). August 1-6, 2010 Singapore*. Ed. by R. Magjarevic, C. T. Lim, and J. C. H. Goh. Vol. 31. IFMBE Proceedings. Berlin, Heidelberg: Springer Berlin Heidelberg, pp. 1288–1291. DOI: 10.1007/978-3-642-14515-5_327.
- Andersen, M. S. (2018). “How sensitive are predicted muscle and knee contact forces to normalization factors and polynomial order in the muscle recruitment criterion formulation?” In: *International Biomechanics* 135, pp. 1–16. DOI: 10.1080/23335432.2018.1514278.
- AnyBody Technology (2023). *AnyBody Tutorials*. AnyBody Technology. URL: <https://anyscript.org/tutorials/> (visited on 06/05/2023).
- Arnason, A., A. Tenga, L. Engebretsen, and R. Bahr (2004). “A prospective video-based analysis of injury situations in elite male football: football incident analysis”. In: *The American journal of sports medicine* 32.6, pp. 1459–1465. DOI: 10.1177/0363546504262973.
- Atkinson, G. and A. M. Batterham (2015). “True and false interindividual differences in the physiological response to an intervention”. In: *Experimental physiology* 100.6, pp. 577–588. DOI: 10.1113/EP085070.
- Auer, S., S. Kubowitsch, and S. Dendorfer (2023). “Kombinierter Einfluss von psychologischen und biomechanischen Faktoren auf die muskulären Belastungen beim Fußballspie-

- len : Ein neuer Ansatz zur Prävention von Muskelverletzungen? Ein neuer Ansatz zur Prävention von Muskelverletzungen?" In: *Orthopadie (Heidelberg, Germany)* 52.11, pp. 876–881. DOI: 10.1007/s00132-023-04437-8.
- Auer, S., S. Kubowitsch, F. Süß, T. Renkawitz, W. Krutsch, and S. Dendorfer (2021). "Mental stress reduces performance and changes musculoskeletal loading in football-related movements". In: *Science and Medicine in Football* 5.4, pp. 323–329. DOI: 10.1080/24733938.2020.1860253.
- Auer, S., S. Kubowitsch, Werner Krutsch, T. Renkawitz, F. Süß, and S. Dendorfer (2020). "EFFECT OF MENTAL DEMAND ON KNEE FORCES IN PROFESSIONAL YOUTH SOCCER PLAYERS". In: *ISBS Proceedings Archive* 38.1, p. 104. URL: <https://commons.nmu.edu/isbs/vol38/iss1/28>.
- Aurand, A. M., J. S. Dufour, and W. S. Marras (2017). "Accuracy map of an optical motion capture system with 42 or 21 cameras in a large measurement volume". In: *Journal of Biomechanics* 58, pp. 237–240. DOI: 10.1016/j.jbiomech.2017.05.006.
- Bartels, T., S. Proeger, K. Brehme, M. Pyschik, K.-S. Delank, S. Schulze, R. Schwesig, and G. Fieseler (2016). "The SpeedCourt system in rehabilitation after reconstruction surgery of the anterior cruciate ligament (ACL)". In: *Archives of orthopaedic and trauma surgery* 136.7, pp. 957–966. DOI: 10.1007/s00402-016-2462-4.
- Benditz, A., S. Auer, J. F. Spörrer, S. Wolkerstorfer, J. Grifka, F. Süß, and S. Dendorfer (2018). "Regarding loads after spinal fusion, every level should be seen separately: a musculoskeletal analysis". In: *European Spine Journal* 27.8, pp. 1905–1910. DOI: 10.1007/s00586-018-5476-5.
- Blair, S., G. Duthie, S. Robertson, W. Hopkins, and K. Ball (2018). "Concurrent validation of an inertial measurement system to quantify kicking biomechanics in four football codes". In: *Journal of Biomechanics* 73, pp. 24–32. DOI: 10.1016/j.jbiomech.2018.03.031.
- Bloemsaat, J. G., R. G. J. Meulenbroek, and G. P. van Galen (2005). "Differential effects of mental load on proximal and distal arm muscle activity". In: *Experimental brain research* 167.4, pp. 622–634. DOI: 10.1007/s00221-005-0066-2.
- Born, D.-P., C. Zinner, P. Düking, and B. Sperlich (2016). "Multi-Directional Sprint Training Improves Change-Of-Direction Speed and Reactive Agility in Young Highly Trained Soccer Players". In: *Journal of Sports Science & Medicine* 15.2, pp. 314–319.
- Brandes, R., F. Lang, and R. F. Schmidt (2019). *Physiologie des Menschen*. Berlin, Heidelberg: Springer Berlin Heidelberg. 1062 pp. DOI: 10.1007/978-3-662-56468-4.
- Brickenkamp, R., L. Schmidt-Atzert, and D. Liepmann (2016). *d2-R. d2 Test of Attention - Revised*. 1st ed. Oxford: Hogrefe Ltd.
- Bussey, M. (2002). *Sports Biomechanics*. Routledge. DOI: 10.4324/9780203474563.

- Carnes, M. E. and G. D. Pins (2020). “Skeletal Muscle Tissue Engineering: Biomaterials-Based Strategies for the Treatment of Volumetric Muscle Loss”. In: *Bioengineering (Basel, Switzerland)* 7.3. DOI: 10.3390/bioengineering7030085.
- Cooper, C. L. (1986). *Stress Research. Issues for the Eighties*. New York: Wiley & Sons. 149 pp.
- Corbett, M. (2015). “From law to folklore: work stress and the Yerkes-Dodson Law”. In: *Journal of Managerial Psychology* 30.6, pp. 741–752. DOI: 10.1108/JMP-03-2013-0085.
- Damsgaard, M., J. Rasmussen, S. T. Christensen, E. Surma, and M. de Zee (2006). “Analysis of musculoskeletal systems in the AnyBody Modeling System”. In: *Simulation Modelling Practice and Theory* 14.8, pp. 1100–1111. DOI: 10.1016/j.simpat.2006.09.001.
- David, S., I. Komnik, M. Peters, J. Funken, and W. Potthast (2017). “Identification and risk estimation of movement strategies during cutting maneuvers”. In: *Journal of science and medicine in sport* 20.12, pp. 1075–1080. DOI: 10.1016/j.jsams.2017.05.011.
- Diamond, D. M., A. M. Campbell, C. R. Park, J. Halonen, and P. R. Zoladz (2007). “The temporal dynamics model of emotional memory processing: a synthesis on the neurobiological basis of stress-induced amnesia, flashbulb and traumatic memories, and the Yerkes-Dodson law”. In: *Neural Plasticity* 2007, p. 60803. DOI: 10.1155/2007/60803.
- Dorn, T. W., A. G. Schache, and M. G. Pandy (2012). “Muscular strategy shift in human running: dependence of running speed on hip and ankle muscle performance”. In: *Journal of Experimental Biology* 215.13, pp. 1944–1956. DOI: 10.1242/jeb.075051.
- Düking, P., D.-P. Born, and B. Sperlich (2016). “The SpeedCourt: Reliability, Usefulness, and Validity of a New Method to Determine Change-of-Direction Speed”. In: *International journal of sports physiology and performance* 11.1, pp. 130–134. DOI: 10.1123/ijsp.2015-0174.
- Dupré, T., M. Dietzsch, I. Komnik, W. Potthast, and S. David (2019). “Agreement of measured and calculated muscle activity during highly dynamic movements modelled with a spherical knee joint”. In: *Journal of biomechanics* 84, pp. 73–80. DOI: 10.1016/j.jbiomech.2018.12.013. URL: <http://www.sciencedirect.com/science/article/pii/S0021929018309035>.
- Ekstrand, J., M. Hägglund, and M. Waldén (2011a). “Injury incidence and injury patterns in professional football: the UEFA injury study”. In: *British journal of sports medicine* 45.7, pp. 553–558. DOI: 10.1136/bjism.2009.060582.
- Ekstrand, J., M. Hägglund, and M. Waldén (2011b). “Epidemiology of muscle injuries in professional football (soccer)”. In: *American Journal of Sports Medicine* 39.6, pp. 1226–1232. DOI: 10.1177/0363546510395879.

- Faber, H., A. J. van Soest, and D. A. Kistemaker (2018). “Inverse dynamics of mechanical multibody systems: An improved algorithm that ensures consistency between kinematics and external forces”. In: *PloS one* 13.9, e0204575. DOI: 10.1371/journal.pone.0204575.
- Fluit, R., M. S. Andersen, S. Kolk, N. Verdonschot, and H. F. J. M. Koopman (2014). “Prediction of ground reaction forces and moments during various activities of daily living”. In: *Journal of Biomechanics* 47.10, pp. 2321–2329. DOI: 10.1016/j.jbiomech.2014.04.030.
- Friston, K. J. (2006). *Statistical Parametric Mapping. The Analysis of Functional Brain Images*. Burlington: Elsevier Science. 689 pp. URL: <https://ebookcentral.proquest.com/lib/kxp/detail.action?docID=282095>.
- Fritz, J., J. Kröll, and H. Schwameder (2019). “Influence of body segment parameter estimation on calculated ground reaction forces in highly dynamic movements”. In: *Journal of biomechanics* 84, pp. 11–17. DOI: 10.1016/j.jbiomech.2018.12.008.
- Fukuchi, C. A., R. K. Fukuchi, and M. Duarte (2019). “Effects of walking speed on gait biomechanics in healthy participants: a systematic review and meta-analysis”. In: *Systematic reviews* 8.153. DOI: 10.1186/s13643-019-1063-z.
- Hart, S. G. and L. E. Staveland (1988). “Development of NASA-TLX (Task Load Index): Results of Empirical and Theoretical Research”. In: *Human Mental Workload*. Vol. 52. Advances in Psychology. Elsevier, pp. 139–183. DOI: 10.1016/S0166-4115(08)62386-9.
- Hicks, J. L., T. K. Uchida, A. Seth, A. Rajagopal, and S. L. Delp (2015). “Is my model good enough? Best practices for verification and validation of musculoskeletal models and simulations of movement”. In: *Journal of biomechanical engineering* 137.2, p. 020905. DOI: 10.1115/1.4029304.
- Higashihara, A., T. Ono, J. Kubota, T. Okuwaki, and T. Fukubayashi (2010). “Functional differences in the activity of the hamstring muscles with increasing running speed”. In: *Journal of sports sciences* 28.10, pp. 1085–1092. DOI: 10.1080/02640414.2010.494308.
- Higuchi, T., K. Imanaka, and T. Hatayama (2002). “Freezing degrees of freedom under stress: Kinematic evidence of constrained movement strategies”. In: *Human Movement Science* 21.5-6, pp. 831–846. DOI: 10.1016/S0167-9457(02)00174-4.
- Ivarsson, A. and U. Johnson (2010). “Psychological Factors as Predictors of Injuries Among Senior Soccer Players. A Prospective Study”. In: *Journal of Sports Science & Medicine* 9.2, pp. 347–352.
- Ivarsson, A., U. Johnson, and L. Podlog (2013). “Psychological predictors of injury occurrence: a prospective investigation of professional Swedish soccer players.” In: *Journal of Sport Rehabilitation* 22, pp. 19–26.

- Jansen, P., J. Lehmann, B. Fellner, G. Huppertz, O. Loose, L. Achenbach, and W. Krutsch (2019). “Relation of injuries and psychological symptoms in amateur soccer players”. In: *BMJ open sport & exercise medicine* 5, e000522. DOI: 10.1136/bmjsem-2019-000522.
- Jones, F. (2001). *Stress. Myth, theory, and research*. 1. publ. Harlow, England: Prentice Hall. 310 pp.
- Junge, A., D. Rösch, L. Peterson, T. Graf-Baumann, and J. Dvorak (2002). “Prevention of soccer injuries: a prospective intervention study in youth amateur players”. In: *The American journal of sports medicine* 30.5, pp. 652–659. DOI: 10.1177/03635465020300050401.
- Karatsidis, A., M. Jung, H. M. Schepers, G. Bellusci, M. de Zee, P. H. Veltink, and M. S. Andersen (2019). “Musculoskeletal model-based inverse dynamic analysis under ambulatory conditions using inertial motion capture”. In: *Medical Engineering & Physics* 65, pp. 68–77. DOI: 10.1016/j.medengphy.2018.12.021.
- Keogh, E. and C. A. Ratanamahatana (2005). “Exact indexing of dynamic time warping”. In: *Knowledge and Information Systems* 7.3, pp. 358–386. DOI: 10.1007/s10115-004-0154-9.
- Konrad, P. (2005). *The ABC of EMG*. Noraxon INC. USA. 60 pp.
- Larsen, F. G., F. P. Svenningsen, M. S. Andersen, M. de Zee, and S. Skals (2020). “Estimation of Spinal Loading During Manual Materials Handling Using Inertial Motion Capture”. In: *Annals of biomedical engineering* 48.2, pp. 805–821. DOI: 10.1007/s10439-019-02409-8.
- Lazarus, R. S. and S. Folkman (1984). *Stress, Appraisal, and Coping*. New York: Springer Publishing Company. 445 pp. URL: <http://swb.eblib.com/patron/FullRecord.aspx?p=423337>.
- Lohse, K. R. and D. E. Sherwood (2012). “Thinking about muscles: the neuromuscular effects of attentional focus on accuracy and fatigue”. In: *Acta Psychologica* 140.3, pp. 236–245. DOI: 10.1016/j.actpsy.2012.05.009.
- Loose, O., B. Fellner, J. Lehmann, L. Achenbach, V. Krutsch, S. Gerling, P. Jansen, P. Angele, M. Nerlich, and W. Krutsch (2019). “Injury incidence in semi-professional football claims for increased need of injury prevention in elite junior football”. In: *Knee Surgery, Sports Traumatology, Arthroscopy* 27.3, pp. 978–984. DOI: 10.1007/s00167-018-5119-8.
- Lund, M. E., S. Tørholm, S. T. Simonsen, and B. K. Englund (2021). *The AnyBody Managed Model Repository (AMMR)*. Version 2.3.4. Zenodo. DOI: 10.5281/zenodo.5060249. URL: <https://zenodo.org/record/5060249> (visited on 02/15/2022).
- Lundberg, U., M. Forsman, G. Zachau, M. Eklöf, G. Palmerud, B. Melin, and R. Kadefors (2002). “Effects of experimentally induced mental and physical stress on motor unit

- recruitment in the trapezius muscle”. In: *Work & Stress* 16.2, pp. 166–178. DOI: 10.1080/02678370210136699.
- Marras, W. S., K. G. Davis, C. A. Heaney, A. B. Maronitis, and W. G. Allread (2000). “The influence of psychosocial stress, gender, and personality on mechanical loading of the lumbar spine”. In: *Spine* 25.23, pp. 3045–3054.
- Mayo, J. and J. Ojeda (2020). “Influence of the kinematic constraints on dynamic residuals in inverse dynamic analysis during human gait without using force plates”. In: *Multibody System Dynamics* 50.3, pp. 305–321. DOI: 10.1007/s11044-020-09739-9.
- McCall, A., G. Dupont, and J. Ekstrand (2018). “Internal workload and non-contact injury: a one-season study of five teams from the UEFA Elite Club Injury Study”. In: *British Journal of Sports Medicine* 52.23, pp. 1517–1522. DOI: 10.1136/bjsports-2017-098473.
- Mendez-Villanueva, A., M. Buchheit, B. Simpson, and P. C. Bourdon (2013). “Match play intensity distribution in youth soccer”. In: *International journal of sports medicine* 34.2, pp. 101–110. DOI: 10.1055/s-0032-1306323.
- Nilsson, T., A. H. Östenberg, and M. Alricsson (2016). “Injury profile among elite male youth soccer players in a Swedish first league”. In: *Journal of exercise rehabilitation* 12.2, pp. 83–89. DOI: 10.12965/jer.1632548.274.
- Nimbarte, A. D., M. J. Al Hassan, S. E. Guffey, and W. R. Myers (2012). “Influence of psychosocial stress and personality type on the biomechanical loading of neck and shoulder muscles”. In: *International Journal of Industrial Ergonomics* 42.5, pp. 397–405. DOI: 10.1016/j.ergon.2012.05.001.
- Ojeda, J., J. Martínez-Reina, and J. Mayo (2016). “The effect of kinematic constraints in the inverse dynamics problem in biomechanics”. In: *Multibody System Dynamics* 37.3, pp. 291–309. DOI: 10.1007/s11044-016-9508-9.
- Pallarès-López, R., F. Costa Alvim, M. Febrer-Nafria, L. Luporini Menegaldo, and J. M. Font-Llagunes (2019). “Assessment of residual reduction procedures for high-speed tasks”. In: *Gait & posture* 73, pp. 116–119. DOI: 10.1016/j.gaitpost.2019.07.191.
- Pastorino, E. and S. Doyle-Portillo (2019). *What is psychology? Foundations, applications & integration*. Fourth edition. Boston, MA: Cengage. 1 online resource.
- Pataky, T. C. (2012). “One-dimensional statistical parametric mapping in Python”. In: *Computer Methods in Biomechanics and Biomedical Engineering* 15.3, pp. 295–301. DOI: 10.1080/10255842.2010.527837.
- Pensgaard, A. M., A. Ivarsson, A. Nilstad, B. E. Solstad, and K. Steffen (2018). “Psychosocial stress factors, including the relationship with the coach, and their influence on acute and overuse injury risk in elite female football players”. In: *BMJ open sport & exercise medicine* 4.1, e000317. DOI: 10.1136/bmjsem-2017-000317.
- Pieri, E. de, M. E. Lund, A. Gopalakrishnan, K. P. Rasmussen, D. E. Lunn, and S. J. Ferguson (2018). “Refining muscle geometry and wrapping in the TLEM 2 model for

- improved hip contact force prediction”. In: *PloS one* 13.9, e0204109. DOI: 10.1371/journal.pone.0204109.
- Praagman, M., E. K. J. Chadwick, F. C. T. van der Helm, and H. E. J. Veeger (2006). “The relationship between two different mechanical cost functions and muscle oxygen consumption”. In: *Journal of Biomechanics* 39.4, pp. 758–765. DOI: 10.1016/j.jbiomech.2004.11.034.
- Praagman, M., H. Veeger, E. Chadwick, W. Colier, and F. van der Helm (2003). “Muscle oxygen consumption, determined by NIRS, in relation to external force and EMG”. In: *Journal of Biomechanics* 36.7, pp. 905–912. DOI: 10.1016/S0021-9290(03)00081-2.
- Putzer, M., I. Ehrlich, J. Rasmussen, N. Gebbeken, and S. Dendorfer (2016). “Sensitivity of lumbar spine loading to anatomical parameters”. In: *Journal of Biomechanics* 49.6, pp. 953–958. DOI: 10.1016/j.jbiomech.2015.11.003.
- Rasmussen, J., M. Damsgaard, and M. Voigt (2001). “Muscle recruitment by the min/max criterion — a comparative numerical study”. In: *Journal of Biomechanics* 34.3, pp. 409–415. DOI: 10.1016/S0021-9290(00)00191-3.
- Rebelo, A., J. Brito, A. Seabra, J. Oliveira, and P. Krstrup (2014). “Physical match performance of youth football players in relation to physical capacity”. In: *European journal of sport science* 14 Suppl 1, pp. 148–156. DOI: 10.1080/17461391.2012.664171.
- Reilly, M. and K. Kontson (2020). “Computational musculoskeletal modeling of compensatory movements in the upper limb”. In: *Journal of Biomechanics* 108, p. 109843. DOI: 10.1016/j.jbiomech.2020.109843. URL: <https://www.sciencedirect.com/science/article/pii/S0021929020302669>.
- Riemer, R. and E. T. Hsiao-Wecksler (2009). “Improving net joint torque calculations through a two-step optimization method for estimating body segment parameters”. In: *Journal of Biomechanical Engineering* 131.1, p. 011007. DOI: 10.1115/1.3005155.
- Sakai, R., Y. Ohtaki, N. Sakaguchi, N. Takahira, T. Kenmoku, K. Yoshida, and M. Ujihira (2018). “Analysis of Forearm Muscle Activity Aiming at Prevention of Refractory Tennis Elbow: Comparison of One-Handed Backhand Stroke Form”. In: *SM Orthopedics & Muscular System* 2.1, p. 1002.
- Selye, H. (1976). “The stress concept”. In: *Canadian Medical Association Journal* 115.8, p. 718.
- Skals, S., M. K. Jung, M. Damsgaard, and M. S. Andersen (2017). “Prediction of ground reaction forces and moments during sports-related movements”. In: *Multibody System Dynamics* 39.3, pp. 175–195. DOI: 10.1007/s11044-016-9537-4.
- Slimani, M., J. S. Baker, F. Cheour, L. Taylor, and N. L. Bragazzi (2017). “Steroid hormones and psychological responses to soccer matches: Insights from a systematic review and meta-analysis”. In: *PloS one* 12.10, e0186100. DOI: 10.1371/journal.pone.0186100.

- Srinivasan, D., S. E. Mathiassen, D. M. Hallman, A. Samani, P. Madeleine, and E. Lyskov (2016). “Effects of concurrent physical and cognitive demands on muscle activity and heart rate variability in a repetitive upper-extremity precision task”. In: *European Journal of Applied Physiology* 116.1, pp. 227–239. DOI: 10.1007/s00421-015-3268-8.
- Storn, R. and K. Price (1997). “Differential Evolution – A Simple and Efficient Heuristic for global Optimization over Continuous Spaces”. In: *Journal of Global Optimization* 11.4, pp. 341–359. DOI: 10.1023/A:1008202821328.
- Swanik, C. B., T. Covassin, D. J. Stearne, and P. Schatz (2007). “The relationship between neurocognitive function and noncontact anterior cruciate ligament injuries”. In: *The American journal of sports medicine* 35.6, pp. 943–948. DOI: 10.1177/0363546507299532.
- Vondrák, V., J. Rasmussen, M. Damsgaard, and Dostál Zdenek (2006). “The algorithms of mathematical programming in muscle recruitment and muscle wrapping problems”. In: *III European Conference on Computational Mechanics*, p. 194.
- Weber, T., S. Dendorfer, S. K. Bulstra, J. Grifka, G. J. Verkerke, and T. Renkawitz (2016). “Gait six month and one-year after computer assisted Femur First THR vs. conventional THR. Results of a patient- and observer- blinded randomized controlled trial”. In: *Gait & Posture* 49, pp. 418–425. DOI: 10.1016/j.gaitpost.2016.06.035.
- Weinhandl, J. T., B. S. Irmischer, and Z. A. Sievert (2017). “Effects of Gait Speed of Femoroacetabular Joint Forces”. In: *Applied bionics and biomechanics*. DOI: 10.1155/2017/6432969.
- Wibawa, A. D., N. Verdonschot, J. P. K. Halbertsma, J. G. M. Burgerhof, R. L. Diercks, and G. J. Verkerke (2016). “Musculoskeletal modeling of human lower limb during normal walking, one-legged forward hopping and side jumping: Comparison of measured EMG and predicted muscle activity patterns”. In: *Journal of Biomechanics* 49.15, pp. 3660–3666. DOI: 10.1016/j.jbiomech.2016.09.041.
- Wijsman, J., B. Grundlehner, J. Penders, and H. Hermens (2013). “Trapezius muscle EMG as predictor of mental stress”. In: *ACM Transactions on Embedded Computing Systems* 12.4, pp. 1–20. DOI: 10.1145/2485984.2485987.
- Winter, D. A. (2009). *Biomechanics and motor control of human movement*. 4th ed. Hoboken, N.J: Wiley. 370 pp. DOI: 10.1002/9780470549148. URL: <http://onlinelibrary.wiley.com/book/10.1002/9780470549148>.
- Wu, J. Z., K.-N. An, R. G. Cutlip, M. E. Andrew, and R. G. Dong (2009). “Modeling of the muscle/tendon excursions and moment arms in the thumb using the commercial software anybody”. In: *Journal of Biomechanics* 42.3, pp. 383–388. DOI: 10.1016/j.jbiomech.2008.11.008+.

- Zajac, F. E. (1989). “Muscle and tendon: properties, models, scaling, and application to biomechanics and motor control”. In: *Critical reviews in biomedical engineering* 17.4, pp. 359–411.
- Zhou, S., D. L. Lawson, W. E. Morrison, and I. Fairweather (1995). “Electromechanical delay in isometric muscle contractions evoked by voluntary, reflex and electrical stimulation”. In: *European Journal of Applied Physiology* 70.2, pp. 138–145. DOI: 10.1007/BF00361541.
- Zinner, C., D.-P. Born, and B. Sperlich (2017). “Ischemic Preconditioning Does Not Alter Performance in Multidirectional High-Intensity Intermittent Exercise”. In: *Frontiers in physiology* 8, p. 1029. DOI: 10.3389/fphys.2017.01029.

Acknowledgments

Even though I have declared that I wrote this thesis independently, it would not have been possible without assistance from others. The greatest thanks are owed to Sebastian as my supervisor for making my doctorate possible and carefully guiding me through it. I would also like to thank my mentors for their willingness and support during my work. Furthermore, my thesis has benefited enormously from the professional exchange and the pleasant working atmosphere in the laboratory. For this I would like to express my gratitude to all my colleagues over the years. Last but not least, I also know that without my family and closest friends, many things would not have worked out this way. I am extremely grateful for their tremendous support throughout my academic career.

Declaration of authorship

I, Simon Auer, born on 24.03.1993 in Kelheim declare that this thesis titled, “Musculoskeletal models in highly dynamic motion: effects of model parameters and mental stress” and the work presented in it are my own. I confirm that

- this work was done wholly or mainly while in candidature for a research degree at this University.
- where any part of this thesis has previously been submitted for a degree or any other qualification at this University or any other institution, this has been clearly stated.
- where I have consulted the published work of others, this is always clearly attributed.
- where I have quoted from the work of others, the source is always given. With the exception of such quotations, this thesis is entirely my own work. I did not receive paid help from mediation and advisory services e.g. PhD consultants.
- I have acknowledged all main sources of help.
- where the thesis is based on work done by myself jointly with others, I have made clear exactly what was done by others and what I have contributed myself.

Regensburg, 26.06.2023

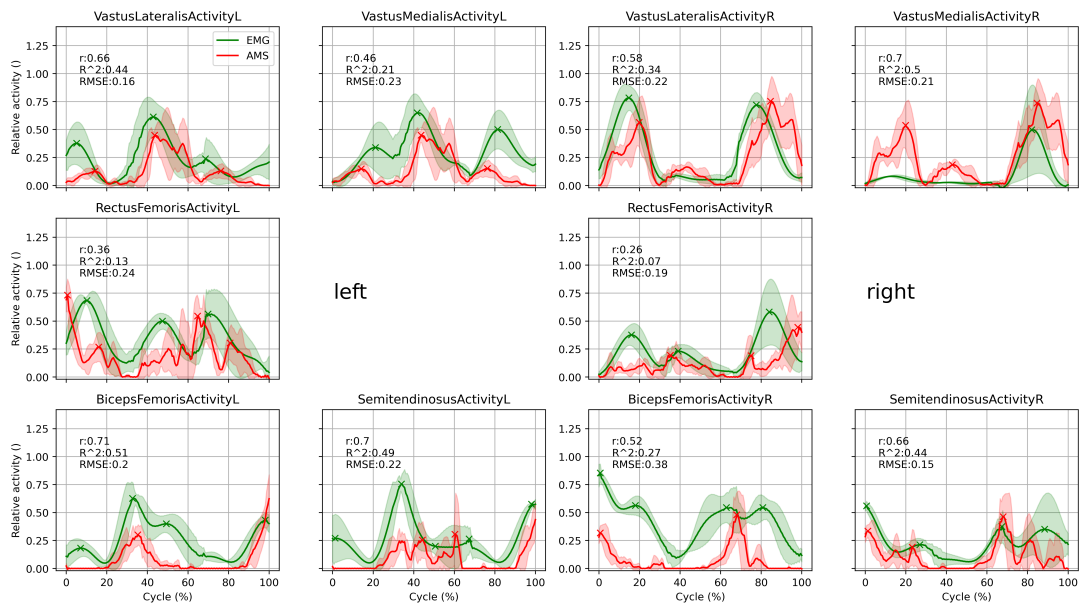


Simon Auer, M.Sc.

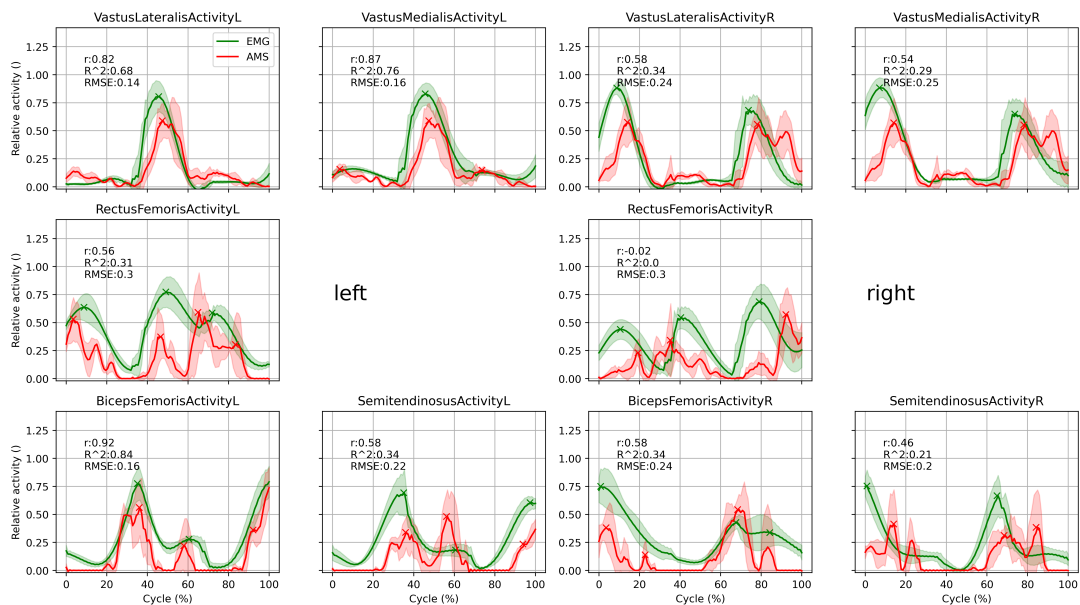
Appendix A

Supplementary material to chapter 3

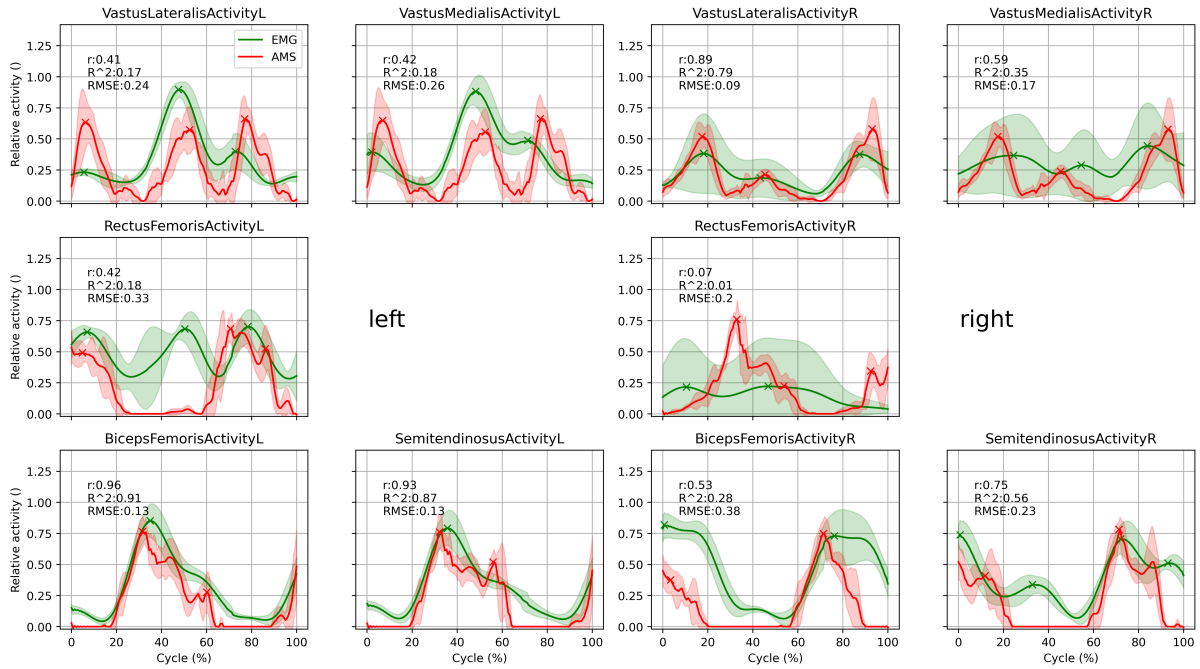
Graphs for muscle activity in EMG and AMS for the S2 scenario for every subject.



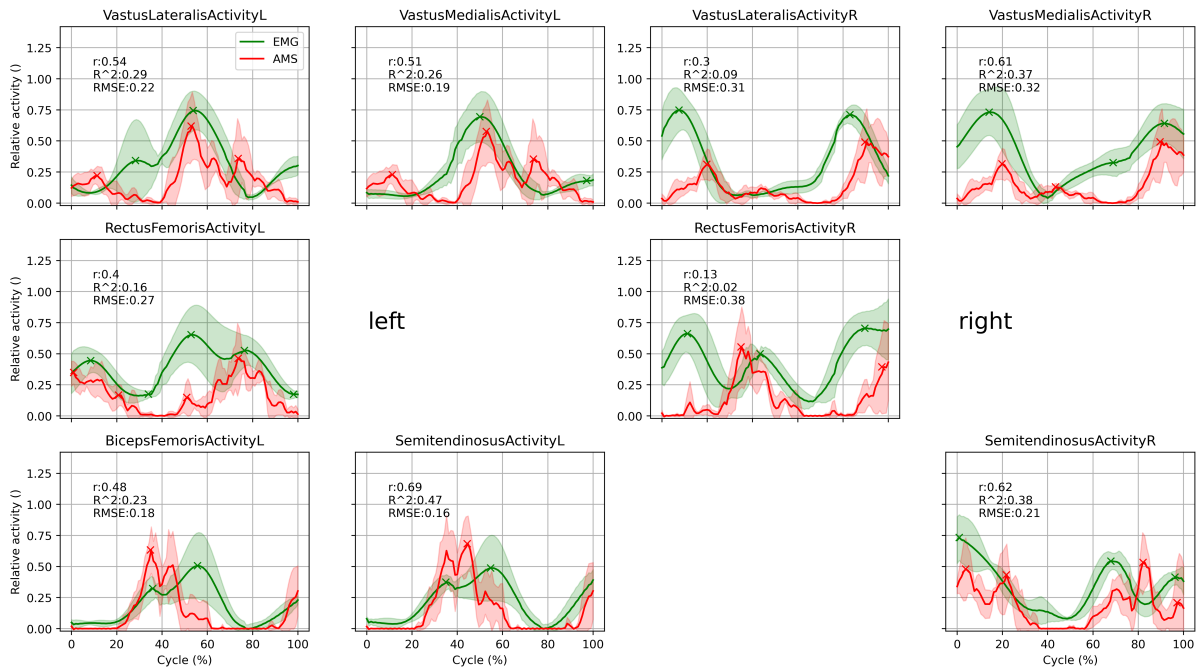
(a) Subject 1



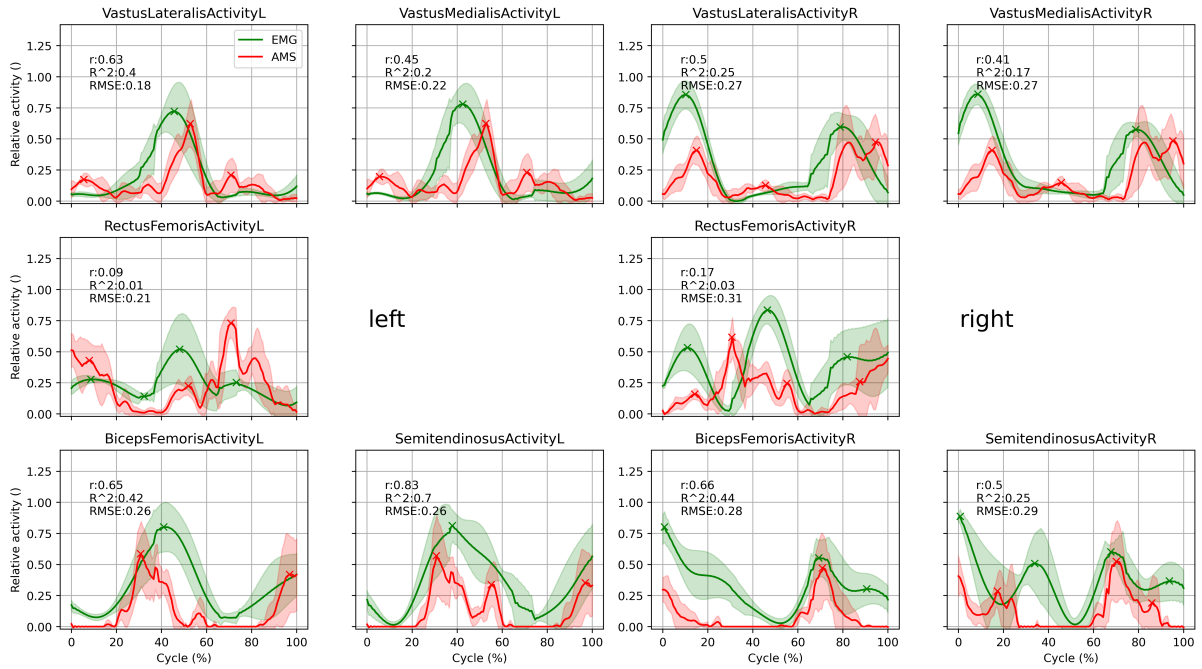
(b) Subject 2



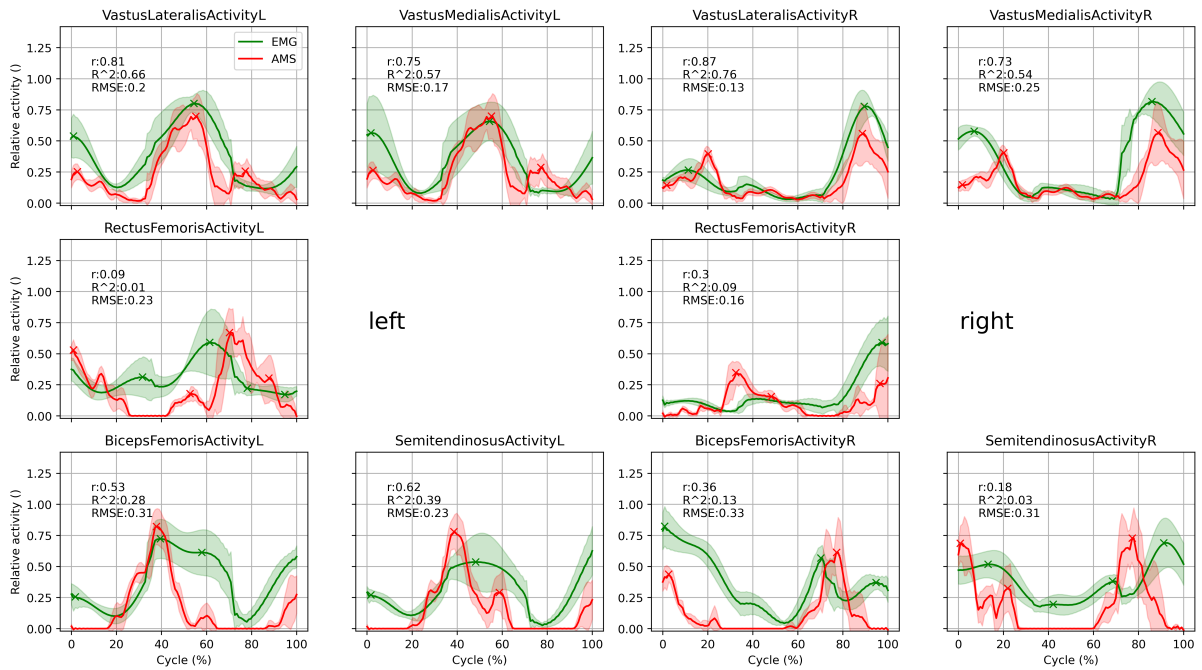
(c) Subject 3



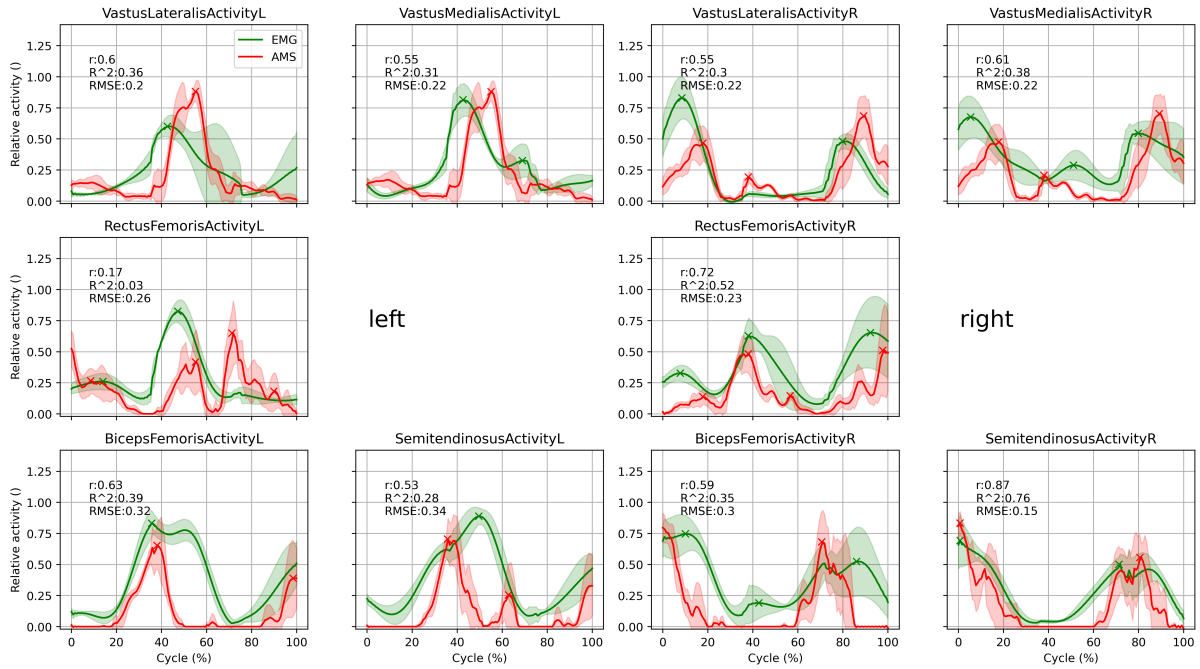
(d) Subject 4



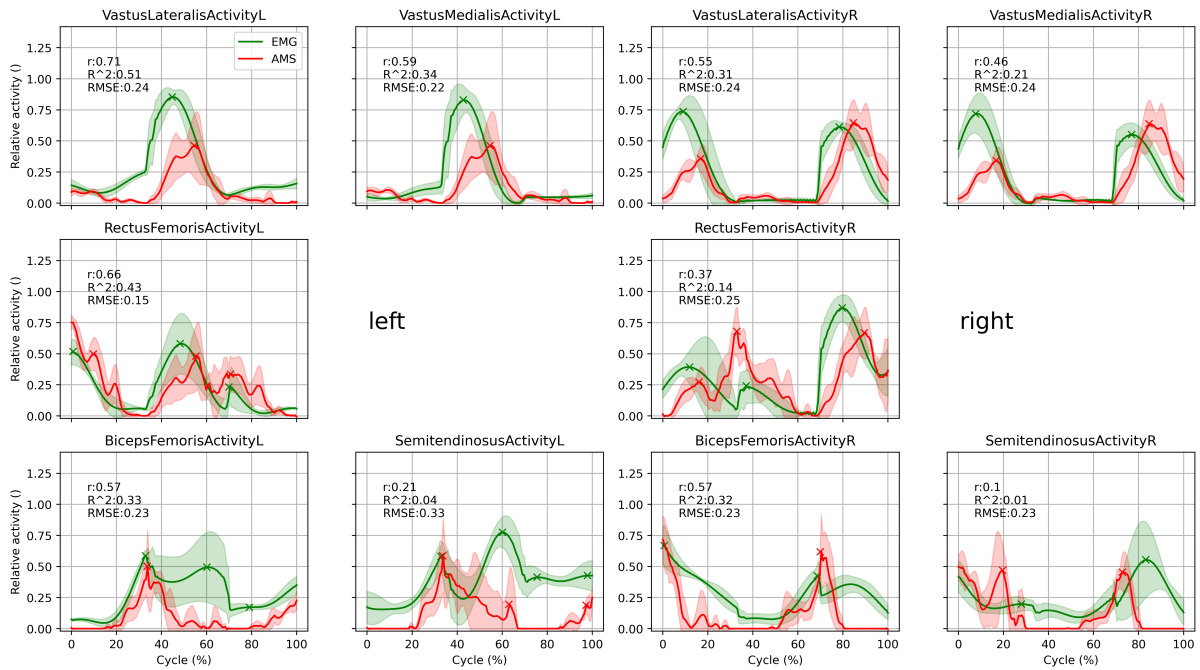
(e) Subject 5



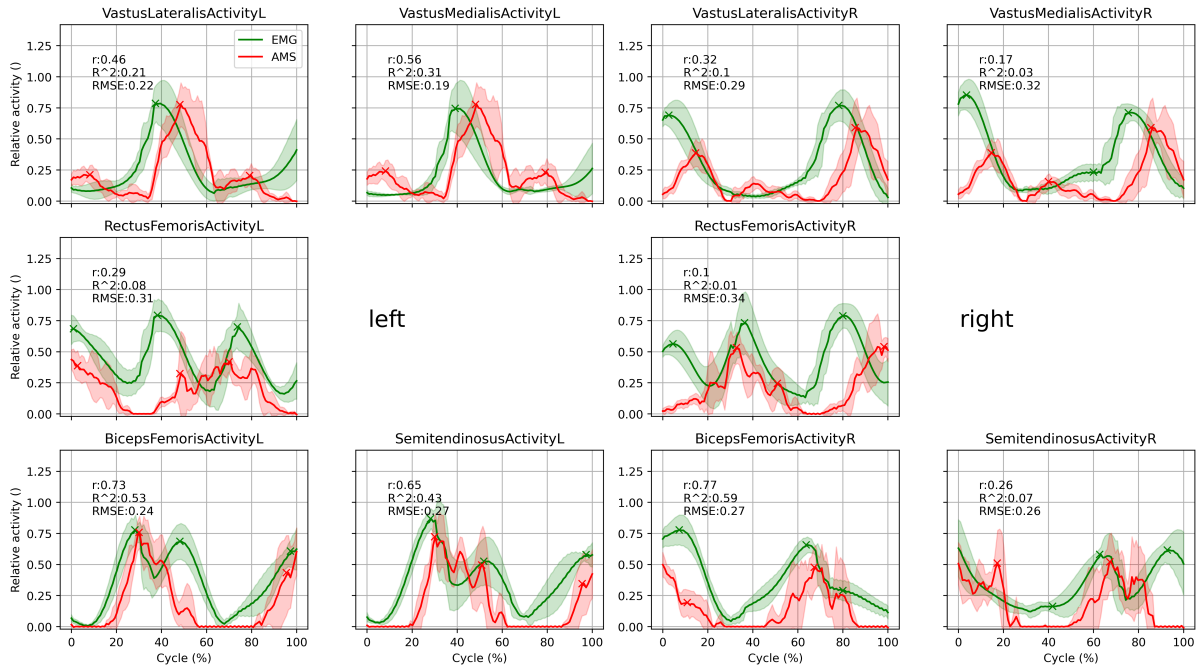
(f) Subject 6



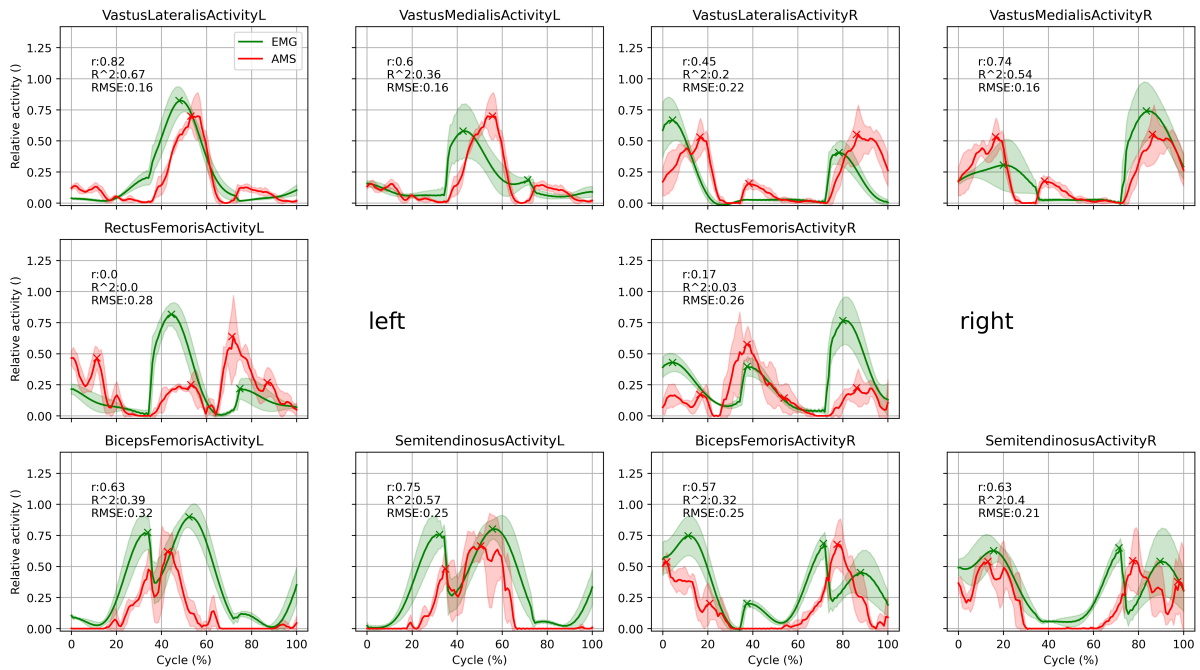
(g) Subject 7



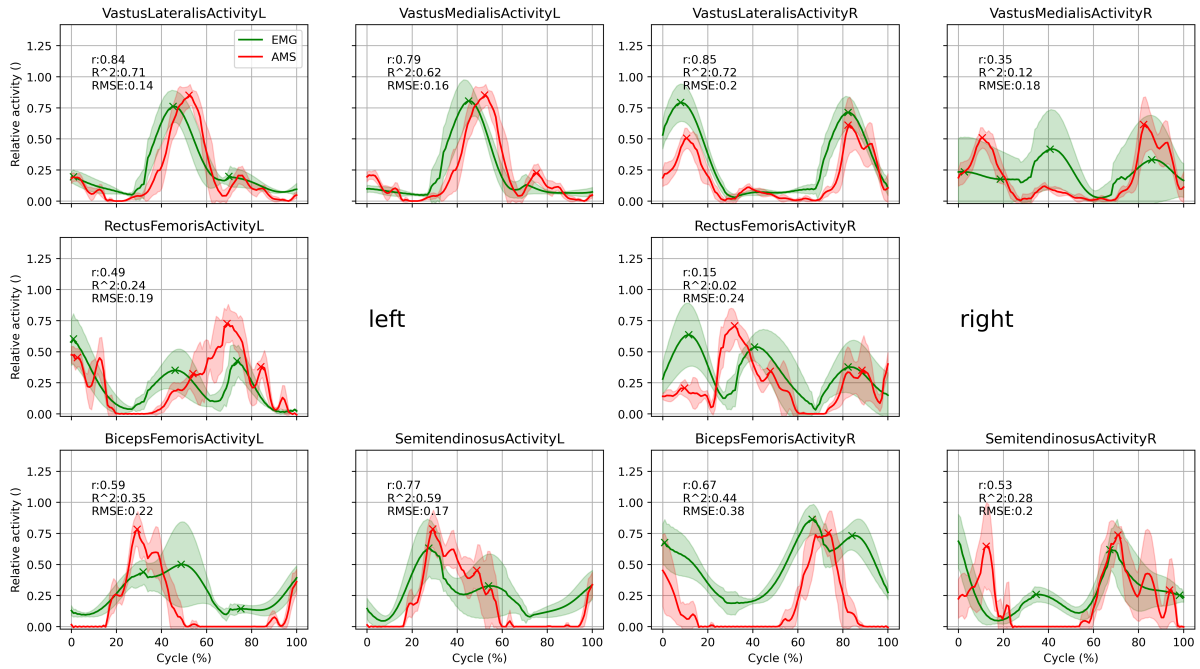
(h) Subject 8



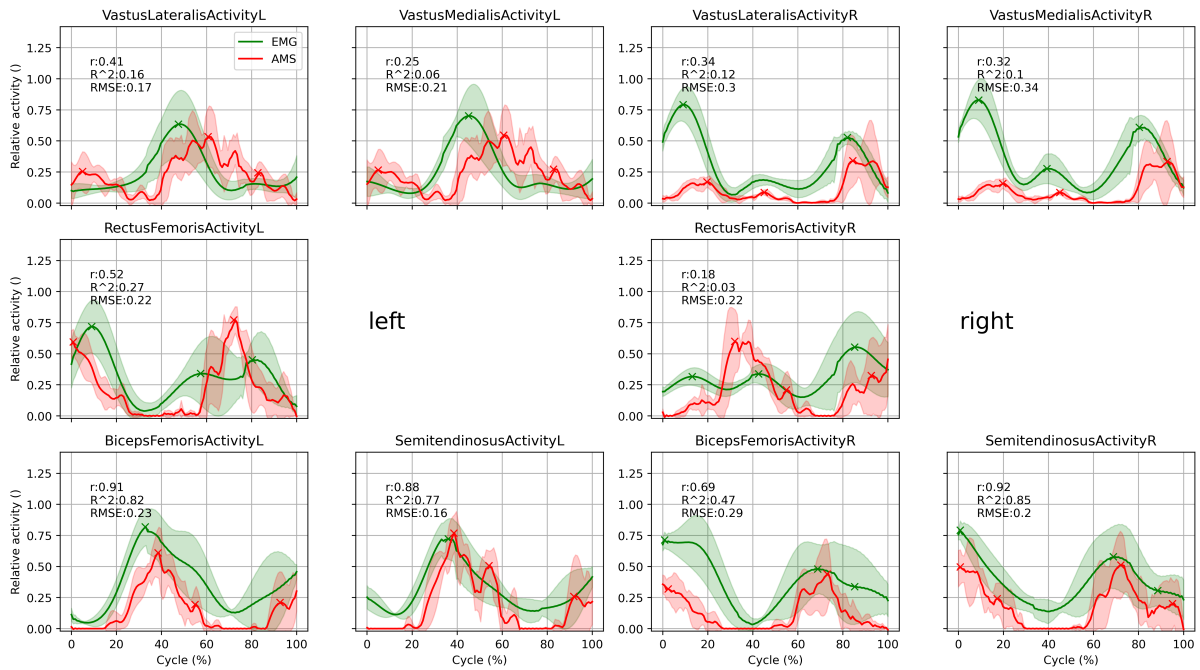
(i) Subject 9



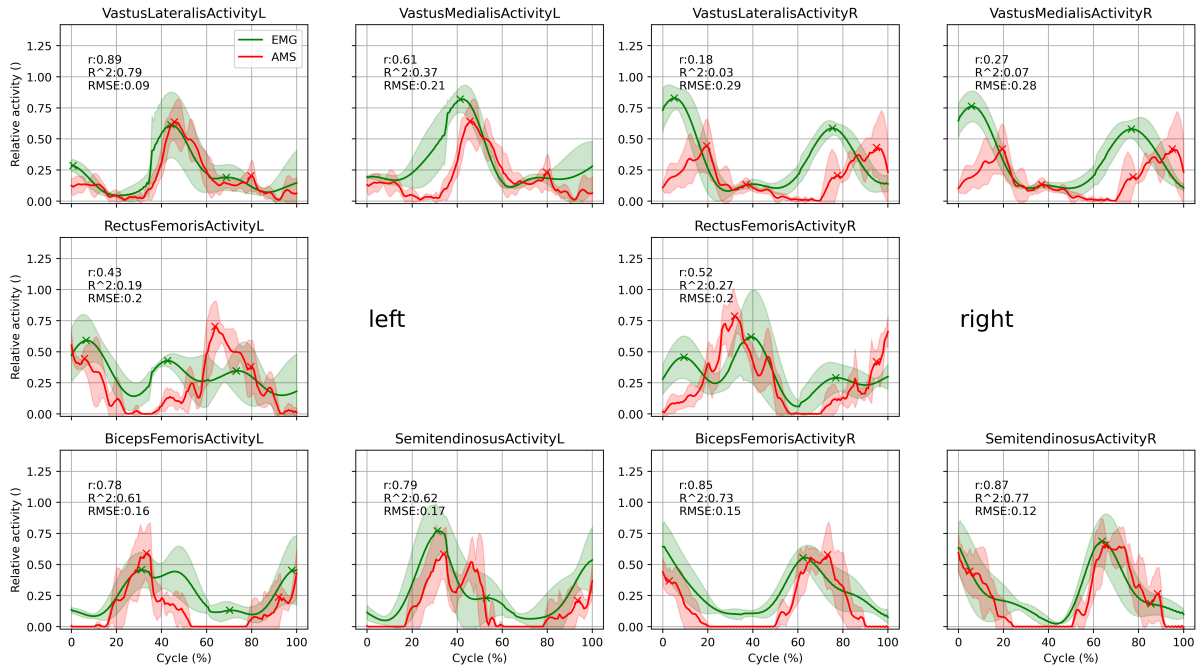
(j) Subject 10



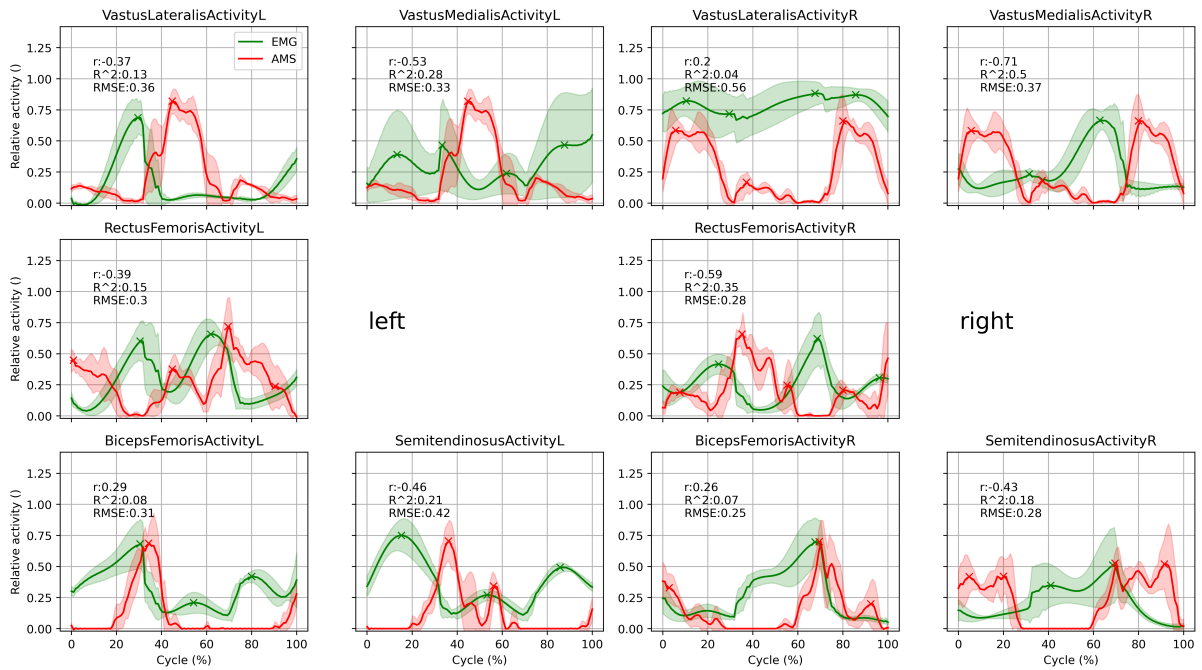
(k) Subject 11



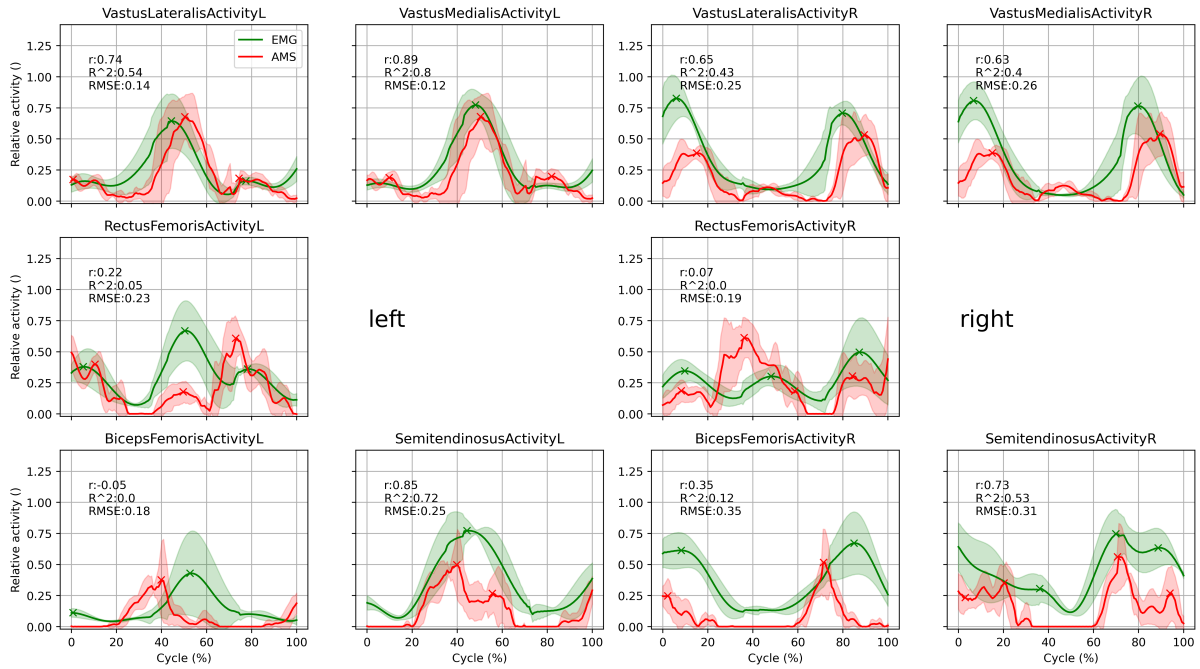
(l) Subject 12



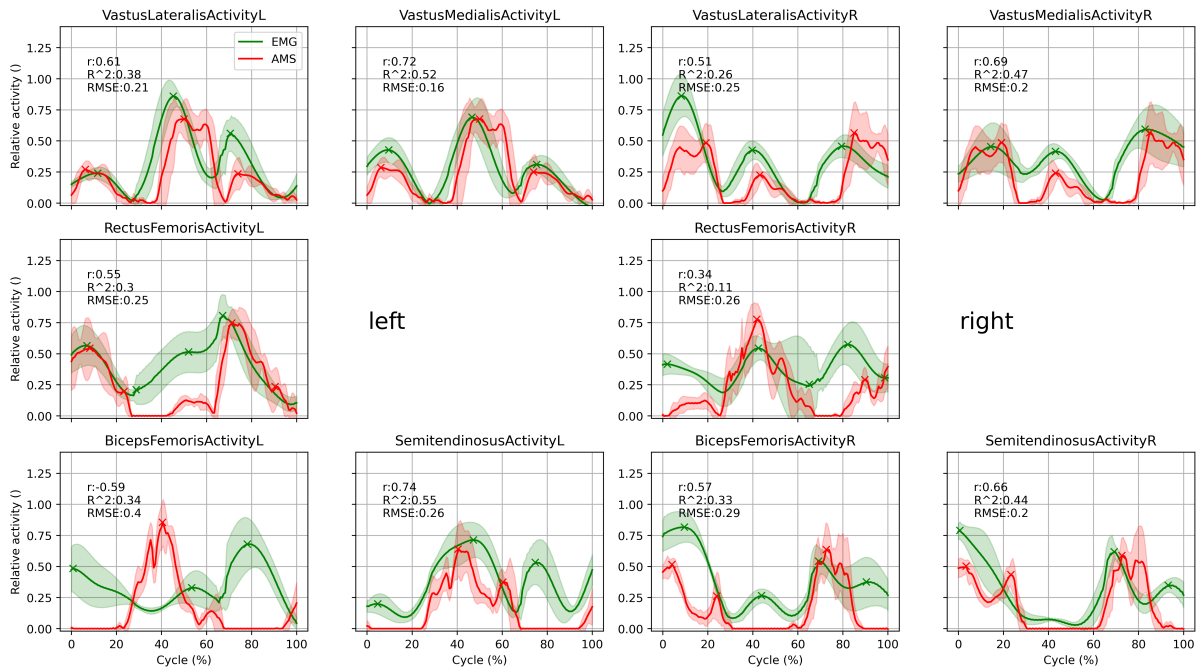
(m) Subject 13



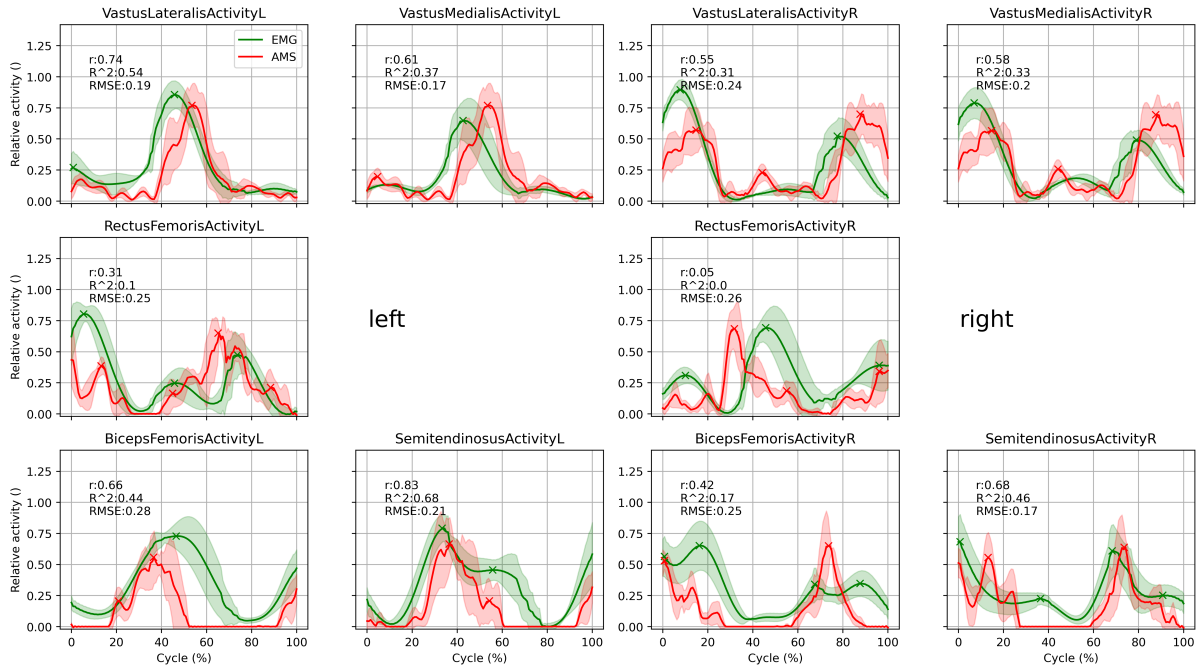
(n) Subject 14



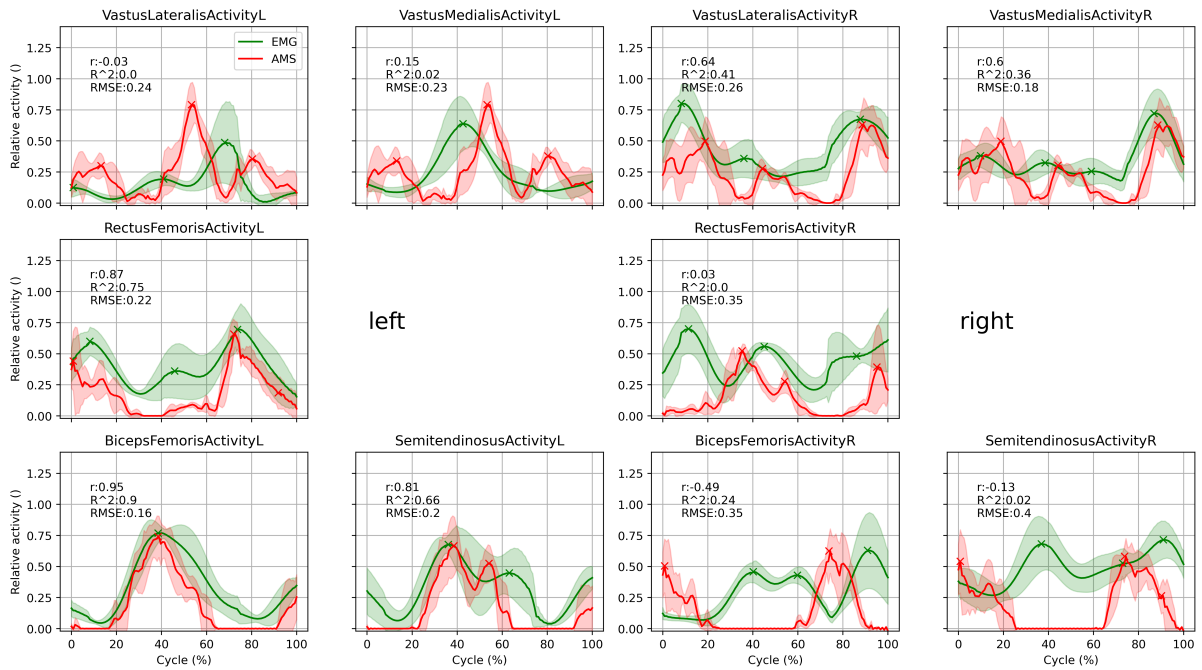
(o) Subject 15



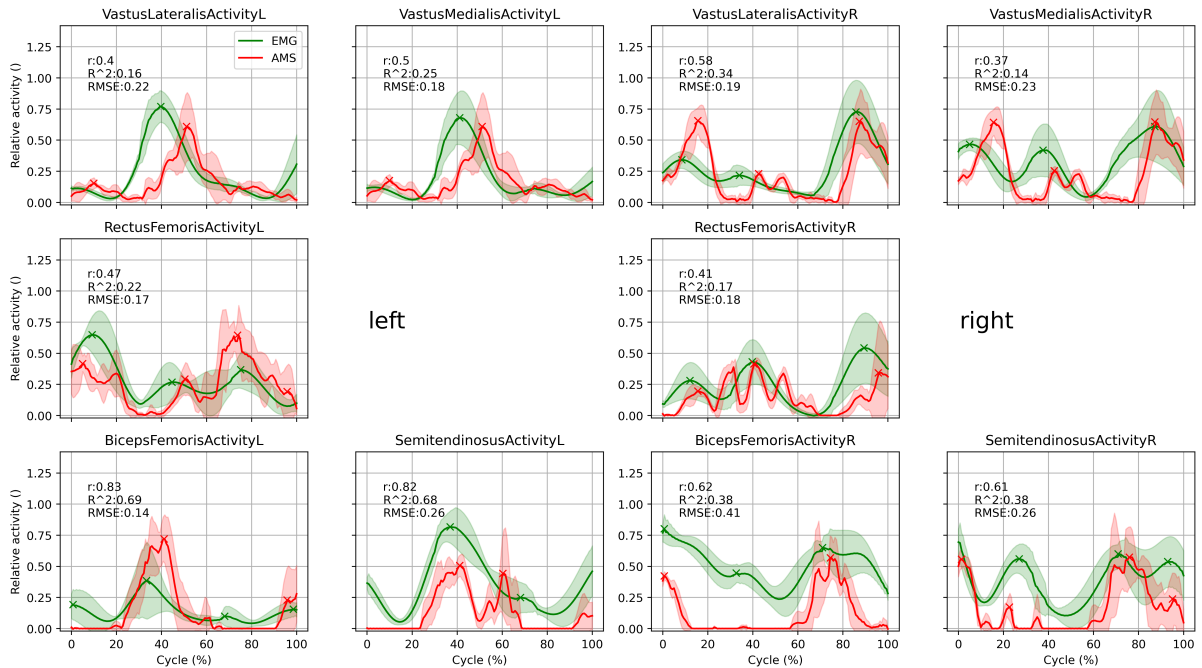
(p) Subject 16



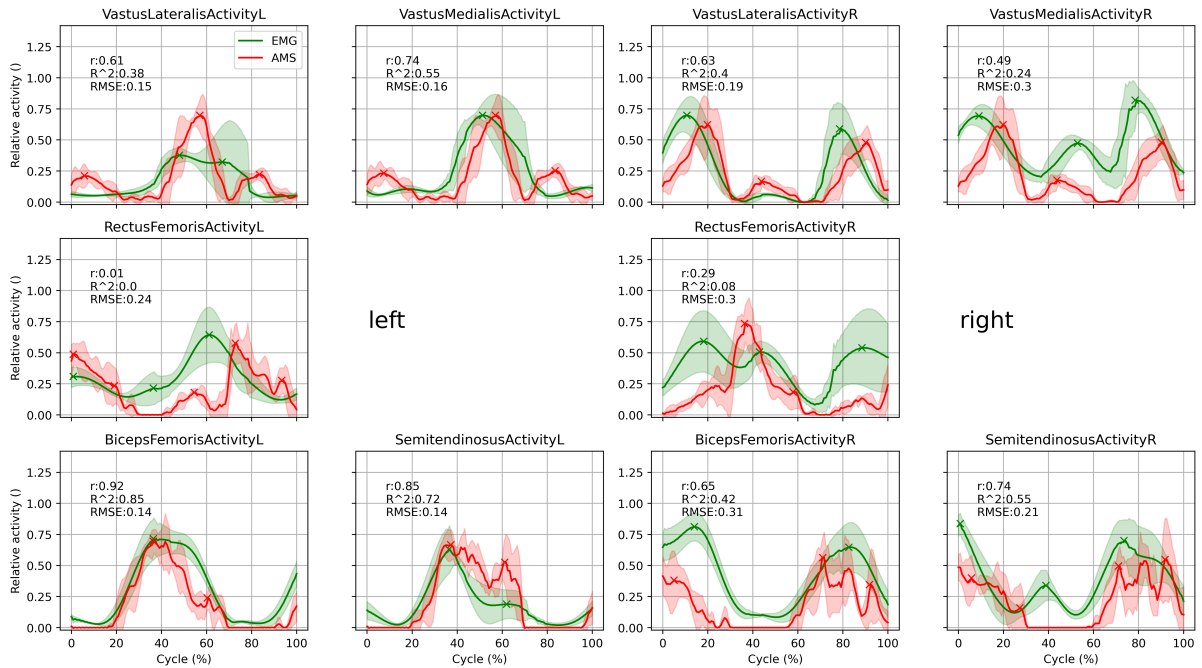
(q) Subject 17



(r) Subject 18



(s) Subject 19



(t) Subject 20

Figure A.1: Muscle activity in electromyography (EMG) (green) and AMS (red) for the S2 scenario for every subject. Including the statistics of Pearson correlation r and coefficient of determination R^2 .

Appendix B

Supplementary material to chapter 4

Listing B.1: Python code for the optimization of the body segment parameters.

```
import scipy
import numpy as np
from pathlib import Path
from anypytools import AnyPyProcess
from anypytools.macro_commands import Load, OperationRun, Dump, SetValue

# relative path to AnyBody .h5 output file
path = str(Path('../.. /02_AnyBody/BVH_with_forceplate/Application/' +
               'MocapExamples/BVH_Xsens/').resolve())
BM = 84.3

def run_model(
    lbrScl, thxScl, plvScl, thiScl, shaScl, fooScl, BM, silent=False):
    macro = [
        Load(path + "/Main.any"),
        SetValue("Main.HumanModel.Anthropometrics.SegmentMasses.Lumbar",
                lbrScl*BM),
        SetValue("Main.HumanModel.Anthropometrics.SegmentMasses.Thorax",
                thxScl*BM),
        SetValue("Main.HumanModel.Anthropometrics.SegmentMasses.Pelvis",
                plvScl*BM),
        SetValue("Main.HumanModel.Anthropometrics.SegmentMasses.Right.Thigh",
                thiScl*BM),
        SetValue("Main.HumanModel.Anthropometrics.SegmentMasses.Right.Shank",
                shaScl*BM),
        SetValue("Main.HumanModel.Anthropometrics.SegmentMasses.Right.Talus",
                fooScl*0.2*BM),
        SetValue("Main.HumanModel.Anthropometrics.SegmentMasses.Right.Foot",
                fooScl*0.8*BM),
        SetValue("Main.HumanModel.Anthropometrics.SegmentMasses.Left.Thigh",
                thiScl*BM),
        SetValue("Main.HumanModel.Anthropometrics.SegmentMasses.Left.Shank",
                shaScl*BM),
        SetValue("Main.HumanModel.Anthropometrics.SegmentMasses.Left.Talus",
                fooScl*0.2*BM),
```

```

    SetValue("Main.HumanModel.Anthropometrics.SegmentMasses.Left.Foot",
            fooScl*0.8*BM),
    OperationRun("Main.RunAnalysis.LoadParameters"),
    OperationRun("Main.RunAnalysis.InverseDynamics"),
    Dump("Main.Studies.InverseDynamicStudy.Output."+
    "ModelEnvironmentConnection.HumanGroundResiduals.PosX_Force"),
    Dump("Main.Studies.InverseDynamicStudy.Output."+
    "ModelEnvironmentConnection.HumanGroundResiduals.PosY_Force"),
    Dump("Main.Studies.InverseDynamicStudy.Output."+
    "ModelEnvironmentConnection.HumanGroundResiduals.PosZ_Force"),
    Dump("Main.Studies.InverseDynamicStudy.Output."+
    "BodyModel.Anthropometrics.BodyMassDummy")
]
app = AnyPyProcess(
    anybodycon_path=
    'C:/Program Files/AnyBody Technology/AnyBody.7.3/AnyBodyCon.exe',
    silent=silent)
results = app.start_macro(macro)
return results[0]

```

```
def objfun(designvars):
```

```
    """Calculate the objective function value"""
```

```

    lbrScl = designvars[0]
    thxScl = designvars[1]
    plvScl = designvars[2]
    thiScl = designvars[3]
    shaScl = designvars[4]
    fooScl = designvars[5]
    result = run_model(lbrScl, thxScl, plvScl, thiScl, shaScl, fooScl, BM,
    silent=True)

```

```
if "ERROR" in result:
```

```
    return 9999999
```

```

bodyWeight = np.array(result['BodyModel.Anthropometrics.BodyMassDummy'])[0]
nrm = (bodyWeight*9.81)/100 # normalization of forces to %BW
hgrX = result["ModelEnvironmentConnection."+
    "HumanGroundResiduals.PosX_Force"]
hgrY = result["ModelEnvironmentConnection."+
    "HumanGroundResiduals.PosY_Force"]
hgrZ = result["ModelEnvironmentConnection."+
    "HumanGroundResiduals.PosZ_Force"]

return np.max(np.sqrt(hgrX**2+hgrY**2+hgrZ**2)/nrm)

```

```
def opt_constraint(x):
```

```
    return (x[0] + x[1] + x[2] + x[3] + x[4] + x[5])
```

```

lbrSc10=0.139
thxSc10=0.1894
plvSc10=0.142
thiSc10=0.1
shaSc10=0.0465
fooSc10=0.0145
sumMD = lbrSc10+thxSc10+plvSc10+thiSc10*2+shaSc10*2+fooSc10*2
tol = 0.05 # overall weight tolerance of 5%

constraints = scipy.optimize.NonlinearConstraint(
    opt_constraint, sumMD-tol*sumMD, sumMD+tol*sumMD)

tol2= 0.2
bounds = [
    (lbrSc10-tol2*lbrSc10, lbrSc10+tol2*lbrSc10),
    (thxSc10-tol2*thxSc10, thxSc10+tol2*thxSc10),
    (plvSc10-tol2*plvSc10, plvSc10+tol2*plvSc10),
    (thiSc10-tol2*thiSc10, thiSc10+tol2*thiSc10),
    (shaSc10-tol2*shaSc10, shaSc10+tol2*shaSc10),
    (fooSc10-tol2*fooSc10, fooSc10+tol2*fooSc10)
]
initial_guess = (lbrSc10, thxSc10, plvSc10, thiSc10, shaSc10, fooSc10)

solution = scipy.optimize.differential_evolution(
    objfun, bounds, constraints=constraints)

```

Listing B.2: Python code for the optimization of the GRFP parameters with C3D input.

```

import scipy
import numpy as np
from pathlib import Path
from anypytools import AnyPyProcess
from anypytools.macro_commands import Load, OperationRun, Dump, SetValue

subject = 'Subject_997'
trial = 'Jump_003'
filename = '/' + subject + '_' + trial
# relative path to AnyBody .h5 output file
path = str(Path('../..'/02_AnyBody/C3D_SquatJump/Application/' +
    'MocapExamples/Plug-in-gait_Simple/').resolve())
firstFrame = 850
lastFrame = 1150
contactStop = 947 # extracted manually from ForcePlate Data
contactStart = 1057
contactDurationC3D = contactStart - contactStop

def run_model(LDH, LVH, silent=False):

```

```

macro = [
    Load(path + "/FullBody_GRFPrediction.main.any"),
    SetValue("Main.EnvironmentModel.ForcePlates."+
    "GRF_Prediction_Right.Settings.LimitDistHigh", LDH),
    SetValue("Main.EnvironmentModel.ForcePlates."+
    "GRF_Prediction_Left.Settings.LimitDistHigh", LDH),
    SetValue("Main.EnvironmentModel.ForcePlates."+
    "GRF_Prediction_Right.Settings.LimitVelHigh", LVH),
    SetValue("Main.EnvironmentModel.ForcePlates."+
    "GRF_Prediction_Left.Settings.LimitVelHigh", LVH),
    OperationRun("Main.RunAnalysis.LoadParameters"),
    OperationRun("Main.RunAnalysis.InverseDynamics"),
    Dump("Main.Studies.InverseDynamicStudy.Output."+
    "ModelEnvironmentConnection.HumanGroundResiduals.PosX_Force"),
    Dump("Main.Studies.InverseDynamicStudy.Output."+
    "ModelEnvironmentConnection.HumanGroundResiduals.PosY_Force"),
    Dump("Main.Studies.InverseDynamicStudy.Output."+
    "ModelEnvironmentConnection.HumanGroundResiduals.PosZ_Force"),
    Dump("Main.Studies.InverseDynamicStudy.Output."+
    "BodyModel.Anthropometrics.BodyMassDummy"),
    Dump("Main.Studies.InverseDynamicStudy.Output.EnvironmentModel."+
    "ForcePlates.GRF_Prediction_Right.GRF_point.Opacity"),
    Dump("Main.Studies.InverseDynamicStudy.Output."+
    "EnvironmentModel.ForcePlates.GRF_Prediction_Left."+
    "GRF_point.Opacity")
]
app = AnyPyProcess(
    anybodycon_path=
    'C:/Program Files/AnyBody Technology/AnyBody.7.4/AnyBodyCon.exe',
    silent=silent)
results = app.start_macro(macro)
return results[0]

def objfun(designvars):
    """Calculate the objective function value"""
    LDH = designvars[0]
    LVH = designvars[1]
    result = run_model(LDH, LVH, silent=True)

    if "ERROR" in result:
        raise ValueError("Failed to run model")

    bodyWeight = np.array(
        result['BodyModel.Anthropometrics.BodyMassDummy'])[0]
    nrm = (bodyWeight*9.81)/100 # normalization of forces to %BW
    hgr = np.sqrt(max(abs(result[
        "ModelEnvironmentConnection.HumanGroundResiduals.PosX_Force"]
        ]))*2

```

```

+ max(abs(result [
    "ModelEnvironmentConnection.HumanGroundResiduals.PosY_Force"]))*2
+ max(abs(result
["ModelEnvironmentConnection.HumanGroundResiduals.PosZ_Force"]))*2)/nrm

rightGRFOnOff = np.array(result [
    'EnvironmentModel.ForcePlates.GRF_Prediction_Right.'+'
    'GRF_point.Opacity'
])
leftGRFOnOff = np.array(result [
    'EnvironmentModel.ForcePlates.GRF_Prediction_Left.'+'
    'GRF_point.Opacity'
])
contactDurationAMS = 0
for i in range(len(rightGRFOnOff)):
    if rightGRFOnOff[i] == 1 or leftGRFOnOff[i] == 1:
        contactDurationAMS += 1
contactDiffAbs = int(contactDurationAMS - contactDurationC3D)
contactDiffRel = contactDiffAbs/contactDurationC3D*100

return hgr + 0.7*abs(contactDiffRel)

def opt_constraint(x):
    return (np.sqrt(x[0]**2 + x[1]**2) - 0.05)

bounds = [(0.005, 0.3), (0.5, 15)]
initial_guess = (0.035, 0.8)

solution = scipy.optimize.differential_evolution(
    objfun, bounds=bounds)

```

Listing B.3: Python code for the optimization of the GRFP parameters with BVH input.

```

import scipy
import pandas as pd
import numpy as np
from pathlib import Path
from anypytools import AnyPyProcess
from anypytools.macro_commands import Load, OperationRun, Dump, SetValue
import mvnx

subject = 'Subject_997'
trial = 'Jump_003'
filename = '/' + subject + '_' + trial
# relative path to AnyBody .h5 output file
path = str(Path('../..//02_AnyBody/BVH_with_forceplate/Application/'+'
    'MocapExamples/BVH_Xsens/').resolve())
# relative path to Xsens .h5 output file

```

```

mvnxFile = Path(
    '../.. /03_Xsens/' + subject + '/out/' + trial + '.mvnx').resolve()
mvnxData = mvnx.MVNX(str(mvnxFile))
firstFrame = 850
lastFrame = 1150

# Xsens Ground contact detection:
contMVNX = pd.DataFrame(mvnxData.get_info('footContacts'))
contactDurationMVNX = 0
for i in range(firstFrame, lastFrame):
    if contMVNX['LeftFoot_Heel'][i] == [1.0] or \
        contMVNX['LeftFoot_Toe'][i] == [1.0] or \
        contMVNX['RightFoot_Heel'][i] == [1.0] or \
            contMVNX['RightFoot_Toe'][i] == [1.0]:
        contactDurationMVNX += 1

def run_model(LDH, LVH, silent=False):
    macro = [
        Load(path + "/Main.any"),
        SetValue("Main.EnvironmentModel.ForcePlates."+
            "GRF_Prediction_Right.Settings.LimitDistHigh", LDH),
        SetValue("Main.EnvironmentModel.ForcePlates."+
            "GRF_Prediction_Left.Settings.LimitDistHigh", LDH),
        SetValue("Main.EnvironmentModel.ForcePlates."+
            "GRF_Prediction_Right.Settings.LimitVelHigh", LVH),
        SetValue("Main.EnvironmentModel.ForcePlates."+
            "GRF_Prediction_Left.Settings.LimitVelHigh", LVH),
        OperationRun("Main.RunAnalysis.LoadParameters"),
        OperationRun("Main.RunAnalysis.InverseDynamics"),
        Dump("Main.Studies.InverseDynamicStudy.Output."+
            "ModelEnvironmentConnection.HumanGroundResiduals.PosX_Force"),
        Dump("Main.Studies.InverseDynamicStudy.Output."+
            "ModelEnvironmentConnection.HumanGroundResiduals.PosY_Force"),
        Dump("Main.Studies.InverseDynamicStudy.Output."+
            "ModelEnvironmentConnection.HumanGroundResiduals.PosZ_Force"),
        Dump("Main.Studies.InverseDynamicStudy.Output."+
            "BodyModel.Anthropometrics.BodyMassDummy"),
        Dump("Main.Studies.InverseDynamicStudy.Output."+
            "EnvironmentModel.ForcePlates.GRF_Prediction_Right.OnOff"),
        Dump("Main.Studies.InverseDynamicStudy.Output."+
            "EnvironmentModel.ForcePlates.GRF_Prediction_Left.OnOff")
    ]
    app = AnyPyProcess(
        anybodycon_path=
            'C:/Program Files/AnyBody Technology/AnyBody.7.3/AnyBodyCon.exe',
        silent=silent)
    results = app.start_macro(macro)

```

```

    return results[0]

def objfun(designvars):
    """Calculate the objective function value"""
    LDH = designvars[0]
    LVH = designvars[1]
    result = run_model(LDH, LVH, silent=True)

    if "ERROR" in result:
        raise ValueError("Failed to run model")

    bodyWeight = np.array(
        result['BodyModel.Anthropometrics.BodyMassDummy'])[0]
    nrm = (bodyWeight*9.81)/100 # normalization of forces to %BW
    hgr = np.sqrt(max(abs(result[
        "ModelEnvironmentConnection.HumanGroundResiduals.PosX_Force"
    ])**2
    + max(abs(result[
        "ModelEnvironmentConnection.HumanGroundResiduals.PosY_Force"
    ])**2
    + max(abs(result[
        "ModelEnvironmentConnection.HumanGroundResiduals.PosZ_Force"
    ])**2)/nrm
    rightGRFOnOff = np.array(
        result['EnvironmentModel.ForcePlates.'+
        'GRF_Prediction_Right.OnOff'])
    leftGRFOnOff = np.array(
        result['EnvironmentModel.ForcePlates.'+
        'GRF_Prediction_Left.OnOff'])
    contactDurationAMS = 0
    for i in range(len(rightGRFOnOff)):
        if rightGRFOnOff[i] == 1 or leftGRFOnOff[i] == 1:
            contactDurationAMS += 1
    contactDiffAbs = int(contactDurationAMS - contactDurationMVNX)
    contactDiffRel = contactDiffAbs/contactDurationMVNX*100

    return hgr + 0.7*abs(contactDiffRel)

def opt_constraint(x):
    return (np.sqrt(x[0]**2 + x[1]**2) - 0.05)

bounds = [(0.005, 0.3), (0.1, 15)]
initial_guess = (0.035, 0.8)

solution = scipy.optimize.differential_evolution(
    objfun, bounds=bounds)

```
